UNIVERSITY OF CUKUROVA
INSTITUTE OF NATURAL AND
APPLIED SCIENCES

**MSc THESIS**

**Eser AKRAY**

# TUNABLE TRANMISSION SPECTRUM OF A PERIODICALLY CORRUGATED WAVEGUIDE

DEPARTMENT OF ELECTRICAL AND
ELECTRONICS ENGINEERING

ADANA, 2006

**ABSTRACT**

**MSc THESIS**

**TUNABLE TRANMISSION SPECTRUM OF A PERIODICALLY CORRUGATED WAVEGUIDE**



**Eser AKRAY**

**DEPARTMENT OF ELECTRICAL AND ELECTRONICS ENGINEERING**
**INSTITUTE OF NATURAL AND APPLIED SCIENCES**
**UNIVERSITY OF CUKUROVA**



Supervisor: Prof. Dr. Victor POGREBNYAK
Year: 2006, Pages: 172
Jury : Prof. Dr. Victor POGREBNYAK
Prof. Dr. Süleyman GÜNGÖR
Doç. Dr. Turgut İKİZ



Analysis of electromagnetic wave propagation in periodic structures is of considerable interest due to their extensive use in many fields of electrical and electronics engineering and technology such as quantum- and optoelectronics, photonic crystals, fiber grating sensors and microwaves.

Although the applications of periodic structures are well developed, there are still some basic experimental problems, such experimental problem as tunability mechanism of the transmission spectrum in a planar periodically corrugated waveguide, which need more detailed investigation.

Aside from considerable interest to the propagation of waves in periodic structures great interest to the propagation of waves in disordered structures by scientists has never been remained behind that of periodic structures as well.

In this thesis, the tunability of the transmission spectrum of a planar periodically corrugated waveguide was investigated theoretically and experimentally at the microwave range of frequency. Measurement of the transmission properties showed that the location of the gap in the frequency spectrum as well as its width depends on the relative position of two corrugated plates. The transmission varies from zero to a maximum value upon shifting one periodic plate with respect to another on the half period of the corrugation. The results confirm the theoretical prediction of the transformation of tunabilty of the transmission spectrum from a band structure form to a gapless one upon such a shift of one of the plates.

Then the effect of randomizing period of a corrugated waveguide was investigated. The corrugated waveguide having randomized periods was designed, manufactured, and its transmission spectrum was investigated experimentally. The experimental results are in a good agreement with the known theoretical predictions.



Keywords: Electromagnetic wave, planar waveguide, Bragg reflection, periodicity, tunable frequency spectrum

# ÖZ

## YÜKSEK LİSANS TEZİ

**PERİYODİK OLARAK OLUKLU BİR DALGA KILAVUZUNUN AYARLANABİLİR İLETİM SPEKTRUMU**

**Eser AKRAY**

**ÇUKUROVA ÜNİVERSİTESİ**
**FEN BİLİMLERİ ENSTİTÜSÜ**
**ELEKTRİK-ELEKTRONİK MÜHENDİSLİĞİ ANABİLİM DALI**

Danışman : Prof. Dr. Victor POGREBNYAK
Yıl: 2006, Sayfa: 172
Jüri : Prof. Dr. Victor POGREBNYAK
Prof. Dr. Süleyman GÜNGÖR
Doç. Dr. Turgut İKİZ

Periyodik yapılardaki elektromanyetik dalga yayılımının analizi, kuantum- ve optoelektronik, fotonik kristaller, fiber grating sensörler ve mikrodalga gibi teknoloji ve fiziğin birçok alanında kendine geniş kullanım alanı bulmasından dolayı hatırı sayılır bir ilgiye sahiptir.

Periyodik yapılar fiziksel olarak çok iyi geliştirilmiş olmalarına karşın, örnek olarak düzlemsel periyodik olarak oluklu dalga kılavuzundaki dalga yayılımı gibi, daha detaylı incelenmesi gereken deneysel bazı problemler hala mevcuttur. Bu tezde yapıldığı gibi böyle bir çalışma periyodik yapıları özelliklerini kontrol etmenin yeni bir ilkesini geliştirmeye yol açacaktır.

Periyodik yapılardaki dalga yayılımına ilginin yanında, düzensiz yapılardaki dalga yayılımına olan ilgi de hiçbir zaman periyodik yapılara olan ilginin gerisinde kalmamıştır.

Bu tezde düzlemsel periyodik olarak oluklu dalga kılavuzunun iletim spektrumunun ayarlanabilirliği mikrodalga frekansında teorik ve deneysel olarak incelenmiştir. İletim özelliklerinin ölçümü göstermiştir ki durdurma ve geçirme bantlarının frekans spektrumundaki yeri (ve genişliği) oluklu plakaların birbirine göre olan pozisyonuna bağlıdır. İletim bir plakanın diğerine göre oluğun yarım periyodu kadar kaydırılmasıyla sıfırdan maksimum değere kadar değişir. Deneysel sonuçlar bir plakanın diğerine göre kaydırılmasıyla, teorik olarak beklenen bant yapılı bir biçimden tamamen bantsız bir yapıya dönüşümü gerçeklemiştir.

Daha sonra periyodik olarak oluklu bir dalga kılavuzunun periyodu randomize edilerek iletim spektrumu deneysel olarak incelendi. Deneysel sonuçlar bilinen teorik öngörülerle iyi bir uyum içindedir.

Anahtar kelimeler: Elektromanyetik dalga, düzlemsel dalga kılavuzu, Bragg yansıması, periyodiklik, ayarlanabilir frekans spektrumu

**ACKNOWLEDGMENT**

I would like to express my thankful feelings to the head of the department Prof. Dr. Süleyman Güngör who provided me the necessary condition to work, and Associate Prof. Turgut İkiz for the evaluation of the results of the work.

I thank MSc. student Neşet Küçükaltun very much for his co-operation and contribution to the experiments, Res. Asst. Mustafa Zateroğlu and Zehan Kesilmiş for their help about necessary logistics they provided as well.

I also would like to thank my sisters Derya and Pırıl Akray, and my cousin Mert Toprak very much for their considerable contributions.

Because it is impossible to state the crucial positive contributions of my supervisor Prof. Dr. Victor POGREBNYAK towards my personality and career with words, I express my endless gratitude to him only. Because it is the only thing that I am able to do. The contributions he has made towards those of mine will live with me forever.

**CONTENTS** **PAGE**

**LIST OF FIGURES** **PAGE**

## NOTATIONS

| | |
|---|---|
| $d$ | Average thickness of the waveguide |
| $d_r$ | A resonance thickness of the waveguide |
| $\xi$ | Amplitude of the corrugations |
| $a$ | Period of the corrugations |
| $\theta$ | Phase shift between the upeer and the lower plates |
| $\Delta x$ | Phase shift between the upeer and the lower plates |
| $\varphi(x, y)$ | The *z*-component of field |
| $\omega$ | Wave frequency |
| $\varepsilon$ | Dielectric constant of the medium |
| $c$ | Velocity oflight |
| $a_n$ | Fourier series coefficient |
| $b_n$ | Fourier series coefficient |
| $k_{yn}$ | Transverse component of the wave vector **k** |
| $k_x$ | Longitudinal component of the wave vector **k** |
| $n$ | Number of harmonics |
| $f_g$ | Bragg gap |
| $\delta f_g$ | Width of the Bragg gap |
| $k_0^{(0)}$ | Wave numbers for smooth waveguide |
| $\omega_p$ | The cutoff frequency of each mode |
| $\delta\omega_p$ | Shifts of cutoff frequencies |
| $\omega_{pm}^{\pm}$ | Splitted cutoff frequencies in resonance case |
| $\delta\omega_{pm}$ | Band gap seperating the cutoff frequencies in resonance case |

# 1. INTRODUCTION

Periodic structures are widely encountered in nature in the form of crystals. They can also be generated simply by a standing wave, i.e., an acoustic wave in a fluid or solid, or an electromagnetic wave in a nonlinear or active medium. Large periodic structures can be developed by just simply repeating a basic unit. These have been factors in generating the interest of scientists to study their characteristics.

The considerable interest to the periodic structures, besides, stems from the fact that propagating modes interact with a structural periodicity in different manners. The interaction could be constructive leading to the generation of a new mode, or destructive resulting in the filtration of a mode. Understanding the nature of the modal interaction is of great help for the design of wave processing devices such as mode couplers, filters, or resonators. In fact, two special properties made periodic structures so unique and important: 1) their eigenmodes consist of an infinite number of space-harmonics with phase velocities varying from zero to infinity; and 2) they can support propagating waves only in well-specified propagation bands. The uniqueness of the first property is that it allows the periodic structure to support waves that have a very low phase velocity and therefore can be efficiently coupled to relatively slowly moving charges or sources. It also allows the coupling of different types of waves, or similar waves in different modes, without requiring them to have inherently identical wave vectors (in the absence of the periodicity). In other words, the periodic structure has an inherent wave vector ($q = {}^{2\pi}\!/_{a}$, where $a$ is the period of the structure) that is adjustable by the designer and can be used to conserve the momentum (or the wave vector) in the coupling between any two waves. The second property is commonly known as the distributed feedback (Bragg reflection), which is a result of the cumulative reflection from each unit cell in the structure. In certain frequency bands the propagation- wave vector can only be complex. This implies that a wave propagating in the structure with a frequency in the stopband will encounter successive reflection, i.e., “distributed feedback,” and thus cannot extend far away from its source. This is the reason for the presence of forbidden bands in crystals. All types of waves exhibit the above properties when they propagate in a periodic structure. The wave could be an acoustic, electromagnetic, magnetoelastic, plasma, electron, or water wave. The structure could have a periodic boundary, a periodic support, or a periodic bulk parameter (i.e., index of refraction, plasma density, electric potential, nonlinearity constant, gain, density, etc.) The only requirement is that the propagation properties of the wave are somehow related to the perturbed parameter.

Interest is also very strong in the field of optical multilayers, which have many applications: filters, antireflection films, beam splitters, and polarizers. The theory of stratified optical thin films was elegantly and considerably investigated. The study of slow wave structures was mainly stimulated by the development of microwave tubes where a periodic structure is used to slow the wave, which could then couple to the relatively slow electron beam.

On the other hand, in 1987, it was suggested the possibility of making periodic dielectric structures in which light cannot propagate in any direction for certain frequency intervals. These frequency intervals are known as photonic bandgaps, and they are analogous to the electronic bandgaps in semiconductor materials that can be related to the periodic arrangement of atoms on a crystal lattice. The new dielectric materials are often referred to as photonic crystals. Since then, a new field of research has started that seeks to understand the new physics of these materials and to take advantage of the new material properties for making novel optical components. Photonic crystals can be incorporated in existing optical components with the purpose of improving their optical properties. Photonic crystals are also interesting for making novel cavities and lasers. Components based on photonic crystals draw interest in use for integrated optics because it is possible to confine and manipulate light in a small spatial region.

Analysis of electromagnetic wave propagation in periodic structures is of considerable interest. When periodic structures interact with electromagnetic waves amazing and unique features result. In particular, characteristics such as frequency stop-bands, pass-bands and band-gaps could be identified. These applications are seen in such fields as quantum- and optoelectronics, photonic crystals, fiber grating sensors, microwaves, as well for the close relation of this analysis in the investigation of a two dimensional electron gas in semiconductors, high temperature superconductors, and also in carbon nanotubes. Periodic waveguides are also used in the tokamak approach to fusion energy production.

The principal physical phenomenon resulting from properties of a periodic structure is the Bragg reflection, or Bragg resonance, resulting in the opening of the forbidden gap in the electromagnetic spectrum of the structure. Bragg's law is simply the mathematical formulation of the constructive interference of waves travelling along the axis of the periodic waveguide. The Bragg reflection occurs both in the case of unbounded periodic medium as well as in a case of bounded periodic structure like a periodic waveguide.

Despite the fact that the physics of periodic structures is well developed, there are still some basic experimental problems, such as wave propagation in a planar periodically corrugated waveguide, which need more detailed investigation.

It is the first aim of this thesis to design and investigate the planar periodically corrugated waveguide with the tunable transmission spectrum theoretically and experimentally at the microwave range of frequency.

This is very promising from a practical point of view, if the periodicity is introduced into the waveguide by the lateral modulation. In this case the spectrum and transmission properties of the waveguide become controllable as there is the opportunity to change the lateral modulation profile. For example, the gap can be tuned by a shift of one periodic boundary. In planar geometry, the tailoring of the lateral modulation is a simple enough problem for microwave devices and a solvable problem in nanotechnology.

Aside from considerable interest to the propagation of waves in periodic structures great interest to the propagation of waves in disordered structures by scientists has never been remained behind that of periodic structures.

What makes disordered systems interesting is that interference effects can survive the random multiple scattering. Examples of such interference effects are coherent backscattering or weak localization (Kuga and Ishimaru, 1984: Van Ablada and Lagendjik, 1985), and short and long range intensity correlations (Freund et al, 1988).

Huge number of studies in the field of photonic structures have shown that the existence of photonic gaps does not require long range periodic order. Therefore, investigation of disorder effects in photonic structures has a fundamental importance in pure and applied physics.

A small impurity inside such a photonic band gap material will give rise to a naturally localized mode around this impurity. Moreover, since unintentional positional disorders are always present in the PBG (Photonic Band Gap) structures, it is important to address the influence of disorders on the photonic band gaps, cavity modes, and especially waveguides.

Not only does the interest come from light propagation in disordered metallic and dielectric photonic crystals but also the propagation of electrons in amorphous (semi)conductors. Besides, these fields mutually interact with each other in a manner such as that existence of photonic band gaps, localization of classical waves in disordered photonic systems, defect modes are reminiscent of what is observed in electronic case. In other words, complete analogy to electronic Bloch bands in crystalline solids can be settled. For instance, it is well known that the amorphous semiconductors have similar band gaps compared to their crystalline counterparts.

Various phenomena that are common for electron transport have now also been found to exist for light waves (Sheng, 1995). Important examples are the optical magnetoresistance (Sparenberg et al, 1997), Anderson localization (John, 1984: Anderson, 1985: Daliehaouch et al, 1991: Wiersma et al, 1997: Chabanov and Genack, 2001), and universal conductance fluctuations (Scheffold and Maret, 1998). In the case of Anderson localization the interference effects are so strong that the transport comes to a halt and the light becomes localized in randomly distributed modes inside the system. Important applications of multiple light scattering include medical imaging (Yodh and Chance, 1995) and diffusing wave spectroscopy, where interference in multiple scattering is used to study the dynamics of optically dense colloidal systems (Maret and Wolf, 1987: Pire et al, 1988).

Along with lots of work done in the fields of (semi)conductors and photonic structures regarding investigation of the effect of disorder in literature (and also in microwave frequency range), majority of studies, although field scattering by rough surface has been of interest due to its applications in radar and communication, concerning the effect of disorder in the microwave frequency range, to our knowledge, remain in the limit of scattering from rough surfaces which are modelled by Gaussian height distribution and Monte Carlo simulation in microwave frequency range. Only small part of studies have seemed different. For example, Kuhl and Stöckmann (2001) showed that there is a close correspondence between one-dimensional tight-binding systems, and the propagation of microwaves through a single-mode waveguide with inserted scatterers. Also, they presented exemplary results on the transmission through random arrangements of scatterers as well as through sequences with correlated disorder. Nonetheless, wave propagation phenomena in a waveguide having random, but correlated surface still need additional investigation.

Moreover, since satisfactory studies have been done in the field of photonic crystals showing the effect of disorder we can use the field of photonic crystals in the same way for our purpose by doing analogy as the scientists working on the photonic crystals take advantage of the similarities between photonic crystals and (semi)conductors, i.e. because of this correspondence it is a common practice to speak of photonic crystals and photonic band gaps in this thesis upon doing modelling for the random waveguide we designed.

The second objective of this thesis is to try to create a suitable mathematical and geometrical model for the random waveguide that we designed which we have found Electromagnetic Band Gap experimentally. Upon doing it, we will mostly take advantage of the studies in photonic crystals field which have been investigated almost all different aspects of the effect of the disorder. Besides, we will get help from plane-wave approximation, and a partially ordered system; photonic quasi-crystal; that we will shortly discuss here, in which the scattering elements are assembled in a non-periodic but deterministic way.

Moreover, over 1500 publications and 10 books are reviewed, and over 200 of which are chosen and put the present thesis in order to constitute the 'Previous Studies' section. Such a review may light the way for one who wants to attempt to the topics wave propagation in periodic, and random/disordered structures.

## 1.1. Publications of the Results

The experimental and theoretical results concerning the periodically corrugated waveguide in this thesis were discussed in both national and international conferences, and published in the proceedings of the conferences and in a journal. Below are the list of the names of the conferences we participated and discussed our results, and the name of the journal we published.

1. Pogrebnyak V.A., **Akray E**., Kucukaltun A.N., 2005. Tunable Gap in the Transmission Spectrum of a Periodic Waveguide. Applied Physics Letters (Appl. Phys. Lett), Vol. 86, pp. 151116-151118.
2. Pogrebnyak V.A., **Akray E**., Kucukaltun A.N., 2005. Tunable Electron Transport in the Lateral Nanostructure. Proceedings of 2005 NSTI Nanotechnology Conference & Trade Show, 8-13 May 2005, Anaheim, California, Vol. 3, pp. 61-63, Nano Science Technology Institute, U.S.A.
3. Pogrebnyak V.A., **Akray E**., Kucukaltun A.N., 2005. Ayarlanabilir Mikrodalga Filtresi Olarak Periyodik Oluklu Dalga Kılavuzu. TUBITAK National Metrology Institute, National Conference of 1st RF and Microwave Measurement, 26-28.09.2005.
4. Pogrebnyak V.A., Hasar U.C., Inan O. E., Eraslan T., **Akray E**., Kucukaltun A.N., 2004. 'Tunable Stop Bands in a Spectrum of Periodically Corrugated Waveguide.' URSİ-TÜRKİYE'2004 2nd National Congress, Bilkent University, Ankara, TURKEY, p.p. 48-50.

# 2. LITERATURE REVIEW

Because wave propagation in periodic structures has been of great interest, and many publications and studies are devoted from several and different field of physics and technology it is suitable to classify into special parts the following studies having been done up to now.

Abundance of publications and studies is also valid for the topic "wave in random/disordered media". Therefore, previous studies concerning this topic are classified in its respective part.

## 2.1. Wave in Periodic Structures

Periodic structures are abundant in nature and they have fascinated artists and scientists alike. When they interact with electromagnetic waves amazing features result. In particular, characteristics such as frequency stop-bands, pass-bands and band-gaps could be identified.

### 2.1.1. Theory of Wave Propagation in Periodic Structures

The dispersion properties and the fields of electromagnetic waves are investigated for propagation in a stratified infinite medium by Tamir (1964). The stratification is characterized by a dielectric constant which, along one coordinate, is modulated sinusoidally about an average value. A systematic and comprehensive study is presented for the case of H modes for which the pertinent wave equation is in the form of a Mathieu differential equation. The modes and dispersion characteristics are analyzed in terms of a "stability" chart, which is customary in the study of the Mathieu equation. Results are obtained for an unbounded medium and for a waveguide filled with the modulated medium. Also, the reflection occurring at an interface between free space and a semi-infinite medium of this type is examined. In addition to these rigorous results for arbitrary values of modulation, simple analytical expressions are given for all of these cases where the modulation in the dielectric is small. It is shown that the fields are then expressible in terms of the fundamental and the two nearest space harmonics. The fields within a unit cell in the stratified medium are calculated for both small and large modulation and for frequencies up through the second pass band. It is of interest that the variation of the fields is not, in general, simply related to the variation of the dielectric constant within a cell.

Richard (1983) describes and classifies the differential equations with periodically varying coefficients. Various methods of solution to this type of equations are proposed. In the last chapter, some of the systems, in the analysis of which should be applied for the solution of these equations, are involved. The features of periodically time-varying systems for practical use are outlined.

Theoretical analysis on the Bragg reflection characteristics of millimeter waves in a periodically plasma-induced semiconductor waveguide is presented by Matsumoto (1986). The plasma is assumed to be generated by light illumination. Numerical examples are given which show the dependence of the Bragg reflection characteristics on the length of the plasma-induced section and on the plasma density. Since the period can be changed by altering the illumination pattern, this type of periodic structure may be developed to tunable filters or tunable DBR oscillators for millimeter-wave region.

Ishimaru (1991) discusses the periodic structure which are used in many applications, such as optical gratings, phased arrays and frequency-selective surfaces. He starts with the Floquet-mode representation of waves in periodic structures. Guided waves along periodic structures and plane-wave incidence on periodic structures are discussed using integral equations and Green's function. An interesting question regarding the Rayleigh hypotesis for scattering from sinusoidal surface is discussed. Also included are the coupled-mode theory and co-directional and contra-directional couplers.

A general formulation for the characterization of corrugated waveguides is presented by Esteban et al (1991). The formulation is based on modal expansion in the different smooth-walled waveguides which constitute the corrugated structure and on the use of mode matching at discontinuities. The use of an admittance matrix formulation and a suitable root-finding algorithm leads to a rigorous and efficient technique. Dispersion curves are presented for corrugated waveguides of circular and rectangular cross sections. As predicted by other authors, complex modes have been obtained for deep corrugations. The effect of the finite thickness and width of teeth and slots on the dispersion behavior is also shown.

The transmission and reflection spectrum of the coupled-waveguide Bragg-reflection filter are computed by a new method by Weber (1993). The filter is based on the use of a Bragg grating to obtain contradirectional coupling between two dissimilar waveguides. The analysis shows that the tuning range should be similar to that of a simple Bragg grating filter, but with the advantage of having the output separated from the input. This device could also be used as a selective tap in a wavelength-division multiplexing System.

Mode coupling of Love waves in an orthotropic thin film having periodically corrugated surfaces over an isotropic elastic half space is considered by Hawwa (1994). Six modes are coupled by both surfaces by means of three simultaneous resonant conditions. On the basis of the weakness of the corrugations, the method of multiple scales is used to derive the coupled-mode equations. These equations together with relevant boundary conditions form a two-point boundary-value problem, which is solved numerically. The filter frequency response of a corrugated film designed as a stop-band filter is calculated. Enhanced filter characteristics are achieved when tapered corrugations are imposed. A narrow pass-band filter is also designed. Its high quality factor presents the fascinating features that might be realized by including the periodic corrugations in the design of SAW devices.

A polarization-independent narrow-band Bragg reflector based on a novel phase-shifted grating structure is proposed and analyzed by Huang et al (1996). Operation and design principles for the proposed grating structure as an polarization-independent optical filter are described. Robustness of the polarization-independent filter against modal birefringence and polarization effects in grating couplings and modal losses are examined and verified. Tunability of the polarization-independent filter is also studied and demonstrated.

A structure with two periodicities can couple up to six modes under a case of simultaneous resonance resulting in a stop-band interaction. The method of multiple scales is employed by Hawwa (1997) to analyze the modal coupling in a two-dimensional acoustic duct with rigid periodically undulated walls as well as in an elastic plate having periodically corrugated outerfaces, leading to the coupled-mode equations. The comparison between the three possible cases of interaction under simultaneous resonance are given in terms of the power reflection coefficient spectrum as a function of frequency. The strength of the stop-band interaction is found to be strongly related to the number of direct couplings between the incident and reflected modes.

The study of Asfar's (1997) concerns a rectangular waveguide embodiment of a recent invention of a narrowband waveguide filter concept. This concept is an outgrowth of work in the area of nonuniform periodic-structure waveguide filters using the perturbation method of multiple scales and a numerical method for the solution of stiff two-point boundary-value problems. These efforts were concerned with stop band filter characteristics of boundary periodic corrugations and the effect of periodic structure nonuniformities on controlling the filter frequency response. It was noted that techniques of antenna array analysis and synthesis, and particularly those concerned with controlling the radiation pattern of arrays, are directly applicable to periodic waveguide stopband frequency response. The current excitation of the antenna array elements, in both magnitude and phase, are analogous to the amplitude and phase of periodic corrugations. The spatial array current distributions are, by a one-to-one correspondence, similar to the spatial distribution of the corrugations so that the frequency response becomes similar in shape to the corresponding radiation pattern of the array. Of particular interest in the case is the analog of the difference mode radiation pattern of a phased array radar. This analogy is the narrow bandpass filter described in the sequel.

In the papers of Rahmat-Samii's (2001 and 2003), the objective is to provide an in-depth understanding of the EBG (Electromagnetic Band Gap) phenomena and present representative applications. Among the structures addressed in this presentation are: (a) FSS (Frequency Selective Surface) structures, (b) PBG

(Photonic Band Gap) crystals, (c) smart surfaces for communication antenna applications, (d) surfaces with perfectly magnetic conducting properties (PMC), (e) creation of materials with negative permittivity and negative permeability, (f) surfaces with reduced edge diffraction effects and (g) reduction of mutual coupling among array antenna elements. In the last several years, there have been numerous published conference papers and journal articles dealing with the characterizations and applications of EBG structures. The interested readers need to perform detailed literature search for up-to-date publications addressing this topic.

Pogrebnyak (2003) predicted the geometric resonance in a periodicaly corrugated waveguide. It is shown that for a change in thickness of the waveguide, at some of its value, one of the cut-off frequencies would split into two, seperated by the forbidden gap, while other cut-off frequencies experience only slight shifts due to the periodicity. The resonant splitting forms the single spectral line in the forbidden gap of the electromagnetic spectrum of the waveguide.

An analytical model for calculating the reflection and transmission coefficients of a Bragg reflector with periodic structure is reported by Purica et al (2003). Using explicit expressions for these coefficients the reflectivity of the periodic structures was simulated for different pairs of layer materials ($SiO_1$ /$Si_3$NN*poly-SU $SO_2$, SU airgap and SiOdAu) and layer thickness. The method allows the rapid evaluation of reflectance of Bragg reflector with periodic structure.

Wave phenomena in a planar periodically corrugated waveguide are investigated in detail by Pogrebnyak (2004). It is shown that the corrugations causes resonant interaction between the transverse modes (standing waves). The interaction results in the non-Bragg nature resonances, which divide the spectrum of the mode into the subminizones and give rise to Bragg reflections. The width of the non-Bragg gap as well as the Bragg gap depends on the relative position of two periodic plates. It varies from zero to a maximum value upon shifting one periodic plate with respect to another on the half period of the corrugation. When a frequency of the electromagnetic wave coincides with one of the gaps, only unidirectional propagation along grooves is allowed in the waveguide. Thus, the shift of the plates switches the two-dimensional guiding structure to the unidirectional guide and creates the photonic stripe phase in such a periodic waveguide.

### 2.1.2. Experimental Studies and Applications in Periodic Structures

Although we classify the publications as being experimental and application in this section most of them also contains theoritical part.

The theory and recent applications of waves in periodic structures are reviewed by Elachi (1976). Both the Floquet and coupled waves approach are analyzed in some detail. The theoretical part of the paper includes wave propagation in unbounded and bounded active or passive periodic media, wave scattering from periodic boundaries, source radiation (dipole, Cerenkov, transition, and Smith-Purcell) in periodic media, and pulse transmission through a periodic slab. The applications part covers the recent development in a variety of fields: distributed feedback oscillators, filters, mode converters, couplers, second-harmonic generators, deflectors, modulators, and transducers in the fields of integrated optics and integrated surface acoustics.

In the study of Yariv's (1977) the theory and device applications of periodic thin-film waveguides are dealt. Topics treated include mode solutions, optical filters, distributed feedback lasers (DFB), distributed Bragg reflector (DBR) lasers, grating couplers, and phase matching in nonlinear interactions.

Wave propagation along a rectangular waveguide with slowly varying width has been investigated with the help of field theory and approximate circuit theory by Mallick and Sanyal (1978). In the field theory approach, two different methods of analysis have been attempted. Many properties of the modulated periodic structure, e.g., the frequency dependence of the propagation constant, group and phase velocities and the electric field axial variation for the fundamental space harmonic and its filter-like property have been investigated. The magnetic field lines on the H-plane for a typical case exhibit an expected configuration. Experimental results show close agreement with analysis. It is concluded that this structure supports the fast fundamental space harmonic.

A planar dielectric waveguide having finite periodic rectangular corrugation is investigated analytically and experimentally, in case of surface waves propagating at an angle to the corrugation by Tsuji (1983). In analytical considerations, a finitely corrugated guide is regarded as consisting of many step discontinuities connected by a length of uniform slab waveguide, and its propagation characteristics in the Bragg interaction region are derived from a cascaded connection of the transmission matrix expressing a step discontinuity. Although the present method takes only surface wave modes into account and neglects the wave with continuous spectrum, the calculated results show an excellent agreement with experimental ones which are performed for art H-guide in the microwave region.

In the paper of Tsuji's (1983), a dielectric waveguide with finite corrugation in length is investigated analytically and experimentally, in a case of surface waves propagating at an angle of the corrugation. In analytical considerations, a partially corrugated guide is regarded as consisting of many step discontinuities connected by a length of uniform slab waveguide, and its propagation characteristics in the Bragg interaction region are derived from a cascaded connection of the transmission matrix expressing a step discontinuity.

The waveguide properties of periodic waveguide structures on 112˚-$LiTaO_3$ are studied experimentally and theoretically at frequencies close to the Bragg stopband by Hratmann et al (1995). On admittance curves of long transducer type test structures it is seen that additional attenuation appears at both the high and low frequency sides of the stopband in that the resonances at these frequencies are suppressed. In addition, strong spurious resonances are seen in the lower half of the stopband region. Direct laser probe measurements have shown that the amplitude distribution in the transverse direction across the waveguide changes significantly versus frequency. Propagation ranges from (a) weak single mode guiding at low frequency to (b) strong multi-mode guiding near the lower stopband frequency then (c) a region without any guided modes and strong side radiation near the upper stopband frequency and (d) a return to weak single mode guiding at frequencies well above the stopband.

Lin et al (2001) demonstrate a long-period fiber grating composed of an etched corrugated structure that can be used as a wavelength- and loss-tunable band-rejection filter. The tunabilities are based on the index modulation capable of being varied in the corrugated structure under externally applied mechanical forces. The new type of fiber filter enables wavelength and loss tuning ranges of more than 40 nm and 25 dB by adjusting the applied amounts of torsion and tensile forces, respectively.

A numerical model based on a scalar beam propagation method is applied to study light transmission in photonic bandgap (PBG) waveguides by Abeeluck (2002). The similarity between a cylindrical waveguide with concentric layers of different indices and an analogous planar waveguide is demonstrated by comparing their transmission spectra that are numerically shown to have coinciding wavelengths for their respective transmission maxima and minima. Furthermore, the numerical model indicates the existence of two regimes of light propagation depending on the wavelength. Bragg scattering off the multiple high-index/low-index layers of the cladding determines the transmission spectrum for long wavelengths. As the wavelength decreases, the spectral features are found to be almost independent of the pitch of the multi-layer Bragg mirror stack. An analytical model based on an antiresonant reflecting guidance mechanism is developed to accurately predict the location of the transmission minima and maxima observed in the simulations when the wavelength of the launched light is short. Mode computations also show that the optical field is concentrated mostly in the core and the surrounding first high-index layers in the short-wavelength regime while the field extends well into the outermost layers of the Bragg structure for longer wavelengths. A simple physical model of the reflectivity at the core/high-index layer interface is used to intuitively understand some aspects of the numerical results as the transmission spectrum transitions from the short- to the long-wavelength regime.

Mizrahi et al (2003) demonstrate that a planar Bragg reflection waveguide consisting of a series of dielectric layers may form an acceleration structure. It is shown that an interaction impedance per wavelength of over l00Ω is feasible with existing materials, Silica ($\varepsilon = 2.1$) and Zirconia ($\varepsilon = 4$), and if materials of high dielectric coefficient become available in the future. They may facilitate an interaction impedance per wavelength closer to 500 Ω

Zhang et al (2003) design and analyze a periodic dielectric Bragg grating waveguide temperature sensor ranging from room temperature to over 1200˚C. By using this sensor combined with a wavelength shifting detector and radiation detection schemes, a wide range thermometer can be built. Temperature can be measured in two ways using the thermal sensor. This sensor has many applications including in aerospace structures.

Yang (2005) investigates the two microstrip line periodic structures respectively loaded with capacitance and resonant elements. The theoretical analyses describe the difference of the two bandgaps happening to the resonant elements loaded periodic structure. From the k-p diagrams, it is found that the stopband obeying Bragg's law can be enhanced by increasing the capacitance in the loads. Based on the theory, both the capacitively loaded and resonant elements loaded periodic structures are realized in two-layer microstrip lines. The equivalent LC values are extracted with quasi-static method, and they are used for circuit optimization, Besides this, the method to improve the bandstop performance is proposed and validated theoretically and experimentally.

### 2.1.3. Photonic Crystals

Photonic crystals are periodic structures that can reflect electromagnetic (EM) waves in all directions within a certain frequency range. These structures can be used to control and manipulate the behavior of EM waves.

Yariv (1973) introduces the coupled-mode theory. The problem of propagation and interaction of optical radiation in dielectric waveguides is cast in the coupled-mode formalism. This approach is useful for treating problems involving energy exchange between modes. A derivation of the general theory is followed by application to the specific cases of electrooptic modulation, photoelastic and magnetooptic modulation, and optical filtering. Also treated are nonlinear optical applications such as second-harmonic generation in thin films and phase matching.

Economou and Zdetsis (1989) considered a muffin-tin periodic potential ( $-\delta$ inside the spheres and zero outside), and reported results based on a systematic study of bands and gaps in periodic configurations of spheres (in the results reported here the periodic lattice was fcc; however, they made calculations for the bcc structure as well with similar results). Using the augmented-plane-wave method they systematically studied the location of gaps for positive energy and for various values of $\delta$ and the sphere $a$. The results are applicable to the problem of classical-wave propagation in composite media and relevant to the problem of optical localization.

Ho et al (1990) report calculations for the photonic band structure of periodic arrangements of dielectric spheres in the fcc and diamond structures. Expanding the EM fields with a plane-wave basis set, they solve Maxwell's equation exactly, taking the vector nature of the EM field fully into account. Comparasion of the calculational results of the fcc structure with experiment indicates that while the experimental data and theory agree well over most of Brillouin zone, there are two symmetry points ($W$ and $U$) where the experiment indicates a gap while calculations show that propagating modes exist. They believe the fcc structure exhibits a pseudogap rather than a full photonic band gap exists over most, but not all, of the Brillouin zone, resulting in a region of low density of dtates rather than a forbidden frequency gap. On the other hand, it is found that the diamond dielectric structure does possess a full photonic band gap. This gap exists for refractive-index contrast as low as 2.

By the use of a position-dependent dielectric constant and the plane-wave method, Plihal and Maradudin (1991) have calculated the photonic band structure for electromagnetic waves in a structure consisting of a periodic array of parallel dielectric rods of circular cross section, whose intersections with a perpendicular plane form a triangular lattice. The rods are embedded in a background medium with a different dielectric constant. The electromagnetic waves are assumed to propagate in a plane perpendicular to the rods, and two polarizations of the waves are considered. Absolute gaps in the resulting bands structures are found for waves of both polarizations, and the dependence of the widths of these gaps on the ratio of the dielectric constants of the rods and of the bacground, and on the fraction of the total volume occupied by the rods, is investigated.

Using a plane-wave expansion method Datta et al (1992) have computed the band structure for a scalar wave propagating in periodic lattices of dielectric spheres (dielectric constant $\varepsilon_a$) in a uniform dielectric background ($\varepsilon_b$). All of the lattices studied (simple cubic, bcc, fcc, and diamond) do possess a full band gap. The optimal values of the filling ratio $f$ of spheres and of the relative dielectric constant for the existence of a gap are obtained. The minimum value of the relative dielectric constant for creating a gap is also obtained. These results are applicable to the problem of the classical wave-propagation in composite media and relavant to the problem of classical-wave localization.

In the paper of Villeneuve et al (1992), it is shown that two-dimensional square and hexagonal lattices generate photonic band gaps common to both polarizations. they examine two structures: (a) one consisting of long parallel rods of square cross section whose centers lie at the corners and center of a regular hexagon (or equivalently at the corners of a regular triangle). In structure (b), the rods are just touching when their filling fraction is 91 %; this corresponds to the close-packed condition. When the filling fraction is larger than 91 % the rods overlap. In both structures, the refraction index of the background may be greater than that of the rods in cylindrical holes in a dielectric material, or maybe less as in dielectric loss in air. Although the material of low index need not be air,

Villeneuve et al (1992) discussed that periodic arrays of rods with either a square or circular cross section located at the corners of a square lattice exhibit photonic band gaps common to $s$ and $p$ polarizations. The overlap of $s$ and $p$ gaps is generated in arrays of low-index rods embedded in a dielectric background of higher index. The overlap does not occur between the same bands in arrays of rods with a square cross section and a circular cross section. Arrays of rods with a circular cross section require a lower index contrast to generate a band gap than rods with a square cross section, but do not necessarily yield larger gaps at higher index contrasts.

The photonic band structure in a two-dimensional dielectric array is investigated using the coherent microwave transient spectroscopy (COMITS) technique by Robertson et al (1992). The array consists of alumina-ceramic rods arranged in a regular square lattice. The dispersion relation for electromagnetic waves in this photonic crystal is determined directly using the phase sensitivity of COMITS. The experimental results are compared to theoritical predictions obtained using the plane-wave expansion technique. Configurations with the electric field parallel and perpendicular to the axis of the rods are investigated.

Using the transfer-matrix method, Sigalas et al (1994) calculate the transmisson coefficient versus the frequency of the incident electromagnetic waves propagating in photonic-band-gap structures constructed from dispersive and highly absorbing materials. They study how the band gaps are affected by the presence of polariton gaps and/or absorbtion. Also, the possible difficulties of their experimental investigation are discussed.

Chan et al (1994) considered both dielectric rods in air background, and the inverse structures with air rods in a high dielectric background. They found that a whole class of structures with rhombohedral symmetry possesses sizeble photonic gaps. These structures can be generated by connecting lattice points in A7 structure by cylinders and a few structures that are known to possess photonic band gaps are in fact members of this "parent" structure. This class of structures also allows the authors to explore more systematically the criteria favorable for gap formation.

Sigalas et al (1995) calculate the transmission and absorbtion of electromagnetic waves propagating in two-dimensional (2D) and 3D periodic metallic photonic band-gap (PBG) structures. For 2D systems, there is substantial difference between the *s*- and *p*-polarized waves. The *p*-polarized waves exhibit behaviour similar to the dielectric PBG's. But, the *s*-polarized waves have a cutoff frequency below which there are no propagating modes. For 3D systems, the results are qualitatively the same for both polarizations but there are important differences related to the topology of the structure. They also study the role of the defects in the metalic structures.

Scalora et al (1996) examine optical pulse propagation through a 30-period, GaAs/AlAs, one-dimensional, periodic structure at the photonic band-edge transmission resonance. It is predicted that theoretically—and demonstrate experimentally—an approximate energy, momentum, and form invariance of the transmitted pulse, as well as large group index (up to 13.5). The group index is tunable and many orders of magnitude more sensitive to variation in material refractive index than for bulk material. They interpret this observation in terms of time dependent electromagnetic states of the pulse-crystal system.

Li et al (1996) study theoretically the propagation of electromagnetic waves through periodic structures consistent of layered materials with an intensity-dependent dielectric constant. They find the transmission properties to be strongly modulated by both frequency and intensity in the presence of nonlinearity. The transmission diagram in the frequency versus amplitude plane exhibits distinctive features depending upon whether the Kerr coefficient is positive or negative. These features, though complicated, can be understood through the analysis of stable periodic orbits of the corresponding nonlinear mapping. These systems exhibit bistability and multistability most strongly near the upper band edges and between the basins of stable periodic orbits. Resonance transmissions via soliton formation are analyzed through a simple mechanical analogy. They also discuss the switching threshold and the feasibility of making a switch utilizing such a structure.

The first experimentally observed ultrasonic full band gap in periodic bidimensional composites for the longitudinal wave mode is described in Montero de Espinosa's et al (1998) paper. The structure consists of an aluminum alloy plate with a square periodic arrangement of cylindrical holes filled with mercury. No propagation wave exists at the frequency range between 1000–1120 kHz irrespective of the measurement direction. The experiment was performed by means of an ultrasonic transmission technique, and a measurement of the position dependence of the acoustic amplitude was also performed.

The idea of the linear combination of atomic orbitals method, well known from the study of electrons, is extended to the classical wave case by Lidorikis et al (1998). The Mie resonances of the isolated scatterer in the classical wave case are analogous to the atomic orbitals in the electronic case. The matrix elements of the two-dimensional tight-binding (TB) Hamiltonian are obtained by fitting to ab initio results. The transferability of the TB model is tested by reproducing accurately the band structure of different 2D lattices, with and without defects, and at two different dielectric contrasts.

The reflection properties of gratings, such as those found in the core of an optical fiber, previously have been interpreted in terms of evanescent or propagating wave behavior in different parts of the grating by Sterke (1998). According to this interpretation, nonuniform gratings can thus be understood in a similar way to one-dimensional quantum well structures. He exploits this similarity to develop an analytic theory for deep Bragg superstructure gratings. Using a method similar to the tight-binding method from condensed matter physics, the author finds approximate analytic expressions for the high- and low-reflectance frequency regions of such gratings.

Sigalas et al (1998) study the transmission of electromagnetic waves propagating in two-dimensional photonic crystals having triangular structure. The transmission has been calculated using the transfer matrix method. They find that for dielectric constant ratios higher than 12.25, there is a full photonic band gap for both polarizations and for out-of-plane incident angle as high as 85°.

Lourtioz et al (1999) present several experimental and theoretical studies showing the feasibility of active photonic crystals controlled either by electrical elements or by light. The controllability of photonic crystals at centimeter wavelengths is proposed with the periodic insertion of diodes along the wires of a two-dimensional (2-D) metallic structure. For only three crystal periods with commercially available devices, more than 30 dB variations of the crystal transmission are predicted over a multigigahertz range by switching the diodes. From calculation models, a tight analogy is shown between these crystals and those consisting of discontinuous metallic rods with dielectric inserts. The numerical models as well as the proposed technology are validated by experimental measurements on 2-D crystals with either continuous or discontinuous metallic rods. The partial control of a 3-D layer-by-layer dielectric structure at millimeter wavelengths is also demonstrated in the second part of the work. A laser light is used to modulate the transmission level of defect modes by photo-induced free carrier absorption. The overall results are expected to contribute to further devopments of switchable electromagnetic windows as well as to tunable waveguide structures in the microwave and millimeter wave domains.

For the first time, it is shown that the transmittivity of wave guides created as rectilinear defects in periodic elastic band-gap materials oscillates as a function of frequency by Kafesaki et al (2000). The results are obtained using the finite difference time domain method for elastic waves propagating in two-dimensional inhomogeneous media. The oscillations of the transmittivity are due to the richness of modes in the elastic systems and, mainly, due to the periodicity of the potential in the direction of the wave propagation. Results are presented for a periodic array of Pb and Ag cylinders inserted in an epoxy host, as well as for Hg cylinders in an Al host.

García-Pablos et al (2000) study elastic band gaps in nonhomogeneous periodic finite media. The finite-difference time domain method is used for the first time in the field of elastic band-gap materials. It is used to interpret experimental data for two-dimensional systems consisting of cylinders of fluids (Hg, air, and oil) inserted periodically in a finite slab of aluminum host. The method provides good convergence, can be applied to realistic finite composite slabs, even to composites with a huge contrast in the elastic parameters of their components, and describes well the experiments.

El-Kady et al (2000) theoretically study three-dimensional metallic photonic-band-gap (PBG) materials at near-infrared and optical wavelengths. The main objective of the paper is to find the importance of absorption in the metal and the suitability of observing photonic band gaps in this structure. For that reason, the authors study simple cubic structures and the metallic scatterers are either cubes or interconnected metallic rods. Several different metals have been studied (aluminum, gold, copper, and silver). Copper gives the smallest absorption and aluminum is more absorptive. The isolated metallic cubes are less lossy than the connected rod structures. The calculations suggest that isolated copper scatterers are very attractive candidates for the fabrication of photonic crystals at the optical wavelengths.

Temelkuran et al (2000) report on fabrication of a layer-by-layer photonic crystal using highly doped silicon wafers processed by semiconductor micromachining techniques. The crystals, built using (100) silicon wafers, resulted in an upper stop band edge at 100 GHz. The transmission and defect characteristics of these structures were found to be analogous to metallic photonic crystals. They also investigated the effect of doping concentration on the defect characteristics. The experimental results agree well with predictions of the transfer matrix method simulations.

Propagation of electromagnetic waves through a two-dimensional triangular lattice has been studied for different values of refractive index contrast between the constituent dielectrics, and for angles of incidence both in and out of the plane of periodicity by Foteinopoulou et al (2000) . Transmission results have been obtained both experimentally and with the transfer matrix technique, and good agreement has been found between the two. Comparison with band structure calculations has also been made.

In the research of Li's et al (2000), a different application concept: using low index contrast 2-D photonic crystal has been investigated. A further study of a superprism phenomenon, which demonstrated an ultra-high dispersion ability possessed by photonic crystal tells that this unique dispersion ability does not require a complete band gap. The dispersion curve ($\omega - k$ curve) of Bloch states folds back into Brillouin zone at every time when wavevector $k$ reaches its edge. In 2-D crystal, it is dispersion surface that folding effect generates band-gap when the lattice possesses large enough index contrast. Each time dispersion curve folds back, anisotrophy of lattice itself is imbedded into the dispersion curve of nextband. During the multiple folding of Bloch state at the edge of Brillouin zone, this anisotrophy is accumulated. One can image that as far as the lattice structure exists, a superprism effect could exist. The advantages of using low index-contrast crystal are that we can avoid scattering issue when trying to build planar waveguide structure by thin thickness of 2-D photonic crystal, so that a waveguide superprism device can be realized. Along with this, the fabrication of low index-contrast 2-D lattice will be much easier than those conventional crystals with complete band gap.

The transverse-magnetic photonic-bandgap-guidance properties are investigated for a planar two-dimensional (2-D) Kagomé waveguide configuration using a full-vectorial plane-wave-expansion method by Nielsen et al (2000). Single-moded well-localized low-index guided modes are found. The localization of the optical modes is investigated with respect to the width of the 2-D Kagomé waveguide, and the number of modes existing for specific frequencies and waveguide widths is mapped out.

Bayındır et al (2001) report experimental observation of a full photonic band gap in a two-dimensional Penrose lattice made of dielectric rods. Tightly confined defect modes having high quality factors were observed. Absence of the translational symmetry in Penrose lattice is used to change the defect frequency within the stop band. They also achieved the guiding and bending of electromagnetic waves through a row of missing rods. Propagation of photons along highly localized coupled-cavity modes is experimentally demonstrated and analyzed within the tight-binding approximation.

A planar photonic crystal waveguide based on the semiconductor-on-insulator (SOI) materials system is analyzed theoretically by Søndergaard et al (2002). Two-dimensional (2-D) calculations and comparison with dispersion relations for the media above and below the finite-height waveguide are used to obtain design guidelines. Three-dimensional (3-D) calculations are given for the dispersion relations and field profiles. The theoretically predicted frequency intervals, where the waveguide supports leakage-free guidance of light, are compared with an experimental measurement for propagation losses. Two out of three frequency intervals coincide with low-measured propagation losses. The poor guidance of light for the third frequency interval is explained theoretically by investigating the vertical localization of the guided modes.

Bayındır et al (2002) propose and demonstrate a type of composite metamaterial which is constructed by combining thin copper wires and split ring resonators (SRRs) on the same board. The transmission measurements performed in free space exhibit a passband within the stop bands of SRRs and thin wire structures. The experimental results found are in good agreement with the predictions of the transfer matrix method simulations.

Using a three-dimensional finite-difference time-domain method, Kafesaki et al (2004) present an extensive study of the losses in two-dimensional (2D) photonic crystals patterned in step-index waveguides. They examine the origin of these losses and their dependence on the various system parameters such as the filling ratio, the lattice constant, the shape of the holes, and the propagation direction. Furthermore, the authors examine the possibility of studying these losses using an approximate 2D model; the validity and limitations of such a model are discussed in detail.

Moussa et al (2005) experimentally and theoretically studied a left-handed structure based on a photonic crystal sPCd with a negative refractive index. The structure consists of triangular array of rectangular dielectric bars with dielectric constant 9,61. Experimental and theoretical results demonstrate the negative refraction and the superlensing phenomena in the microwave regime. The results show high transmission for the structure for a wide range of incident angles. Furthermore, surface termination within a specific cut of the structure excite surface waves at the interface between air and PC and allow the reconstruction of evanescent waves for a better focus and better transmission.

Koschny et al (2005) study the frequency dependence of the effective electromagnetic parameters of left-handed and related metamaterials of the split ring resonator and wire type. It is shown that the reduced translational symmetry speriodic structured inherent to these metamaterials influences their effective electromagnetic response. To anticipate this periodicity, a periodic effective medium model is formulated which enables to distinguish the resonant behavior of electromagnetic parameters from effects of the periodicity of the structure. They use this model for the analysis of numerical data for the transmission and reflection of periodic arrays of split ring resonators, thin metallic wires, cut wires, as well as the left-handed structures. The analysis shows that the periodicity of the structure can be neglected only for the wavelength of the electromagnetic wave larger than 30 space periods of the investigated structure.

Weiss et al (2006) study the distribution of resonance widths $P(\Gamma)$ for three-dimensional (3D) random scattering media and analyze how it changes as a function of the randomness strength. The authors are able to identify in $P(\Gamma)$ the system inherent fingerprints of the metallic, localized, and critical regimes. Based on the properties of resonance widths, they also suggest a criterion for determining and analyzing the metal-insulator transition. The theoretical predictions are verified numerically for the prototypical 3D tight-binding Anderson model.

### 2.2. Wave in Random Media

The following two studies show the behaviour of wave in random media generally. In the subsections, random media are classified into such parts as scattering from rough surfaces, wave behaviour in a waveguide having random/rough surfaces. And also localization part is needed to add because the general behaviour of waves is explained by localization phenomenon in disordered media.

A novel theory is developed by Ogura (1975) to cope with the difficulty of the multiple-scattering problem in a random medium (RM). The theory is given for a one-dimensional homogeneous RM which is represented by a strictly stationary random process. Some possible forms of the stochastic solution are determined by a group-theoric consideration based on the shift-invariance property of the homogeneous RM. It is shown that there are two kinds of solutions in one-dimensional RM: a travelling-wave mode and a cutoff mode. For a Gaussian RM with small fluctuation, an approximate stochastic solution given in the possible form is obtained in terms of multiple Wiener integrals with respect to the Brownian-motion process. The law of large numbers is shown to hold concerning the fluctuarions of the phase and amplitude. The average value of the wave and the transmission coefficient of a medium with finite thickness are also studied using the stochastic solution.

Edrei et al (1989) present a new numerical method for calculating the interference phenomena for waves propagating through random media. The model is applied to calculate probability distribution functions for the transmission $P(T)$ in one and two dimensions, $T$ being the transmission coefficient. The model reproduces the analytical predictions for one dimension, and yields new results for two-dimensional systems. The distribution function $P(T)$ in two dimensions, in the diffusive regime, is found to be close to a Gaussian with a variance proportional to the mean, in agreement with the results of diagrammatic calculations. A crossover of the distribution to log-normal behaviour typical for strong localization is obtained.

### 2.2.1. Scattering of Waves by Rough Surfaces

Field scattering by rough surface has been of interest due to its applications in radar and communications. Recent years have seen the development of robust and efficient numerical techniques for exact calculations of rough surface scattering. In the below paragraphs one can find many kinds of solution of wave scattering in rough surface and the applications.

A one-dimensional random rough surface is modeled by Brockelman and Hagfoors (1966) as a Gaussian noise signal. The effect of shadowing in the case of backscattering of waves from such a surface is studied in the geometic optic limit by analyzing the Gaussian noise signal in a digital computer. It is found that presently accepted theories for the shadowing effect are of doubtful validity.

It has often been suggested in lunar studies that measurements of radar cross-polarization factor *D* should yield information on the target's surface roughness and dielectric properties. The paper of Krishen et al (1966) describes an experimental effort to obtain quantitative data on $\langle D \rangle$, the average value of *D,* for randomly rough targets having Gaussian distribution of slopes. The dependence of $\langle D \rangle$ on various parameters is shown graphically, and extension to M.I.T. data of lunar crosspolarization is discussed.

Specular point densities for several models of randomly rough surfaces with a Gaussian height distribution are derived by Seltzer (1972). Both area densities and volume densities conditioned by the surface height variate and surface curvatures are obtained. Several shadowing functions are compared with digital computer simulation results, and the application of the slope conditional shadowing function as a modifying factor for specular point densities is described.

A one-dimensionally rough random surface with known statistical properties was generated by Axline and Fung (1978) by digital computer. This surface was divided into many segments of equal length. The moments method was applied to each surface segment assuming perfect conductivity to compute the induced surface current and subsequently the backscattered field due to an impinging plane wave. The return power was then calculated and averaged over different segments. Unlike numerical computations of scattering from deterministic surfaces, problems of stability and convergence of the solution existed for random surface scattering. It was shown that the stability of the numerically computed estimate of the backscattered average power depends on *N,* the total number of disjoint surface segments averaged; $\Delta x$, the spacing between surface current points: *D,* the width of each surface segment; and *g,* the width of the window function. Relations were obtained which help to make an appropriate choice of these parameters.

An analytical approach to the problem of scattering by composite random surfaces is presented by Brown (1978). The surface is assumed to be Gaussian so that the surface height can be split (in the mean-square sense) into large ($\zeta_l$) and small ($\zeta_s$) scale components relative to the electromagnetic wavelength. A first-order perturbation approach is used wherein the scattering solution for the large-scale structure is perturbed by the small-scale diffraction effects. The scattering from the large-scale structure (the zeroth-ors perturbation solution) is treated via geometrical optics since $4k_{O^2}\overline{\zeta l^2} \gg 1$. For a given surface height spectrum, this wavenumber can be determined by a combination of mathematical and physical arguments.

Explicit expressions are presented for the radiation fields scattered by rough surfaces by Bahar and Rajan (1979). Both electric and magnetic dipole sources are assumed, thus excitations of both vertically and horizontally polarized waves are considered. The solutions are based on a full-wave approach which employs complete field expansions and exact boundary conditions at the irregular boundary. The scattering and depolarization coefficients are derived for arbitrary incident and scatter angles. When the observation point is at the source these scattering coefficients are related to the backscatter cross section per unit area. Solutions based on the approximate impedance boundary condition are also given, and the suitability of these approximations are examined. The solutions are presented in a form that is suitable for use by engineers who may not be familiar with the analytical techniques and they may be readily compared with earlier solutions to the problem. The full-wave solutions are shown to satisfy the reciprocity relationships in electromagnetic theory, and they can be applied directly to problems of scattering and depolarization by periodic and random rough surfaces.

Full-wave solutions are derived by Bahar (1980) for the scattered radiation fields from rough surfaces with arbitrary slope and electromagnetic parameters. These solutions bridge the wide gap that exists between the perturbational solutions for rough surfaces with small slopes and the quasi-optics solutions. Thus it is shown, for example, that for good conducting boundaries the backscattered fields, which are dependent on the polarization of the incident and scattered fields at low frequencies, become independent of polarization at optical frequencies. These solutions are consistent with reciprocity, energy conservation, and duality relations in electromagnetic theory. Since the full-wave solutions account for upward and downward scattering, shadowing and multiple scatter are considered. Applications to periodic structures and random rough surfaces are also presented.

The study of Eom et al (1983) provides a comparison between the backscattering coefficients computed using Gaussian versus non-Gaussian surface statistics. The computation are performed for a class of surface height distributions and surface correlation functions.

Maystre (1983) introduced a rigorous integral formalism for the problem of scattering of electromagnetic radiation from a cylindrical, perfectly conducting rough surface of arbitrary shape. The computer code obtained from this theory enables him to show that the range over which the incident field affects the surface current density is of the order of the radiation wavelength. This phenomenon is explained using a new approximate theory, able to express the scattered field in the form of an integral whose integrand is known in closed form. Using the rigorous computer code, he shows that the new approximate theory is better than the Kirchhoff approximation in the resonance region. Finally, it is shown that the phenomenon of short interaction range of the incident field permits the rigorous computation of the field scattered from a rough surface of arbitrary width.

Bahar and Fitzwater (1984) use the full wave approach to determine the scattering cross sections for composite models of non-Gaussian rough surfaces. In particular, it is assumed here that the rough surface is characterized by a family of joint height probability densities that have been developed by Beckmann (IEEE Trans. Antennas Propagat., AP-21(2), 169-175, 1973) for non-Gaussian surfaces. These joint height probability densities are expressed as an infinite sum of powers of the correlation coefficient and it is assumed that decorrelation of surface heights implies statistical independence. Using these joint probability density functions Beckmann derives physical optics and geometrical optics approximations for the scattering cross sections.

By means of the Wiener-Hermite (W-H) expansion, Meecham and Lin (1987) are able to represent stochastic field functions using the Gaussian reflecting surface as the basic element. They include three terms. Multiple reflection effects are visible, even for these low-order terms in the expansion. Such reflections can be expected to greatly enhance backscatter at near grazing incidence.

The scattering of electromagnetic and acoustic waves by rough surfaces is studied by Varadan et al (1988) when either the Dirichlet or the Neumann boundary condition prevails. The facet- ensemble method is used to compute the field scattered by rough surfaces. In the present method, the scattering surfaces are modeled by an ensemble of flat facets and, consequently, the scattered field is expressed as a sum of specularly reflected and diffracted fields. The reflected field can be calculated by applying the laws of reflection and refraction. The uniform theory of diffraction (UTD) is used to solve the diffracted field from convex wedges on the surface. The surface models examined are periodic in one instance and random gaussian in the other. The comparison between results from the facet ensemble method and experimental data is good for both types of surfaces.

A numerical method is developed to simulate electromagnetic wave scattering from computer-generated two-dimensional (the surface height varies only with one of the coordinates) randomly rough surfaces by Wu et al (1988). The rough surface generated for scattering simulation is specified only up to the second moment statistics, i.e., the height distribution and the autocorrelation function. The coherent and noncoherent scattering from four different types of random surfaces are examined.

Louza et al (1989) suggest one method of expressing the surface shape is statistically, and in this work the rough surface is described first by Markov chain. The surface heights correspond to the states in the stochastic matrix. They also generated a number of Gaussian surfaces with the same statistical properties as those of the Markov chain. Thus, they have two sets of rough surfaces, one according to Markov chain and the other follows Gaussian distribution. Using ray tracing, the scattered fields by these surfaces are calculated and compared.

Hill (1989) derives first-order results for the reflection coefficient of a waveguide with slightly uneven walls. Specific analytical and numerical results are given for rectangular waveguides and coaxial transmission lines. Simple upper bounds are given for reflection coefficients in terms of the maximum deviation of the waveguide. For typical tolerances the reflection coefficients are very small $\left(<10^{-3}\right)$ but the results are important in precise six-port measurements.

In the work of Louza and Audeh's (1990) the rough surfaces consist of piecewise linear segments or facets having random slopes and variable horizontal projections. Such surfaces are described by the Markov chain and the surface heights correspond to the states in the stochastic matrix. A number of Gaussian surfaces with the same statistical properties as those of the Msrkow surfaces are generated. Thus, there are two sets of rough surfaces, one according to Markov chain and the other follows Gaussian distribution. Using ray tracing, the horizontally polarized field scattered by these surfaces are calculated and compared.

Broschat et al (1990) propose a heuristic algorithm for the bistatic radar cross section for random rough surface scattering based on the phase perturbation approximation. The algorithm satisfies reciprocity, and the results, using a Gaussian roughness spectrum, are superior to those of the original phase perturbation method.

Full wave expressions for the singly and the doubly scattered electromagnetic fields from one dimensional rough surfaces are computed by Bahar and El-Shenawee (1991). The singly scattered like and cross polarized fields are expressed in terms of one dimensional integrals. However the doubly scattered full wave solutions are expressed in terms of two and three dimensional integrals. To compute the like and the cross polarized multiple scattered fields it is necessary to use a supercomputer. The results indicate that the double scatter in the backward direction is significant for near normal incidence when the mean square slopes of the highly conducting rough surfaces are larger than unity.

Yang and Broschat (1992) calculate Bistatic radar cross sections using two modern scattering models: the small slope approximation (both first- and second-order) and the phase perturbation technique. The problem is limited to scalar-wave scattering from two-dimensional, randomly rough Dirichlet surfaces with a Gaussian roughness spectrum. Numerical results for the cross sections are compared to those found using the classical Kirchoff, or physical optics, approximation and perturbation theory. Over a wide range of scattering angles, the new results agree well with the classical results when the latter are considered to be accurate. A comparasion between the new results shows that the phase perturbation method gives better results in the backscattering region for correlation lengths greater than approximately one wavelength, while both the first- and second-order small slope approximations yield greater accuracy in the forward scattering direction at low grazing angles.

A new full wave method is developed by Collin (1992) for scattering from a perfectly conducting rough surface. The new method does not make use of the telegraphist's equations, and takes into account the two-dimensional roughness of the surface from the start. It is shown that the scattering coefficients obtained agree with those given in earlier work. The full wave solutions are also compared with the first-order perturbation solutions, the Kirchhoff-type solutions, and integral equation results.

The Neumann expansion has been used to compute the solutions of the magnetic field integral equation (MFIE) for two-dimensional, perfectly conducting, Gaussian rough surfaces by Wingham and Devayya (1992). For surfaces whose roughness is of a similar order to the incident wavelength, it is shown that the expansion may diverge rapidly. The rate of convergence is compared with the conjugate-gradient (CG) method, whose convergence is sure. When it converges, the Neumann expansion convergence is more rapid. It is concluded that the Neumann expansion is not suitable without qualification as a numerical solution to the rough surface MFIE. Moreover, the failure of the Neumann expansion of the solution of the discrete representation of the MFIE provides strong evidence that the use of the Neumann expansion as a formal solution to the MFIE is open to doubt.

The accuracy of the phase perturbation approximation for scattering from a multiscale Pierson-Moskowitz sea surface is examined by Broschat (1993) for large angles of incidence and wind speeds of 10 and 20 m/s in the paper. Numerical results for the incoherent bistatic radar cross section and the coherent reflection loss are compared with exact integral equation results. The study is limited to scalar-wave scattering from one-dimensional surfaces with Gaussian surface statistics for the Dirichlet problem. It is found that, for the examples studied, the phase perturbation bistatic radar cross section is accurate away from low scattered grazing angles. In addition, it contains approximations to higher order classical perturbation cross section terms that partially account for the incoherent intensity structure in the specular region. Finally, the phase perturbation approximation accurately predicts the coherent reflection loss.

The bistatic scattering cross sections are derived by Bahar (1993) for rough one-dimensional perfectly conducting surfaces using the full wave approach. The surfaces are characterized by four-dimensional Gaussian joint probability density functions for heights and slopes. Thus correlations between the rough surface heights and slopes are accounted for in the analysis. Convergence of the formal series solution is considered. Self-shadowing effects are included. The full wave solutions are compared with the small perturbation solutions, which are polarization dependent, and the specular point (physical optics) solutions, which are independent of polarization. Both the physical optics and the small perturbation solutions can be obtained from the full wave solution.

Ishimaru (1993) et al present analytical and experimental studies on the time-dependent scattering from one-dimensional rough surface. The scattering of a Gaussian beam pulse from a rough surface is investigated analytically using the tangent plane approximation. The two-frequency mutual coherence function is then derived from the scattered field using a stationary phase method. The pulse broadening arid lateral spread for different surface roughnesses and observation ranges are obtained from the analytical results. In the experimental study, the scattering of a wide-band pulse from very. rough surfaces is investigated. The frequency coherence functions as a function of observation angles are derived from scattering cross sections obtained from controlled scattering experiments using a wide-band millimeter wave scatterometer (75-100 GHz). Numerical Monte Carlo simulations are compared with the experimental results showing good agreement.

Using the full wave approach, integral expressions for the double scattered radar cross sections are given by E. Bahar and El-Shenawee (1993). The rough surface is assumed to be characterized by a Gaussian joint probability density function for the surface heights and slopes at two points. The surface height autocorrelation function and its Fourier transform (the rough surface spectral density function) are also assumed to be Gaussian. It is shown that enhanced backscatter is due to double scatter when the rough surfaces mean square slopes and heights are large.

Tateiba and Nanbu (1994) present numerical results in detail for the effective propagation constant of a space where many small spheres with high permittivity are randomly distributed, on the basis of the multiple scattering theory presented before. Their results are valid also for the space where the results given by conventional methods become invalid.

Kaczkowski and Thorsos (1994) give a brief review of a derivation of the standard OE solution, and show how the short series are obtained in their paper. Numerical examples is presented illustrating the rapid convergence and wide accuracy of the various forms of the OE solution in several scattering regimes. The results indicate that the short series provide efficient and accurate alternatives to the standard solution, a finding which is of significant practical value in treating scattering from 2-D surfaces. They also present the alternative forms of the OE solution and give one example for scattering from surfaces with a Gaussian spectrum.

Collin (1994) developes the modifications of the regular full wave theory for rough surface scattering by an incident Gaussian beam instead of a plane wave. The Gaussian beam is produced by a large circular aperture that has a Gaussian illumination. It is shown that provided the incident Gaussian beam has a plane phase front over the extent of the rough surface patch and the linear dimensions of the rough patch are large compared with the surface height correlation length, the normalized scattering cross-section is the same as for an incident plane wave.

De Boer et al (1994) report the first measurement of the distribution function of the fluctuations on the total transmission of multiple scattered light. The shape of the distribution is predominantly Gaussian. A non-Gaussian contribution to the distribution function is found, caused by correlation in the cubed intensity. The scattering diagrams responsible for this new correlation are calculated without free paramaters, and a good agreement is found between experiment and theory.

Scattering of the TE incident wave from a perfectly conducting random rough surface is studied by Pak et al (1994). First, the vector electromagnetic scattering from a two-dimensional rough surface with a surface area of 81 square wavelengths is illustrated. Monte Carlo results show backscattering enhancement for the co-polarized component. Secondly, the TE scattering from a one-dimensional random rough surface with a Gaussian roughness spectrum is studied. Specifically, a grazing incident angle at 86˚ with a surface length of 800 wavelengths is presented. Lastly, backscattering intensities from Gaussian and non-Gaussian rough surfaces are compared. Numerical results are illustrated as a function of rms height and slope.

Nieuwenhuizen and Rossum (1995) calculated the distributions of the angular transmission coefficient and of the total transmission for the multiple scattered waves. The calculation is based on a mapping to the known distribution of eigenvalues of the transmission matrix. The distributions depend on the profile of the incoming beam. The distribution function of the angular transmission distribution grows log normally whereas it decays exponentially.

The one-dimensionally rough surfaces considered in the work of Bahar and Lee's (1995) paper are characterized by four-dimensional Gaussian joint probability density functions for the surface heights and slopes at two points. The expressions for the diffuse scattered fields are used to obtain the random rough cross sections. The full wave solutions are compared with the corresponding small perturbation results and the physical optics results. They are also compared with experimental and numerical results based on Monte Carlo simulations of rough surfaces. The earlier assumption that the surface heights and slopes can be considered to be uncorrelated are examined, and the impact of self shadow is considered in detail. The impact of the commonly used assumption that the radii of curvature is very large compared to the wavelength is also examined in detail. These results are in agreement with the duality and reciprocity relationships in electromagnetic theory.

A Monte-Carlo finite-difference time-domain (FDTD) technique is developed by Hastings et al (1995) for wave scattering from randomly rough, one-dimensional surfaces satisfying the Dirichlet boundary condition. Both single-scale Gaussian and multiscale Pierson-Moskowitz surface roughness spectra are considered. Bistatic radar cross sections are calculated as a function of scattering angle for incident angles of 0, 45, 70, and 80 degrees measured from the vertical. The contour path FDTD method is shown to improve accuracy for incident angles greater than 45 degrees. Results compare well with those obtained using a Monte-Carlo integral equation technique.

By means of perturbation theory and a computer simulation approach Sanchez-Gil et al (1995) study the transmission of *p*-polarized electromagnetic waves through a thin, free-standing metal film. The illuminated (upper) surface is a one-dimensional, randomly rough surface: the back surface is planar. The plane of incidence is perpendicular to the generators of the rough surface. The film is sufficiently thin that two surface plasmon polaritons it supports in the absence of the roghness have distinct wave numbers $q_1(\omega)$ and $q_2(\omega)$ at the frequency $\omega$ of the incident wave. As a consequence, the angular dependence of the intensity of the incoherent component of the transmitted field displays satellite peaks at angles of transmission $\theta_t$ that are related to the angle of incidence $\theta_0$ by $\sin\theta_t = -\sin\theta_0 \pm (c/\omega)\left[q_2(\omega) - q_1(\omega)\right]$, in addition to the enhanced transmission peak.

Busch and Soukoulis (1995) present a new method for efficient, accurate calculations of transport properties of random media. It is based on the principle that the wave energy density should be uniform when averaged over length scales larger than the size of the scatterers. The scheme captures the effects of resonant scattering of the individual scatterer exactly, as well as the multiple scattering in a mean-field sense. It has been successfully applied to both “scalar” and “vector” classical wave calculations. Results for the energy transport velocity are in agreement with experiment. This approach is of general use and can be easily extended to treat different types of wave propagation in random media.

A new approach based on the original full wave solutions for the like and cross scattering cross sections of composite (multi-scale) random rough surfaces is presented by Bahar and Zhang (1995). The rough sea surfaces are assumed to be characterized by the Pearson-Moskowitz spectral density function. The probability density functions (pdf's) for the rough surface heights and slopes are assumed to be Gaussian. The backscatter incoherent like and cross polarized cross sections are calculated using this new full wave approach.

The full wave solutions for the fields diffusely scattered from two-dimensional random rough surfaces are used to evaluate the scatter cross sections by Bahar and Lee (1996). Unlike the original full wave solution this full wave solution accounts for rough surface height and slope correlations and can, therefore, be used for a wide range of surface roughness scales. The computation time is relatively sort compared to the numerical results based on Monte Carlo simulations (even for one-dimensional random rough surfaces). The full wave scatter cross sections for the twodimensional random rough surfaces are shown to reduce to the small perturbation and physical optics solutions in their appropriate regions of validity. It is also shown that there is good agreement between the full wave results and experimental data or numerical results based on Monte Carlo simulations

Despite the recent development of analytical and numerical techniques for problems of scattering from two-dimensional rough surfaces, very few experimental studies were available for verification. In the paper, Chan et al (1996) present the results of millimeter-wave experiments on scattering from twodimensional conducting random rough surfaces with Gaussian surface roughness statistics. Machine-fabricated rough surfaces with controlled roughness statistics were examined. Special attention was paid to surfaces with large rms slopes (ranging from 0.35 to 1.00) for which enhanced backscattering is expected to take place. Experimentally, such enhancement was indeed observed in both the copolarized and cross-polarized returns. In addition, it was noticed that at moderate angles of incidence, the scattering profile as a function of observation angle is fairly independent of the incident polarization and operating frequency. This independence justifies the use of the geometric optics approximation embodied in the Kirchhoff formulation for surfaces with large surface radius of curvature. When compared with the experimental data, this analytical technique demonstrates good agreement with the experimental data.

The backscattering from a random medium is analytically studied by Ito and Adachi (1997). The result gives a mathematical foundation to the cumulative forward-scatter single-backscatter (CFSB) approximation. The multiple scattering effects on backscattering of a plane wave incidence are examined for both Fresnel and Fraunhofer scatterings with various correlation functions of turbulence. As a result, it is found that the multiple scattering effect on the backscattering is sensitive to the statistical properties of the fluctuating medium.

A theoretical analysis of the statistical distributions of the reflected intensities from random media is presented by Garcia-Martin et al (1998). Random matrix theory is used to analytically deduce the probability densities in the localization regime. Numerical calculations of the coupling to backward modes in surface corrugated waveguides are also put forward for comparison. Interestingly, the speckle distributions are found to be independent of the transport regime. Despite the scattering being highly nonisotropic, the predicted probability densities reproduce accurately the numerical results.

Peral and Capmany (1997) have developed a generalized Bloch wave approach for the analysis of aperiodic gratings. This method yields both a macroscopic (i.e., reflection or transmission coefficient) as well as a microscopic (i.e., dispersion diagram and microstructure of the propagating internal field) characterization of fiber and waveguide aperiodic gratings.

Warnick and Arnold (1998) present an asymptotic method for computing the backscatter from a rough conducting surface in the physical optics approximation. For intermediate and high frequencies, the backscattering coefficient is determined by an $\alpha$-stable distribution function which generalizes the Gaussian form of the geometric optics limit. The parameters of this distribution are determined by a truncation of the surface height power spectrum, which corrects the nonphysical dependence of the geometrical optics limit on high wavenumber surface components with small feature size. That backscatter in the physical optics approximation is not sensitive to components of the surface spectrum above an effective spectral cutoff wavenumber is shown. They also show that the composite surface model results from a binomial expansion of the multiple convolution of the surface spectrum. This expansion provides higher order correction term to the composite model. This derivation demonstrates that the composite model is valid for surfaces which do not naturally separate into two scales, and for wtich surfaces the theory fixes the optimal scale separation parameter. In addition, the expansion naturally specifies the transition between near-normal and mid-range incidence angle scattering.

Tatarskii et al (1998) use decomposition of an arbitrary PDF in the sum of auxiliary multivariate Gaussian PDF (for a single random variable this method is sometimes used in the Monte-Carlo simulation of a non-Gaussian PDF) to describe the non-Gaussian multivariate PDF. This approach replaces the conventional cumulant expansion. The method suggested in this paper does not lead to negative probabilities and because of its simplicity it successfully replaces the cumulant expansion. The solution obtained is simple enough to perform all necessary calculations and obtain the analytical formulae for joint CF of differences of elevations and for the scattering cross section in the Kirchhoff and other approximations for a non-Gaussian surface with the realistic anisotropic spectrum and PDF of the principal slopes. The results obtained show that deviations from the Gaussian PDF may cause significant differences in the scattering cross section. They consequently consider the following problems, each of which can be solved after the previously discussed problem is solved.

Yoon et al (1999) numerically analyze scattering of electromagnetic waves from building walls by using FVTD method. They consider three different types of rough surfaces such as periodic, random, and composite structures. the bistatic normalized radar cross section (NRCS) is calculated for horizontal and vertical polarization, and the authors take into account of the conventional optical reflection which corresponds to the n-th Bragg reflection for periodic structures. In addition, they investigate what conditions are needed in order to be able to ignore the higher order Bragg reflection for the periodic structures.

Collaro et al (1999) says that electromagnetic scattering is often solved by applying Kirchhoff approximation to the Stratton–Chu scattering integral. In the case of rough surfaces, it is usually assumed that this is possible if the incident electromagnetic wavelength is small compared to the mean radius of curvature of the surface. Accordingly, evaluation of the latter is an important issue. In their paper Collaro et al generalizes the groundwork of Papa and Lennon by computing the mean radius of curvature for Gaussian rough surfaces with no restriction on its correlation function. This is an interesting extension relevant to a variety of natural surfaces. Relations between the surface parameters and the mean radius of curvature are determined and particular attention is paid to the relevant small slope regime.

Bal et al (2000) study transport and diffusion of classical waves in two-dimensional disordered systems and in particular surface waves on a flat surface with randomly fluctuating impedance. They derive from the first principles a radiative transport equation for the angularly resolved energy density of the surface waves. This equation accounts for multiple scattering of surface waves as well as for their decay because of leakage into volume waves. The dependence of the scattering mean free path and of the decay rate on the power spectrum of fluctuations are analyzed.

Toporkov and Brown (2000) discuss the method which is one of the development of robust and efficient numerical techniques for exact calculations of rough surface scattering done recently, typically formulated for time-independent surfaces, can be extended to calculate scattering from time-evolving ocean-like surfaces. Estimates are provided for the choice of parameters in such time-varying simulations. The method of ordered multiple interactions (MOMI) is used to calculate time-varying scattering from surfaces generated according to linear and nonlinear (Creamer) models for incidence angles ranging from normal to low grazing. The average Doppler spectra of backscattered signals obtained from such simulations are compared for different incident angles, polarizations, and surface models. In particular, the simulations show a broadening of the Doppler spectra for nonlinear surfaces, especially at low grazing angles (LGA) and a separation of the vertical and horizontal polarization spectra at LGA for nonlinear surfaces.

By using the Monte Carlo method and numerical finite element approach, bistatic scattering from the fractal and Gaussian rough surfaces is studied by Li and Jin (2000). Difference between these two surfaces and their functional dependence on the surface parameters are discussed. Some novelty conclusions have been achieved.

Numerical simulation of passive microwave remote sensing of ocean surfaces has a strict requirement of accuracy. This is because the key output of the simulations is the difference of brightness temperature between a rough surface and a flat surface. Since the difference can be as small as 0.5 K, it is important to simulate the scattering and emission accurately. In their paper, Zhou et al (2001) perform accurate simulations of transverse electric (TE) and transverse magnetic (TM) waves for ocean surfaces with relative permittivity = 28.9541 + $i$36.8430 at 19 GHz. Because ocean permittivity is large, they used up to 80 points per free space wavelength. To ensure accuracy, a matrix equation obtained from the surface integral equation formulation is solved by matrix inversion. Numerical results are illustrated for rough surfaces with Gaussian spectrum and bandlimited ocean spectrum and bandlimited fractal surfaces. Numerical results indicate that fine discretization is required for ocean-like surfaces with fine scale roughness.

A finite-difference time-domain (FDTD) method for scattering by one-dimensional, rough fluid–fluid interfaces is presented by Hastings et al (2001) . Modifications to the traditional FDTD algorithm are implemented which yield greater accuracy at lower computational cost. Numerical results are presented for fluid–fluid cases modeling water–sediment interfaces. Two different roughness spectra, the single-scale Gaussian roughness spectrum and a multiscale modified power-law spectrum, are used. Results are compared with those obtained using an integral equation technique both for scattering from single-surface realizations and for Monte Carlo averages of scattering from an ensemble of surface realizations. Scattering strengths are calculated as a function of scattering angle for an incident angle of 70 (20 grazing). The results agree well over all scattering angles for the cases examined.

The emission and reflection properties of a two-dimensional (2-D) Gaussian rough sea surface are investigated by Bourlier et al (2001). The emissivity and reflectivity study is of importance for accurate measurement of the temperature distribution of a wind-roughened water surface by infrared thermal imaging. The radius of curvature of the capillary waves being much larger than the wavelength involves the fact that our statistical model is based on the first order geometrical-optics method.

In this 2-D study of Galdi et al (2001), the Gabor-based Gaussian beam (GB) algorithms, in conjunction with the complex source point (CSP) method is applied to aperture-excited field scattering from, and transmission through, a moderately rough interface between two dielectric media. It is shown that the algorithm produces accurate and computationally efficient solutions for this complex propagation environment, over a range of calibrated combinations of the problem parameters. One of the potential uses of the algorithm is as an efficient forward solver for inverse problems concerned with profile and object reconstruction.

In the development of wave scattering models for randomly dielectric rough surfaces, it is usually assumed that the Fresnel reflection coefficients could be approximately evaluated at either the incident angle or the specular angle. However, these two considerations are only applicable to their respective regions of validity. A common question to ask is what are the conditions under which we would choose one or the other of these two approximations? Since these approximations are basically roughness-dependent, how can we handle the in-between cases where neither is appropriate? In their paper, Wu et al (2001) propose a physical-based transition function that naturally connects these two approximations. The like-polarized backscattering coefficients are evaluated with the model and are compared with those calculated with a moment method simulation for both Gaussian and non-Gaussian correlated surfaces. It is found that the proposed transition function provides an excellent prediction for the backscattering coefficient in the frequency and angle trends.

Simulations of electromagnetic waves scattering from two-dimensional perfectly conducting random rough surfaces are performed by Xia et al (2001), using the method of moment (MoM) and the electric field integral equation (EFIE). Scattering from Gaussian conducting rough surfaces of a few hundred square wavelengths are studied numerically using Haar wavelets. A matrix sparsity less than 10% is achieved for a range of root mean square (RMS) height at eight sampling points per linear wavelength. Parallelization of the code is also performed. Simulation results of the bistatic scattering coefficients are presented for different surface RMS heights up to 1 wavelength. Comparsions with sparse-matrix/canonical-grid approach (SM/CG) and triangular discretized (RWGbasis) results are made as well. Depolarization effects are examined for both TE and TM incident waves. The relative merits of the SM/CG method and the present method are discussed.

The light scattering effect by rough surface of amorphous silicon was examined by Kwak et al (2002) by several methods. They newly adopted integral equation method developed by Fung et. al and compared with the first order approximation or high frequency approximation (geometric optics solution) of Kirchhoff method. The surface of amorphous silicon was assumed as Gaussian rough surface. The enhancement of light absorption by surface scattering can be predicted more accurately by the method suggested here.

In surface scattering model applications a large variery of roughness conditions are encountered: some surfaces may be described with one roughness scale and others with more than one roughness scales; some surfaces are correlated exponentially, Gaussian-like or anywhere between the two. In their study, Fung and Tjuatja (2003) want to show the backscattering models in algebraic form: (1) R scattering model whose correlation function behaves like a Gaussian or an exponential function, and (2) a scattering model whose correlation firnclion behaves. like a Gaussian near the origin and nearly an exponential function at large lag distances. It is believed that most surface backscattering problems can be explained with one of the two models. Applications of these models to data interpretation are demonstrated.

Gilbert and Johnson (2003) presented simplified forms for $\sigma^{01}$ and $\sigma^{11}$ for penetrable surfaces under the asumption of a Gaussian random process surface with an isotropic Gaussian correlation function in the paper. These surfaces are admittedly simple compared to many natural surfaces, but the Gaussian model remains commonly applied in many studies.

A problem of interest to underwater acousticians is understanding the relationship between ocean-bottom characteristics and acoustic backscattering statistics. The experimental work done by Becker (2004) focused on examining surface roughness characteristics that cause backscattering strength statistics to deviate from the Rayleigh distribution. Several different scattering surfaces with known height distributions were designed for this study. The surfaces were modeled using a technique that allowed for different height-distribution functions and correlation lengths to be prescribed. Isotropic and anisotropic surfaces were fabricated having both Gaussian and non-Gaussian surface-height distributions. Many independent backscattering measurements were made for different aspects of each surface using a computer-controlled transducer-positioning system. Acoustic backscattering statistics were non-Rayleigh for the anisotropic surfaces when combining measurements from different aspects. Mean scattering strength was found to be dependent on both the surface-height distribution and correlation length. In addition, backscattering strength showed a dependence on the surface-height power distribution.

Monte Carlo simulations are performed by Ohnuki and Chew (2004) to investigate the statistical properties of electromagnetic scattering from 2-D random rough surfaces in 3-D space, and a strategy is developed to solve this high-frequency problem. The surfaces are characterized by perfectly conducting Gaussian random surfaces on a finite plate. This scattering problem is studied for a single realization of a random profile on which the radar cross section depends.

### 2.2.2. Localization in Random Media

Any advancement to the theory of electronic transport in noncrystalline materials requires information about the nature of the eigenstates. Possibly the most important to be acquired from the eigenstates is their localization properties, i.e., to inquire whether the electrons are essentially confined within the finite volumes of the material or are allowed to escape to infinity. This important question has been studied theoritically within the framework of certain simplified models of Anderson's study (1958), so called Anderson localization. It presents a simple model for such processes as spin diffusion or conduction in the "impurity band." These processes involve tranport in a lattice which is in some sense random, and in them diffusion is expected to take place via quantum jumps between localized states. In this simple model the essential randomness is introduced by requiring the energy to vary randomly from site to site. It is shown that at low enough densities no diffusion at all can take place, and the criteria for transport to occur are given. This study is of universal validity. In fact, it has blazed a trail on the observation of localization in disordered media.

Licciardello and Economou (1975) examined various approaches to the problem of localization within Anderson's model for random lattices. A new approximate criterion based on the Economou-Cohen *L(E)* approximation was developed. Results were presented and compared for several real lattices and for various probability distributions of the site energies. The new criterion was shown to be remerkably successful.

The question of localization is examined by employing the localization function method in the limit of infinitesimal disorder for a square-lattice tight-binding model by Soukoulis and Economou (1980). Within numerical accuracy it is found that the localization function equals to 1 within the band; this strongly indicates that all eigenstates become localized for nonzero disorder.

A frequency regime in which electromagnetic waves in a strongly disordered medium undergoing Anderson localization in $d$=3 is suggested by John (1984). In the presence of weak dissipation in $d = 2 + \varepsilon$ it is shown that the renormalized energy absorbtion coefficient increases as the photon frequency $\omega$ approaches a mobility edge $\omega^*$ from the conducting side as $\alpha \sim (\omega^* - \omega)^{-(d-2)\nu/2}, \nu = 1/\varepsilon$. This mobility edge occurs at a frequency compatible with the Ioffe-Regel condition.

A new mechanism for strong Anderson localization of photons in carefully prepared disordered dielectric superlattices with an everywhere real positive dielectric constant is described by John (1987). In three dimensions, two photon mobility edges seperate high- and low-frequency extended states from an intermediate-frequency pseudogap of localized states arising from remnant geometric Bragg resonances. Experimentally observable consequences are discussed.

Using diagrammatic Green's-function methods Arya et al (1986) investigate the criterion for the localization of an electromagnetic wave in a dielectric medium containing randomly distributed metallic spheres. They show by calculating the scattering length using the $t$-matrix approach and Mie theory that this criterion can be satisfied for reasonable values of the concentration of metallic spheres and other experimental parameters. It is proposed that effects of this strong localization can be observed in optical-absorption or –transmission experiments on a suspension of silver particles.

The quantum site and bond percolation problem, which is defined by a disordered tight-binding Hamiltonian with a binary probability distribution, is studied using finite-size-scaling methods by Soukoulis and Grest (1991). For the simple square lattice, authors find that all states are exponentially localized for any amount of disorder, in agreement with the scaling theory of localization and in disagreement with recent claims of a localization transition in two simensions. The localization length $\lambda$ is given by $A\exp\left\{B\left[p/(1-p)\right]^{y}\right\}$ with $y$ very close to 0.5 and $p$ the probability that a site or a bond is present.

Freylikher and Tarasov (1991) presented the resonance approximation method permitting calculation of the frequency correlators of fields propagating in randomly layered media. It was used to find the coherent component, the intensity, and the energy flux of radiation of a point source in an infinite randomly layered medium. It was demonstrated that such a medium acts as a fluctuation waveguide.

Kroha et al (1993) study localization of classical waves in a model of point scatterers, idealizing a random arrangement of dielectric spheres ($\varepsilon = 1 + \Delta\varepsilon$) of volume $V_s$ and mean spacing $a$ in a matrix ($\varepsilon = 1$). At distances $\gg a$ energy transport is diffusive. A self-consistent equation for the frequency dependent diffusion coefficient is obtained and evaluated in the approximation where noncritical quantities are calculated in the coherent potential approximation. Authors find localization for $d = 3$ dimensions in a frequency window centered at $\omega \simeq 2\pi / a$, and for values of the average change in the dielectric constant $\overline{\Delta\varepsilon} = \left(V_s a^{-3}\right)\Delta\varepsilon$ exceeding $\sim 1.7$.

Liu and Sarma (1994) study the Landau level localization and scaling properties of a disordered two-dimensional electron gas in the presence of a strong magnetic fields. The impurities are treated as randomly distributed scattering centers with parametrized potentials. Using a transfer matrix for a finite-width-strip geometry, the localization length as a function of system size and electron energy are calculated. The finite-size localization length is determined by calculating the Lyapunov exponents of the transfer matrix. A detailed finite-size scaling analysis is used to study the critical behaviour near the center of the Landau bands. The influence of varying the impurity concentration, the scattering potential range and its nature, and the Landau level index on the scaling behaviour and on nthe critical exponent is systematically investigated. Particular emphasis is put on studying the effects of finite range of the disorder potential and Landau level coupling on the quantum localization behaviour. On numerical results, carried out on systems much larger than those studied before, indicate that pure $\delta$ function disorder in the absence of any Landau level coupling gives rise to nonuniversal localization properties with the critical exponents in the lowest two Landau levels being substantially different. Inclusion of a finite potential range and/or Landau level mixing may be essential in producing universality in the localization.

Pradhan and Kumar (1994) derive and analyze the statistics of reflection coefficient of light backscattered coherently from an amplifying and disordered optical medium modeled by a spatially random refractive index having a uniform imaginary part in one dimension. Enhancement of reflected intensity owing to a synergy between wave confinement by Anderson localization and coherent amplification by the active medium are found. The study is relevant to the physical realizability of a mirorless laser by photon confinement due to Anderson localization.

Sigalas et al (1996) calculate the average transmission for *s*- and *p*-polarized electromagnetic (EM) waves and consequently the localization length of two-dimensional (2D) disordered systems which are periodic on the average; the periodic systems form a square lattice consisting of infinitely long cylinders parallel to each other and embedded in a different dielectric medium. In particular, authors study the dependence of the localization length on the frequency, the dielectric function ratio between the scatterer and the background, and the filling ratio of the scatterer. It is found that the gaps of the *s*-polarized waves can sustain a higher amount of disorder than those of the *p*-polarized waves, due to the fact that the gaps of the *s*-polarized waves are wider than those of the *p*-polarized waves. For high frequencies, the gaps of both types of waves easily disappear, the localization length is constant and it can take very small values. The optimum conditions for obtaining localization of EM waves in 2D systems is discussed.

Statistical properties of the transmittance ($T$) and reflectance ($R$) of an amplifying layer with one dimensional disorder are investigated by Freilikher et al (1997) analytically within the random phase approximation. Whereas the transmittance at typical realizations decreases exponentially with the layer thickness $L$ just as it does in absorbing media, the average $\langle T \rangle$ and $\langle R \rangle$ are shown to be infinite even for finite $L$ due to the contribution of low probability resonant realizations corresponding to the non-Gaussian tail of the distribution of ln $T$. This tail differs drastically from that in the case of absorption. The physical meaning of typical and resonant realizations is discussed.

Xie et al (1998) study the localization property of a two-dimensional noninteracting electron gas in the presence of a random magnetic field. The localization length is directly calculated using a transfer matrix technique and finite size scaling analysis. Strong numerical evidence is shown that the system undergoes a disorder-driven Kosterlitz-Thouless-type metal-insulator transition. A mean field theory is developed which maps the random field system into a two-dimensional *XY* model. The vortex and antivortex excitations in the *XY* model correspond to two different kinds of magnetic domains in the random field system.

Sirko et al (2000) measure the angular momentum content of modes in a flat, near-circular microwave cavity with a rough perimeter and demonstrate localization in angular momentum space. Introducing the concept of effective roughness, good qualitative agreement are found.

Transport properties of narrow two-dimensional conducting wires in which the electron scattering is caused by side edges roughness have been studied by Makarov and Tarasov (2001). A method for calculating dynamic characteristics of such conductors is proposed which is based on a two-scale representation of the mode wave functions at weak scattering. With this method, fundamentally different *by-height* and *by-slope* scattering mechanisms associated with edge roughness are discriminated. The results for single-mode systems, previously obtained by conventional methods, are proven to correspond to the former mechanism only. Yet the commonly ignored by-slope scattering is more likely dominant. The electron extinction lengths relevant to this scattering differ substantially in functional structure from those pertinent to the by-height scattering. The transmittance of ultraquantum wires is calculated over all range of scattering parameters, from ballistic to localized transport of quasiparticles. The obtained dependence of scattering lengths on the disorder parameters is qualitatively valid for an arbitrary intercorrelation of the boundaries' defects.

The effects of wave localization on the delay time $\tau$ (frequency sensitivity of the scattering phase shift) of a wave transmitted through a disordered waveguide is investigated by Schomerus (2001). Localization results in a separation $\tau = \chi + \chi'$ of the delay time into two independent but equivalent contributions, associated to the left and right end of the waveguide. For N=1 propagating modes, $\chi$ and $\chi'$ are identical to half the reflection delay time of each end of the waveguide. In this case the distribution function P( $\tau$ ) in an ensemble of random disorder can be obtained analytically. For N>1 propagating modes the distribution function can be approximated by a simple heuristic modification of the single-channel problem. A strong correlation between channels with long reflection delay times and the dominant transmission channel is found.

Chabanov and Genack (2001) report measurements of microwave transmission over the first five Mie resonances of alumina spheres randomly positioned in a waveguide. Though precipitous drops in transmission and sharp peaks in the photon transit time are found near all resonances, measurements of transmission fluctuations show that localization occurs only in a narrow frequency window above the first resonance. There the drop in the photon density of states is found to be more pronounced than the fall in the photon transient time above the resonance, leading to a minimum in the Thouless number.

Burin et al (2002) present an analytical approach to random lasing in a one-dimensional medium, consistent with transfer matrix numerical simulations. It is demonstrated that the lasing threshold is defined by transmission through the passive medium and thus depends exponentially on the size of the system. Lasing in the most efficient regime of strong three-dimensional localization of light is discussed. The author argue that the lasing threshold should have anomalously strong fluctuations from probe to probe, in agreement with recent measurements.

Deych et al (2003) numerically study the distribution function of the conductance (transmission) in the one-dimensional tight-binding Anderson and periodic-on-average superlattice models in the region of fluctuation states where single parameter scaling is not valid. It is shown that the scaling properties of the distribution function depend upon the relation between the system's length L and the length $l_s$ determined by the integral density of states. For long enough systems, $L \gg l_s$ , the distribution can still be described within a new scaling approach based upon the ratio of the localization length $l_{loc}$ and $l_s$ . In an intermediate interval of the system's length L, $l_{loc} \ll L \ll l_s$, the variance of the Lyapunov exponent does not follow the predictions of the central limit theorem and this scaling becomes invalid.

Statistical and scaling properties of the Lyapunov exponent for a tight-binding model with the diagonal disorder described by a dichotomic process are considered near the band edge by Deych et al (2003). The effect of correlations on scaling properties is discussed. It is shown that correlations lead to an additional parameter governing the validity of single parameter scaling.

Dominguez-Adamea and Malyshev (2004) present a simple approach to Anderson localization in one-dimensional disordered lattices. They introduce the tight-binding model in which one orbital and a single random energy are assigned to each lattice site, and the hopping integrals are constant and restricted to nearest-neighbor sites. The localization of eigenstates is explained by two-parameter scaling arguments. The size scaling of the level spacing in the bare energy spectrum of the quasi-particle (in the ideal lattice) with the size scaling of the renormalized disorder seen by the quasi-particle is compared. The former decreases faster than the latter with increasing system size, giving rise to mixing and to the localization of the bare quasi-particle wave functions in the thermodynamic limit. Authors also provide a self-consistent calculation of the localization length and show how this length can be obtained from optical absorption spectra for Frenkel excitons.

Transmission of a scalar field through a random medium, represented by a system of randomly distributed dielectric cylinders, is calculated numerically by Markos and Soukoulis (2005). The system is mapped to the problem of electronic transport in disordered two-dimensional systems. Universality of the statistical distribution of transmission parameters is analyzed in the metallic and localized regimes. In the metallic regime, the universality of transmission statistics in all transparent channels is observed. In the band gaps, the authors distinguish a disorder induced (Anderson) localization from tunneling through the system, due to a gap in the density of states. Authors also show that absorption causes a rapid decrease of the mean conductance, but, contrary to the case of the localized regime, the conductance is self-averaged with a Gaussian distribution.

### 2.2.3. Scattering and Propagation of Waves in Waveguides Having Random/Rough Surfaces

Aside from simple random/rough surface scattering, one application field is of significant interest: Scattering and Propagation of Waves in Waveguides Having Random/Rough Surfaces. Many kinds of waveguides such as laser, oceanlike surface, photonic crystal, having disordered surfaces are discussedtheoritically and experimentally.

The Green’s function technique is employed to investigate the influence of the boundary condition perturbations in a number of wave propagation problems by Bass et al (1974). The method permits treatment of multiple scattering on random irregularities of a boundary surface which is of particular importance for waveguide applications. For an average Green’s function the Dyson type equation has been obtained whose solution represents the coherent part of a point source field in a rough waveguide. The eigenfunction spectrum has also been calculated for such waveguides. By means of mutual wave transformation due to the scattering, the waveguide modes acquire additional (lossless) damping and altered phase velocities. Detailed calculations have been carried through for plane acoustical waveguides with statistically rough walls under the Dirichlet and Neumann conditions. The average field’s damping has also been considered for some cases of more complex geometry. In the electromagnetic case the electrical and magnetic solutions are similarly influenced by the wall roughness. Owing to the scattering they acquire longitudinal components of E or H thus becoming quasi-electrical or quasi-magnetic. For these normal waves the damping coefficients (attenuation rates) have been derived. A particular attention is paid to cutoff frequencies in the presence of effective wave conversion to the resonant mode.

Van Albada et al (1990) measured the correlation in the frequency-dependent intensity fluctuations in the total transmission through random dielectric samples, using visible light in a (essentialy) plane-wave geometry. The correlation function, of which the width at half maximum is proportional to $L^{-2}$ ($L$ is the thickness of the sample), decays as $(\Delta\omega)^{-1/2}$. This constitutes the experimental proof for the building up long-range intensity correlations in the propsgstion of classical waves by multiple scattering.

The reflection coefficient of a section of randomly rough waveguide is calculated by Garcia-Molina et al (1990) by using a coordinate transformation. Perturbation analysis is performed, assuming that the amplitude of the roughness is small compared to the average width of the waveguide. A drastic difference at long wavelengths betweenTEM on the one hand and TE and TM on the other hand has been found.

The effect of various islandlike obstacles, placed inside an electron waveguide, and the disordered tunneling modulation on the quantized conductance is theoritically investigated with the use of a model of two coupled chains by Gu et al (1992). The Landaur-Büttiker prescription, the tight-binding approximation, and the transfer matrix method are used to calculate the conductance of this mesoscopic system. The calculated results show that for these structures there are basic plateau structures in the conductance curve as a function of the Fermi energy. In addition, resonance structures are superimposed on the plateaus. However, the accuracy of the quantization and the resonance pattern in the conductance strongly depend on the interchannel tunneling modulations. The resonance structures in the conductance plateaus are smeared when the corresponding tunneling modulation alters smoothly over the obstacle region. Authors also study the variation of the quantized conductance with the Fermi energy for various multiply connected structures and for a system containing a finite-length obstacle with periodically modulated tunneling. A series of features in the conductance curve emerge. Roughness or corrugation always exist on the surface of the obstacles. This efect can be characterized by the randomly modulated tunneling between the two channels. Authors also present the investigation of the influence of the tunneling disorder on the conductance. The effect of disordered interchain tunneling are threefold. Both the localization length and the root-mean-square value of conductance fluctuations depend on the extent of disorder and the Fremi energy. The statistical distribution of conductance fluctuations in this disordering system is also presented. It is found that the statistical distribution can be normal, log-normal, or neither the former nor the latter, depending on the extent of disorder and the Fermi energy. Finally, authors studied the combined effect of both the site-energy disorder and the tunneling disorder on the conductance. It is found that the two disorders are of a very similar nature.

Ogura and Wang (1994) propose a way to treat the scattering problem of guided waves in a waveguide with a slightly rough boundary by applying the stochastic functional approach, which has been used successfully in the scattering problems of a plane scalar or electromagnetic wave in free space from various shaped random rough surfaces and has been shown to be good for treating the multiple scattering effects. As a prototype of the basic theory, only the planar structure of the waveguide and the Dirichlet boundary condition are considered. The waveguide's Green's function is expanded in terms of the Wiener-Hermite stochastic functionals of a homogeneous Gaussian random rough surface. Expressions for the modified normal waves (modes) of the average or coherent Green's function are given for the Dirichlet boundary condition. A mass operator is derived which contains the information of the multiple scattering of the modes from the rough boundary and can be evaluated in an iterative way. The second order statistical moment or the correlation function of the Green's function is also considered. Some numerical examples are given for illustration. It has been shown that the approach used in this paper gives more thorough results than those given by the graphical or Feynman diagram method.

A nonperturbative random-matrix theory is applied to the transmission of a monochromatic scalar wave through a disordered waveguide by Van Langen et al (1996). The probability distributions of the transmittances $T_{mn}$ and $T_n = \Sigma_m T_{mn}$ of an incident mode $n$ are calculated in the thick-waveguide limit, for broken time-reversal symmetry. A crossover occurs from Rayleigh or Gaussian statistics in the diffusive regime to lognormal statistics in the localized regime. A qualitatively different crossover occurs if the disordered region is replaced by a chaotic cavity.

Makarov and Tarasov (1998) address the interference localization of waves in narrow two-dimensional (2D) surface-corrugated waveguides. The problem stated generally consists of two different rather complicated ones. The first lies in the correct description of the wave interaction with randomly rough surfaces, and the other consists in due consideration of multiple scattering of waveguide modes in searching their localization. The approach most frequently used for taking into account the effect of roughness of the underlying surface on wave propagation is reduced, for the most part, to expansion of boundary conditions in terms of the power series of the asperity height, with solving subsequently an impedance-type boundary-value statistical problem. Authors argue that such an approach is unsuitable as applied to wave transfer through narrow surface-corrugated waveguides. It commonly causes wrong dependence of the extinction lengths on the asperity mean height. An alternative method is proposed, derived conformably to the electron transport in rough-bounded quantum wires that eliminates the pointed incorrectness. It provides a way for reasonable distinction of two different physical mechanisms responsible for wave scattering in 2D waveguides. One of them is conditioned by the waveguide width fluctuations (by-height scattering), and the other is governed by the asperity slopes (by-slope scattering). The latter mechanism is shown to dominate the former as a rule, leading to unexpected dependence of the localization length on the r.m.s. asperity height $\sigma$.

A new regime in the transmission of waves through disordered waveguides is predicted by Sanchez-Gil et al (1998), according to which ballistic, diffusive, and localized modes coexist within the same scale length, due to the surface-type disorder. This entangled regime is confirmed by the different behaviors of the transmitted intensities, obtained by means of numerical simulations based on invariant embedding equations for the reflection and transmission amplitudes. Also, an anomalous conductance crossover from quasiballistic transport to localization is encountered.

Exact calculations of transmission and reflection coefficients in surface randomly corrugated optical waveguides are presented by Garcia-Martin et al (1998). As the length of the corrugated part of the waveguide increases, there is a strong preference to forward coupling through the lowest mode. An oscillating behavior of the enhanced backscattering as a function of the wavelength is predicted. Although the transport is strongly nonisotropic, the analysis of the probability distributions of the transmitted waves confirms in this configuration distributions predicted by random matrix theory for volume disorder.

Makarov and Tarasov (1998) analyze wave propagation in a narrow 2D waveguide which properties are substantially controlled by scattering of wave at random rough boundaries. Usually the opposite side boundaries of the waveguides are considered to have exactly the same or sufficiently close statistical properties among all models of such statistically identical rough boundaries two substantially different are distinguished. One of them includes the waveguides with no correlation between the asperities of the opposite edges. Within the other model, correlation between the asperities of the opposite boundaries is exactly the same as the correlation at any waveguide edge.

Bulatov et al (1998) calculate the probability distribution function and the average of the cumulative phase of electromagnetic radiation transmitted through the waveguide with randomly positioned dielectric scatterers. The average phase exhibits a crossover from linear to power-law behavior as a function of frequency. A detailed comparison with experimental results is made and a good agreement is found. The results are consistent with the well-known observation that the scattering mean free path is of the order of the size of scatterers.

The tight-binding model with correlated disorder introduced by Izrailev and Krokhin (1999) has been extended to the Kronig–Penney model by Kuhl et al (2000). The results of the calculations have been compared with microwave transmission spectra through a single-mode waveguide with inserted correlated scatterers. All predicted bands and mobility edges have been found in the experiment, thus demonstrating that any wanted combination of transparent and nontransparent frequency intervals can be realized experimentally by introducing appropriate correlations between scatterers.

The reflection and transmission amplitudes of waves in disordered multimode waveguides are studied by means of numerical simulations based on the invariant embedding equations by Sanchez-Gil et al (1999). In particular, the influence of surface-type disorder on the behavior of the ensemble average and fluctuations of the reflection and transmission coefficients, reflectance, transmittance, and conductance are analyzed. The results show anomalous effects stemming from the combination of mode dispersion and rough-surface scattering: For a given waveguide length, the larger the mode transverse momentum is, the more strongly is the mode scattered. These effects manifest themselves in the mode selectivity of the transmission coefficients, anomalous backscattering enhancement, and speckle pattern both in reflection and transmission, reflectance and transmittance, and also in the conductance and its universal fluctuations. It is shown that, in contrast to volume impurities, surface scattering in quasi-one-dimensional structures (waveguides) gives rise to the coexistence of the ballistic, diffusive, and localized regimes within the same sample.

Exemplary results on the transmission through regular and random arrangements of scatterers as well as through sequences with correlated disorder are presented by Kuhl and Stöckmann et al (2001). There is a close correspondence between one-dimensional tight-binding systems, and the propagation of microwaves through a single-mode waveguide with inserted scatterers. Varying the lengths of the scatterers arbitrary sequences of site potentials can be realized.

The purpose of work of Kawakami's (2002) is twofold. First, a new simple model of photonic crystal structures is presented that can be treated analytically. Second, from the rigorous analysis of propagation and resonance of the models, out two novel properties of waves are pointed in the structure. The first is that there is a waveguide in which a leakage-free guided mode can have the same propagation constant (wavenumber) as that of continuum waves. The second novel property is that there is a resonator in which the wave can be localized, even in the absence of a "full bandgap." These facts disprove some "common beliefs" about photonic crystal structures: many people believe that 1) in a photonic crystal waveguide, a radiation-free guided mode cannot have the same wavenumber as that of continuum modes and 2) in a photonic crystal resonator, lossless localization can take place only if the host photonic crystal has an absolute bandgap. The examples show that such beliefs are overstatements.

Structure of eigenstates in a periodic quasi-one-dimensional waveguide with a rough surface is studied both analytically and numerically by Izrailev et al (2003). A large number of ‘‘regular’’ eigenstates for any high energy were found. They result in a very slow convergence to the classical limit in which the eigenstates are expected to be completely ergodic. As a consequence, localization properties of eigenstates originated from unperturbed transverse channels with low indexes are strongly localized (delocalized) in the momentum (coordinate) representation. These eigenstates were found to have a quite unexpected form that manifests a kind of ‘‘repulsion’’ from the rough surface. The results indicate that standard statistical approaches for ballistic localization in such waveguides seem to be inappropriate.

Israilev and Makarov (2003) present analytical results on transport properties of many-mode waveguides with rough surfaces having long-range correlations. It is shown that propagation of waves through such waveguides reveals a quite unexpected phenomena of a complete transparency for a subset of propagating modes. These modes do not interact with each other and effectively can be described by the theory of one-dimensional transport with correlated disorder. It is also found that with a proper choice of model parameters one can arrange a perfect transparency of waveguides inside a given window of energy of incoming waves. The results may be important in view of experimental realizations of a selective transport in application to both waveguides and electron/optic nanodevices.

Miyazaki et al (2003) investigate numerically optical properties of novel two-dimensional photonic materials where parallel dielectric rods are randomly placed with the restriction that the distance between rods is larger than a certain value. A large complete photonic gap (PG) is found when rods have sufficient density and dielectric contrast. The result shows that neither long-range nor short-range order is an essential prerequisite to the formation of PG’s in the novel photonic material. A universal principle is proposed for designing arbitrarily shaped waveguides, where waveguides are fenced with side walls of periodic rods and surrounded by the novel photonic materials. Highly efficient transmission of light for various waveguides is observed. Due to structural uniformity, the novel photonic materials are well suited for filling up the outer region of waveguides of arbitrary shape and dimension comparable with the wavelength.

Song et al (2005) report the random laser emission from surface corrugated waveguides. Discrete lasing modes, super narrow spectral linewidth, and the existence of lasing threshold behaviour have been observed. Single mode emission is observed by controlling the gain length. The lasing modes are strongly polarized. A theoritical model is presented to explain the localization phenomena.

### 2.3. Partially Disordered Periodic Media

This section and its subsection contain publications studied on the media, and structures behaving like both periodic and random such as quasicrystals etc. Such a structures are very important in order to define the effect of disorder in periodic structures. One significant application of this field is to detect the effects of defects in photonic crystals which are vital in manufacturing.

The transmittivity of a one-dimensional random system that is periodic on average is studied by Freilikher et al (1995). It is shown that the transmission coefficient for frequencies corresponding to a gap in the band structure of the average periodic system increases with increasing disorder when the disorder is weak enough. This property is shown to be universal, independent of the type of fluctuations causing the randomness. In the case of strong disorder the trasmission coefficient for frequencies in allowed bands is found to be a nonmonotonic function of the strength of the disorder. An explanation for the latter behaviour is provided.

Using the transfer-matrix method, Sigalas and Soukoulis (1995) studied the propagation of elastic waves through disordered solid multilayers constructed from two different materials and assumed periodic on the average. Results for different incident angles were reported; the effect of the mixing between longitudinal and transverse type of waves in the case of incident angles different from normal was discussed. They also studied absorbing systems and how the localization length changes in the presence of dissipation.

The transmittivity of a one-dimensional randon system that is periodic on average is studied by Freilikher et al (1995). It is shown that the transmission coefficient for frequencies corresponding to a gapin the band structure of the average periodic system increases with increasing disorder when the disorder is weak enough. This property is shown to be universal, independent of the type of fluctuations causing the randomness. In the case of strong disorder the trasmission coefficient for frequencies in allowed bands is found to be a nonmonotonic function of the strength of the disorder. An explanation for the latter behaviour is provided.

Bayındır et al (2001) report experimental observation of a full photonic band gap in a two-dimensional Penrose lattice made of dielectric rods. Tightly confined defect modes having high quality factors were observed. Absence of the translational symmetry in Penrose lattice was used to change the defect frequency within the stop band. They also achieved the guiding and bending of electromagnetic waves through a row of missing rods. Propagation of photons along highly localized coupled-cavity modes was experimentally demonstrated and analyzed within the tight-binding approximation.

By means of Monte Carlo simulations Deych et al (1998) show that there are two qualitatively different modes of localization of classical waves in 1D random periodic-on-average systems. States from pass bands and band edges of the underlying band structure demonstrate single parameter scaling with universal behavior. States from the interior of the band gaps do not have universal behavior and require two parameters to describe their scaling properties. The transition between these two types of behavior occurs in an extremely narrow region of frequencies. When the degree of disorder exceeds a certain critical value the single parameter scaling is restored for an entire band gap.

Krokhin et al (2002) present experimental and theoretical studies of the transport properties of random 1D site potentials. The key result is that exponentially weak transmissivity of a disordered system may be modifed by finite correlations. It is shown that the long-range correlations give rise to a continuum of extended states, which are separated from localized states by mobility edges. For energies (or frequencies) between the mobility edges, the disordered system is transparent, while it is not outside this interval. The authors propose to exploit this property for filtering of electrical and optical signals.

Wiersma et al (2005) discuss the optical transport properties of complex photonic structures ranging from ordered photonic crystals to disordered strongly-scattering materials, with particular focus on the intermediate regime between complete order and disorder. They start by giving an overview of the field and explain the important analogies between the transport of optical waves in complex photonic materials and the transport of electrons in solids, then discuss amplifying disordered materials that exhibit random laser action and show how liquid crystal infiltration can be used to control the scattering strength of random structures. Also the occurrence of narrow emission modes in random lasers is discussed. Liquid crystals are discussed as an example of a partially ordered system and particular attention is dedicated to quasi-crystalline materials. One-dimensional quasi-crystals can be realized by controlled etching of multi-layer structures in silicon. Transmission spectra of Fibonacci type quasi-crystals are reported and the (self-similar) light distributions of the transmission modes at the Fibonacci band edge are calculated and discussed.

Izrailev and Makarov (2005) review recent developments in the study of low-dimensional models with the so-called correlated disorder. By this term authors mean specific long-range correlations embedded in random potentials, that lead to anomalous transport properties. Second, new results obtained for one dimensional (1D) and quasi-1D structures with the corrugated surfaces resulting in surface scattering are observed. In the latter problem, the case when surface profiles, although described by random functions, contain the long-range correlations along the profiles are also considered.

### 2.3.1. Quasicrystals

Merlin et al (1985) report the first realization of a quasiperiodic (incommensurate) superlattice. The sample, grown by molecular-beam epitaxy, consists of alternating layers of GaAs and AlAs to form a Fibonacci sequence in which the ratio of incommensurate periods is equal to the golden mean $\tau$. X-ray and Raman scattering measurements are presented that reveal some of the unique properties of these novel structures.

Lu and Birman (1986) studied a class of mistakes or faults in quasilattices. The effect of a random distribution of mistakes on the diffraction of 1D, and a special class of 3D, quasilattices is calculated exactly. Mistakes change the diffraction pattern qualitatively: some Bragg peaks decrease in intensity as expected, but some are enhanced. As a result some spots disappear and some new ones appear. The diffuse scattering is also calculated. Results are given comparing calculated diffraction patterns in fivefold, threefold, amd twofold symmetry directions for a 3D quasicrystal with and without mistakes.

An experiment to probe the (quasi)localization of the photon is proposed, in which the optical layers are constructed following the Fibonacci sequence by Kohmoto et al (1987). In this system the one-dimensional theory is strictly valid. Also, it is feasible to construct the system accurately and the parameter may be precisely controlled and measured. Although Anderson localization occurs in quantum-mechanical problem; however, the phonemon is essentially due to the wave nature of the electronic states, and thus could be found in any wave phenomena. The transmission coefficient has a rich structure as a function of the wavelength of light and, in fact, is multifractal. For particular wavelengths for which the resonance is satisfied, the light propagation has scaling with respect to the number of layers, as well as an interesting fluctuation.

A microscopic theory for obtaining the polarized Raman spectrum of Fibonacci chains is developed and applied to GaAs-AlAs heterostructures by Wang and Barrio (1988). The results of the theory, without adjustable parameters, are compared with experimental data, and remarkable agreement is attained. The treatment is performed in real space and, although this system is nonperiodic in a strict sense, it retains many properties usually associated with the translational invariance of crystals. Because of its computational efficiency, this theory is suitable to other finite-size systems.

Desideri et al (1989) present experimental results and their interpretation on the propagation of surface acoustic waves on quasiperiodically corrugated solid. The surface is made of a thousand of grooves engraved according to a Fibonacci sequence. For the first time, they observe the spatial structure of the critical proper modes obtained from an optical diffraction experiment. These special modes are characteristic of quasiperiodic systems and exhibit remarkable scaling features.

Gellerman et al (1994) measured the optical transmision of quasiperiodic dielectric multilayer stacks of $SiO_2(A)$ and $TiO_2(B)$ thin films which are ordered according to a Fibonacci sequence $S_{j+1} = \{S_{j-1}, S_j\}$ with $S_0 = \{B\}$ and $S_1 = \{A\}$ up to the sequence $S_9$ which consists of 55 layers. A scaling of the transmission coefficient with increasing Fibonacci sequences at quarter-wavelength optical thicknesses are observed. This behavior is in a good agreement with theory and can be considered as experimental evidence for the localization of the light waves. The persistence of strong suppression of the transmission (gaps) in the presence of variations in the refractive indices among the layers is surprising.

Hattori et al (1994) observed the dispersion relation of photons transmitting through a photonic one-dimensional quasicrystal arranged in a Fibonacci sequence by measuring the spectrum of the phase change of the transmitted light using a Michelson-type interferometer. The phase spectrum obtained clearly showed the self-similar structure characteristic to dispersion curves of Fibonacci lattices.

Huang and Gong (1998) study the properties of Fibonacci numbers and the transparency of clusters for electrons at some values of the energy. For the *m*th Fibonacci number $Fm$, a set of divisors are obtained by $Fm/k=[Fm/k]$, $1<k\leq Fm$. Interestingly, the numerical and analytical results show that any new divisors of the *m*th Fibonacci sequence will appear periodically in the following Fibonacci sequence. Furthermore, in the mixing Fibonacci system, they perform computer

simulations and analytical calculations to study the transparent properties and spatial distributions of electronic states with the energies determined by the divisors of Fibonacci systems. The results show that the transmission coefficients are unity and the corresponding wave functions have periodiclike features. They also report that an infinite number of one-dimensional disordered lattices, which are composed of some specific Fibonacci clusters, exhibit an absence of localization.

In his book, Stadnik (1999) presents an up-to-date review of the field of quasicrystals, a new form of matter which was discovered only in 1984. the field is inspected from an experimental point of view and the results are anterpreted within the framework of the existing the theoritical models. He discusses the current understanding of the unusual physical properties of quasicrystals, as well as the highlighting the challenges associated with the physical interpretation of the properties of these complex and fascinating materials. A wealth of measured experimental data is presented and important information is given in a convenient tabular form.

### 2.3.2. Defect in Photonic Crystals

A powerful and efficient model recently proposed by the authors based on the leaky mode propagation method is used to characterize photonic bandgap structures incorporating multiple defects, having arbitrary shape and goemetrical parameter values.

Joannopolulos and Cohen (1974) investigate the efects of two types of disorder on the elctronic density of states of III-V semiconductors using simple tight-binding models and the empirical pseudopotential method. For the first type of disorder Authors consider a stoichiometric system with fourfold coordination, all bounds satisfied, variations in the bond lengths and angles, and only *unlike-atom bonds.* Thesecond type of disorder includes the properties of the first with the addition of *like-atom* bonds. These two types of disorder are studied explicitly by taking GaAs as a *prototype* and making various GaAs structures using the atomic positions of certain crystal structures with short-range disorder. These structures are crystals; however, they have atoms in the primitive cells arranged in varying fashions. A comparasion of the trends observed in the densities of states with the inclusion of different types of disorder reveals valuable information concerning the relationship of the structural nature of an amorphous prototype GaAs, for each type of disorder, which the authors believe would be consistent with some of the present experimental radial-distribution-function data. The effects of these types of disorder are discussed in general, and hopefully they will be useful in identifying specific types of disorder in amorphous samples.

Nakayama and Ogura (1977) study the eigenfunction in a one-dimensional random periodic structure, which is related to such problems as density of electronic states in a random crystal etc. They consider the reflection loss due to deformation of a periodic wave guide, a uniform transmission line periodically loaded with shunt susceptances. And it is assumed that the susceptances are described by a stationary random sequence. In their analysis a group-theoretic consideration to determine some possible form of the random eigenfunction is employed. As a result the wave function is given in the form of a successive product of a stationary random sequence, which is to be obtained from a stochastic equation. Assuming the random distortion is an independent Gaussian sequence, the properties of the eigenfunction. Finally, transmission coefficient for such a random structure of finite length is calculated.

Yablanovich et al (1991) could show that if the perfect 3D periodicity is broken by a local defect, local electromagnetic modes can occur within the forbidden band gap. Addition of extra dielectric material locally, inside the photonic crystal, produces “donor” modes. Conversely, removal of dielectric material from the crystal produces “acceptor” modes. It is now possible to make high-Q electromagnetic cavities of ~1 cubic wavelength, for short wavelengths at which metallic cavities are useless. These new dielectric cavities can cover the range from mm waves to uv wavelengths. For the experiments they chose a face-centered-cubic (fcc) photonic crystal employing non-spherical atoms. While they could design the structure at will, donor defects were chosen to consist of a single dielectric sphere centered in an air atom. Likewise, by breaking one of interconnecting ribs, it is easy to create acceptor modes.

It is demonstrated that lattice imperfections in a periodic array of dielectric material can give rise to fully localized electromagnetic states by Meade et al (1991). Calculations are performed by using a plane-wave expansion to solve Maxwell's equations. The frequency of these localized states is tunable by varying the size of the defect. Potential device applications in the microwave and millimeter-wave regime are proposed.

Pendry and MacKinnon (1992) have presented a new formalism for calculating the scattering of photons by complex dielectric structures which opens the field for simulations of all manner of systems, from photonic band structure of materials containing metallic elements, to calcılation of transmission coefficients of arbitrary structures, to simulation of the properties of disordered dielectrics. The method successfully addresses the problems of eliminating the longitudinal modes, of numerical stability, and of speed of computation, in a formulation ideally suited to calculation of transmission coefficients, to the first to be calculated, and successfully compared them to experiment.

Using the transfer-matrix technique to the propagation of electromagnetic waves in dielectric structures, Sigalas et al (1993) calculate the transmission coefficient versus the frequency of the incident wave for different polarizations in two-dimensional periodic and/or random arrangements of dielectric cylinders. This technique has been applied to cases where the plane-wave method fails or becomes too time consuming, such as when the dielctric constant is frequency dependent or has a nonzero imaginary part, and when defects are present in an otherwise periodic system. For all the cases studied, the results compared well with experiment.

An extension of the well-known coherent-potential-approximation is developed by Soukoulis et al (1994) for the study of various properties of random arrangements of spherical dielectric scatterers. Some of the short-range order is taken into account by considering a coated sphere as the basic scattering unit. A generalization of the energy-transport velocity is obtained. The validity of their approach is checked by comparison with experimental results, as well as with numerical calculations. Results for the long-wavelength effective dielectric constant, phase velocity, energy-transport velocity, mean-free path, and diffusion coefficient are presented and compared with experiments on scattering from dielectric spheres. In addition, their findings suggest that the position of the band gaps in periodic dielectric structures are closely related with the range of localized states in random dielectric media.

Ozbay et al (1995) experimentally and theoritically investigated defect structures that were incorporated into a three-dimensional layer-by-layer photonic band-gap crystal. The defects were formed by either adding or removing dielectric material to or from the crystal. For both cases, localized modes with frequencies that lie within the forbidden band gap of the pure crystal were observed. Relatively high peak transmission (10 dB below the incident signal), and high quality factors (2000) were measured. These measurements were in a good agreement with theoritical simulations. Theoritical calculations also predicted very high ($\left(Q>10^{6}\right)$) quality factors for certain cavity structures.

Using the plane-wave expansion method, Sigalas (1997) study the propagation of elastic waves through two-dimensional (2-D) periodic composites which exhibit full band gaps for all the polarizations and directions of the displacements. Defect states created inside those band gaps are also studied by disturbing the periodicity of the lattice. Systems exhibiting such kinds of states can be used as acoustical filters.

Sigalas et al (1998) study defect states in two- and three-dimensional dielectric photonic crystals. They use the transfer-matrix method and calculate the transmission and reflection coefficient of electromagnetic waves. Using the TMM, the band structure of an infinite periodic system can be calculated, but the main advantage of this method is the calculation of transmission and reflection properties of EM waves of various frequencies incident on a finite thickness slab of PBG material. In that case, the material is assumed to be periodic in the directions parallel to the interfaces. The TMM has previously been applied to defects in 2D PBG structures, photonic crystals with complex and frequency dependent dielectric constants, metallic PBG materials, and angular filters. In all these examples, the agreement between theoretical calculations and experimental measurements is very good. The Q factor of the defect states increases exponentially with the thickness of the photonic crystal. However, it saturates at high thickness when absorption is introduced. The higher the absorption, the lower the saturated value of the Q factor.

Zhang et al (1998) have directly observed the Anderson localized wave functions in three dimensions in a new class of photonic band gap systems. Such systems are networks made of one-dimensional waveguides. By adopting a simple scattering geometry in a unit cell, they are able to obtain large photonic band gaps. In the presence of defects or randomness, they have systematically studied the structures of transmission and the localized wave functions inside a gap. The effects due to absorption are investigated. Excellent quantitative agreements between theory and experiments have been obtained.

Sigalas et al (1999) study the transmission of electromagnetic waves propagating in three-dimensional disordered photonic crystals that are periodic on the average with a diamond symmetry. The transmission has been calculated using the transfer matrix method. Two different geometries are studied for the scatterers: spheres and rods connecting nearest neighbors. They find that the gaps of the periodic structure survive to a higher amount of disorder in the rods' case than in the spheres' case. They argue that this is due to the connectivity of the rod structure that exists for any amount of disorder.

A new type of waveguiding mechanism in three-dimensional photonic band-gap structures is demonstrated by Bayındır et al (2000). Photons propagate through strongly localized defect cavities due to coupling between adjacent cavity modes. High transmission of the electromagnetic waves, nearly 100%, is observed for various waveguide structures even if the cavities are placed along an arbitrarily shaped path. The dispersion relation of the waveguiding band is obtained from transmission-phase measurements, and this relation is well explained within the tight-binding photon picture. The coupled-cavity waveguides may have practical importance for development of optoelectronic components and circuits.

Bayındır et al (2001) experimentally investigated the influence of positional disorder on the photonic band gap, defect characteristics, and waveguiding in two-dimensional dielectric and metallic photonic crystals. Transmission measurements performed on the dielectric photonic crystals have shown a stop band even if a large amount of disorder was introduced to these structures. On the other hand, the photonic band gap of the metallic crystals was found to be very sensitive to disorder, while the metallicity gap was not affected significantly. Authors addressed how the transmission characteristics of a cavity were affected in the presence of weak disorder. Since the translational symmetry was broken by disorders, different cavity frequencies were measured when the authors generated defects at various locations. The propagation of photons by hopping through coupled-cavity structures in both dielectric and metallic two-dimensional photonic crystals were demonstrated. Effects of weak disorder on guiding and bending of electromagnetic waves through the coupled-cavity waveguides were also investigated.

Deych et al (2001) study analytically defect polariton states in Bragg multiple quantum well structures and defect-induced changes in transmission and reflection spectra. Defect layers can differ from the host layers in three ways: exciton-light coupling strength, exciton resonance frequency, and interwell spacing. They show that a single defect leads to two local polariton modes in the photonic band gap. Analytical expressions for corresponding local frequencies are obtained as well as for reflection and transmission coefficients. It is shown that the presence of the defects leads to resonant tunneling of the electromagnetic waves via local polariton modes accompanied by resonant enhancement of the field inside the sample, even when a realistic absorption is taken into account. On the basis of the results obtained, recommendations are made regarding the experimental observation of the effects studied in readily available samples.

Agio and Soukoulis (2001) numerically study single-defect photonic crystal waveguides obtained from a triangular lattice of air holes in a dielectric background. It is found that, for medium-high air filling ratios, the transmission has very small values in narrow frequency regions lying inside the photonic band gap—the so-called ministop bands. Two types of ministop bands are shown to exist; one of which is due to the multimode nature of the waveguide. Their dependence on the length of the waveguide and on the air filling ratio is presented.

The field distributions of reflected speckles arising from localized states inside the gap of disordered photonic crystals in two dimensions were studied through numerical simulations using the multiple-scattering method by Zhang et al (2002). The statistics of the Lyapunov exponent of the transmitted waves were also studied. Similar to the case of disordered photonic crystals in one dimension, two types of localized states were found depending on the degree of disorder and the frequency inside the gap. Author's simulation results indicate that the reflection statistics depend on whether or not the localized states are of the normal type. They also depend on whether the reflected angles are in the Bragg direction or not. By separating the field into coherent and diffuse parts, they have studied the statistics of field and phase distributions for both diffuse and total fields as well as their speckle contrasts. It was found that the crossover behavior is very similar to behavior in ballistic to diffusive wave propagation for the transmitted waves and can be described by the random-phasor-sum model (RPS). For the Bragg angle, non-Rayleigh statistics were found for both kinds of localized states. The statisics are sensitive to the degree of disorder. It was found that both the RPS and *K* distribution have limited ranges of validity in this case.

Kaliteevski et al (2003) demonstrated the appearance of photonic minibands within the photonic bandgaps of a disordered system represented by randomly distributed 'vacancies' of air cylinders. The positions of the photonic minibands are defined by the energies of the localized photonic states of the single defect, and their width increases with increase in the concentration of the defects. The appearance of the minibands makes possible the construction of spectral filters with thin transmission bands.

The importance of the defect-mode characterization in photonic bandgap materials is due to the intensive use of defects for ligth localization to design very promising optical devices. This study done by Giorgio et al (2003) provides a new, efficient method to model defects in waveguiding, finite-size photonic bandgap devices and analytical and closed-form expressions for the reflection and transmission coefficients and out-of-plane losses, which is very useful and easily implemented under any operating conditions. Moreover, the method has been applied to examine the capabilities of waveguiding photonic bandgap devices in dense wavelength division multiplexing filtering applications. Therefore, the design of two optical filters for such applications has been carried out and optimal design rules have been drawn using the new model.

The effects of structural disorder in feature position in finite two-dimensional photonic crystals are studied computationally by Frei and Johnson (2004). Under random variation in feature position some structures are not only resistant to disorder, but also show improved transmittance reduction. This apparent increase in band gap strength can be explained in terms of distributions of point defects within the photonic crystal structure. For certain photonic crystal geometries, point defects lead to scattering that reduces transmittance. Similarly, it is shown that some line defects reduce transmittance by acting as waveguides of a subcritical dimension, inhibiting transmission better than the corresponding perfect photonic crystal structures. The open square lattice photonic crystal structure is examined in depth, and other configurations are examined briefly for comparison. Calculations are done using the finite element method to solve the 2-D Maxwell's Equations in the frequency domain.

Unavoidable structural disorder in photonic crystals causes multiple scattering of light, resulting in extinction of coherent beams and generation of diffuse light. Koenderink and Willem (2005) demonstrate experimentally that the diffusely transmitted intensity is distributed over exit angles in a strikingly non-Lambertian manner, depending strongly on frequency. The angular redistribution of diffuse light reveals both photonic gaps and the diffuse extrapolation length, as confirmed by a quantitative diffusion theory that includes photonic band structures. Total transmission corrected for internal reflection shows that extinction increases slower with frequency than Rayleigh's law predicts. Hence disorder affects the high-frequency photonic bandgap of fcc crystals less severely than expected previously.

# 3. THEORY AND EXPERIMENTAL RESULTS ON WAVE PROPAGATION IN PLANAR PERIODICALLY CORRUGATED WAVEGUIDE

## 3.1. Statement and Geometry of the Problem

### 3.1.1. Theory of Wave Propagation in a Planar Smooth Waveguide

Consider a planar periodically corrugated waveguide shown in Fig. 3.1., made of two metal plates, the lower plates of whose profiles is $y_{-d/2}(x) = -d/2 + \xi\cos(qx)$ and that of the upper plate is $y_{d/2}(x) = d/2 + \xi\cos(qx+\theta)$. Where $d$ is the average thickness of the waveguide, $q = 2\pi/a$; $\xi$ and $a$ are amplitude and a period of the corrugations, respectively, the parameter $\theta$ is the phase shift between the upper and lower periodic corrugation. The wave propagation in such a structure can be analysed as follows. The TE wave, having the *x*- and *z*-components of the wave vector in the plane of the waveguide, satisfies to two wave equations. The first wave equation, for the $E_z$ component of the electric field, describes wave propagation along the *z*-axis (along the grooves). The periodicity along the *x*-axis does not affect strongly on wave propagation into the *z*-direction. In the first order approximation, we can neglect by change of parameters of the wave progressing into the *z*-direction. In this case, the eigenvalue problem reduces to solving the two dimensional wave equation

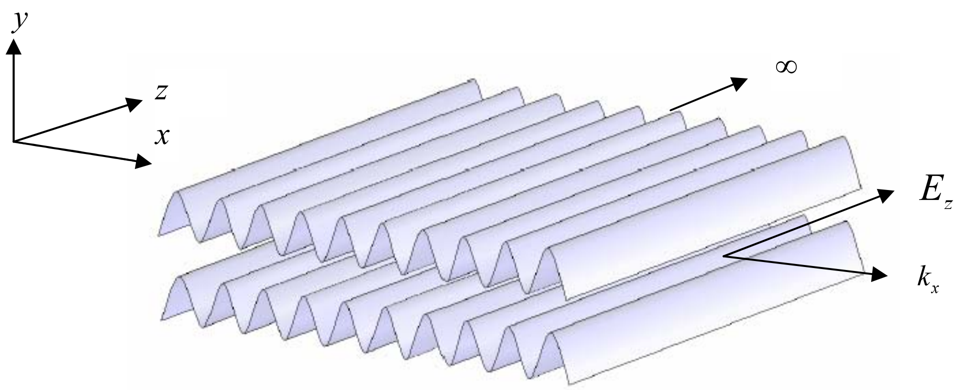


Fig. 3.1. Geometry of a planar periodically corrugated waveguide. The length of the structure along *z*-direction is considered infinite.

$$\frac{\partial^2 E}{\partial x^2}+\frac{\partial^2 E}{\partial y^2}+\varepsilon\frac{\omega^2}{c^2}E=0\,, \tag{3.1}$$

subject to the boundary condition

$$E(x,y_{-d/2}(x))=E(x,y_{d/2}(x))=0\,, \tag{3.2}$$

where $E(x,y)$ is the $z$ component of the electric field $E_z$ of the transverse electric wave, $\omega$ is the wave frequency, $\varepsilon$ is the dielectric constant of the medium, and $c$ is the velocity of light. Due to the boundary periodicity, $E(x,y)$ can be represented in the form of a Fourier series (Floquet's theorem)

$$E(x,y)=\sum_n[a_n\cos(k_{yn}y)+b_n\sin(k_{yn}y)]\times\exp[i(k_x+nq)x]\,, \tag{3.3}$$

where $a_n$ and $b_n$ are the Fourier series coefficients, and $k_{yn}$ and $k_x$ are the transverse and longitudinal components of the wave vector **k**. Eq. (3.1) and Eq. (3.3) gives the following relation

$$\varepsilon\frac{\omega^2}{c^2}-(k_x+nq)^2-k_{yn}{}^2=0\,, \tag{3.4}$$

which is then used for finding the dispersion relation $\omega(\mathbf{k})$. Substitution of Eq. (3.3) into the boundary condition gives a system of linear algebraic equations for the coefficients $a_n$ and $b_n$. By equating to zero the determinant of this system, the allowed values of $k_{yn}$ can be found, hence the frequency spectrum of the waveguide. For small corrugations $\xi/d \ll 1$ and $\xi q \ll 1$, it is sufficient to retain the first three space harmonics. As a result, the following characteristic equation is obtained for the determination of the allowed values of $k_{y0}$ at $k_x = 0$ and cutoff frequencies take such form

$$\tan(k_0 d) = \frac{\xi^2 k_0 k_1}{\tan(dk_1)} - \frac{\xi^2 k_0 k_1 \cos\theta}{\cos(k_0 d)\sin(k_1 d)}, \tag{3.5}$$

where $k_1 = k_{-1} = \sqrt{k_0^2 \pm 2k_x q - q^2}$ are wave numbers of the $n = \pm 1$ harmonics. In Eq. (3.5) and below the subscript, y is dropped in the wavenumbers $k_{yn}$. The solution of Eq. (3.5) is sought by the method of successive approximation with respect to $\xi$, i.e., $k_0 = k_0^{(0)} + \delta k + \ldots$. In the case of smooth boundaries, $\xi = 0$, Eq. (3.5) gives $\tan(k_0{}^{(0)} d) = 0$. Therefore,

$$k_0^{(0)} = \frac{p\pi}{d} \equiv k_{0p}, \qquad \omega_{0p} = \frac{c}{\sqrt{\varepsilon}}\frac{p\pi}{d}, \qquad p = 1, 2, 3, \ldots . \tag{3.6}$$

when successive approximations are performed, the wave number for the wave propagation in the $x$-direction is found by substituting $k_0^{(0)}$ in Eq. (3.6) into Eq. (3.4) as

$$k_x = \sqrt{\varepsilon \frac{\omega^2}{c^2} - \frac{p^2 \pi^2}{d^2}} \tag{3.7}$$

Dispersion curve for smooth waveguide is shown in Fig. 3.2. There are well-known modes and cutoff frequencies in a smooth planar waveguide.

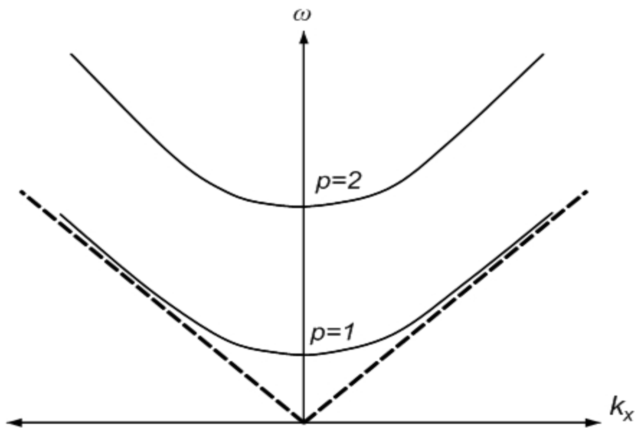


Fig. 3.2. Dispersion curve for smooth waveguide. As explicitly seen, transmission is continuous.

### 3.1.2. Wave Propagation in a Periodically Corrugated Waveguide

In the next approximation, for $\xi \neq 0$, the equations for cutoff frequencies and their shifts, $\delta\omega_p$, with respect to location in the smooth waveguide are

$$\omega_p = \left[1 + \frac{\xi^2}{d} k_1 \cot(dk_1) + (-1)^{p+1} \frac{\xi^2 k_1 \cos\theta}{2d \sin(k_1 d)}\right] \omega_{0p}, \tag{3.8}$$

$$\delta\omega_p = \omega_p - \omega_{p0} = \frac{\xi^2}{d}\left[k_1 \cot(dk_1) + (-1)^{p+1} \frac{k_1 \cos\theta}{2\sin(k_1 d)}\right] \omega_{0p}, \tag{3.9}$$

Equation (3.8) describes a location of a cutoff frequency in the spectrum as a function of the geometric parameters $\xi$, $d$, and $a$ of the periodic waveguide. Dispersion curve for such a periodic structure is shown in Fig. 3.3. Eqs. (3.5) and (3.8) are counterparts of Eq. (3.6) for the smooth waveguide. The last two equations and Eq. (3.5) indicate the nontrivial dependence of $\omega_p$ on the $k_{\pm 1}$ wave numbers and on geometric dimensions of the waveguide. Primarily, Eq. (3.8) displays the resonance behaviour of the system, but of not less importance is the dependence of $\omega_p$ on an angle $\theta$, i.e., a dependence on the phase shift of one periodic boundary with respect to another. As will be seen below, both dependencies cause properties of wave propagation in the waveguide.

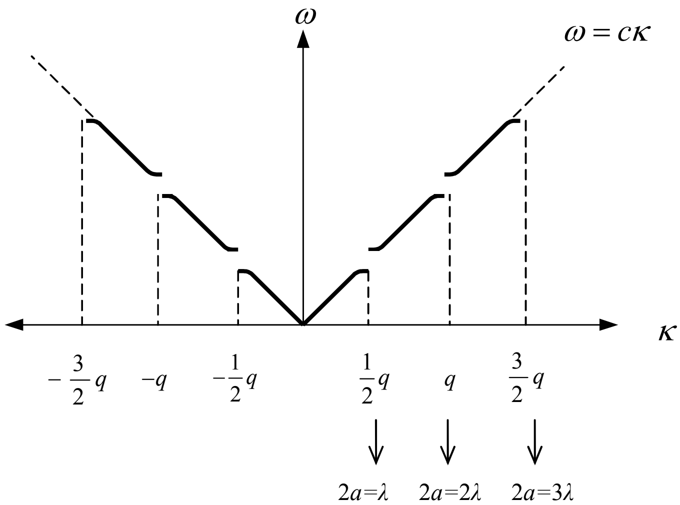


Fig. 3.3. Dispersion curve for a periodic structure. The periodicity brings about the opening of the stop band in the frequency spectrum of the structure. Therefore, transmission is not continuous.

### 3.1.3. Geometric Resonance

It is seen from Eqs. (3.5), (3.8), and (3.9) that resonance occurs in the system if

$$k_1 = \sqrt{k_0^2 - 2k_x q - q^2} = \frac{m\pi}{d} \equiv k_{1m}, \qquad m = 1, 2, 3, ..., \qquad m < p \qquad (3.10)$$

An index $m$ designates the order number of the resonance in the system, and it can be considered as the 'mode' index of the $n = \pm 1$ space harmonics but in the resonance case only. The Bragg resonance, $k_{x,B}^{\pm} = \pm q/2$, is a particular case of Eq. (3.10) at $m=p$. A number of resonances equal the order number of the mode. For example, there are two resonances in the spectrum of the second mode ($p$=2). Eq. (3.7) and (3.10) are the condition of the non-Bragg resonance between transverse modes, and it can be written in such form

$$k_{\pm 1} = \frac{m\pi}{d}, \quad k_0^{(0)} = \frac{p\pi}{d}. \tag{3.11}$$

The physical meaning of the resonance becomes clear if the last equations are rewritten in terms of wavelength ($\lambda = \frac{2\pi}{k}$) of the standing waves associated with the transverse modes ($k_0^{(0)}$ and $k_{\pm 1}$) of the fundamental ($n = 0$) and the $n = \pm 1$ space harmonics

$$d_r = p\frac{\lambda_0}{2} = m\frac{\lambda_1}{2} \tag{3.12}$$

where $d_r$ is the resonance thikness. Equation (3.12) shows that the geometric resonance occurs if the thickness of the waveguide $d_r$ is simultaneously a multiple of half wavelengths of the standing waves associated with the fundamental and the $n = \pm 1$ space harmonics but with different integers $p$ and $m$.

In contrast to the common consideration of the coupling of the longitudinal travelling waves that gives rise to the Bragg reflection, Eqs. (3.11) and (3.12) are the condition of the constructive and destructive interference of the transverse modes (standing waves).

The resonant value $k_{x,p,m}^{\pm}$ of the wave number $k_x$, at which the resonant condition (3.10)-(3.12) holds, can be found from Eq. (3.10)

$$k_{x,p,m}^{\pm} = \pm\frac{1}{2q}(k_{0p}^2 - q^2 - k_{1m}^2), \tag{3.13}$$

Substitution of $k_{x,p,m}^{\pm}$ into Eq. (3.4) gives the resonant frequency

$$\omega_{p,m} = \frac{c}{\sqrt{\varepsilon}}\left\{k_{0p}^2 + \left(\frac{k_{0p}^2 - q^2 - k_{1m}^2}{2q}\right)\right\}^{1/2}, \tag{3.14}$$

For this mode, the resonant thickness, $d_r$, can be found by substituting corresponding values of $k_0$ and $k_1$ in resonance case into Eq. (3.10) and we obtain $\left(p\pi/d\right)^2 = \left(m\pi/d\right)^2 + q^2$. For $a$ = 3.2 cm and $p$=3, the geometric resonance occurs at $d_r = 4.5$ cm and $m$=1 where the conditions $m < p$ and different integers are satisfied. It is suitable here to appoint integer numbers 3 and 1 to $p$ and $m$, respectively, as from this point for our specific calculations.

In the vicinity of resonance, the more accurate solution of Eq. (3.5) shows that this resonant frequency splits into two values $\omega_{pm}^{+}$ and $\omega_{pm}^{-}$, seperated by the forbidden gap $\delta\omega_{pm}$

$$\omega_{pm}^{\pm} = \omega_{p,m}\left[1 \pm \sqrt{2}\,\frac{\xi}{d}\,\frac{\omega_{0p}\omega_{1m}}{\omega_{p,m}^{2}}[1+(-1)^{p-m+1}\cos\theta]^{1/2}\right], \qquad (3.15)$$

$$\delta\omega_{pm} = \omega_{pm}^{+} - \omega_{pm}^{-} = 2\sqrt{2}\,\frac{\xi}{d}\,\frac{\omega_{0p}\omega_{1m}}{\omega_{p,m}}[1+(-1)^{p-m+1}\cos\theta]^{1/2}, \qquad (3.16)$$

where

$$\omega_{0p} = \frac{ck_{0p}}{\sqrt{\varepsilon}}, \qquad \omega_{1m} = \frac{ck_{1m}}{\sqrt{\varepsilon}} \qquad (3.17)$$

From Eq. (3.14) it is seen that the resonant frequency $\omega_{p,m}$ approaches to the cutoff frequency, $\omega_{0p}$, as the expression in the paranthesis $(k_{0p}^2 - q^2 - k_{1m}^2)$ vanishes. Equality of this expression to zero imposes relationship between a thickness and a period of the waveguide and mode indices $p$ and $m$. It means that given cutoff frequency will be resonant under the specific geometric relationship. That is why the resonance can be named as the geometric resonance Eq. (3.15) and (3.16), in such a resonance, take forms

$$\omega_{pm}^{\pm} = \left[1 \pm \sqrt{2}\frac{\xi}{d_r}\frac{m}{p}[1+(-1)^{p-m+1}\cos\frac{2\pi}{a}\Delta x]^{1/2}\right]\omega_{0p}, \tag{3.18}$$

$$\delta\omega_{pm} = \omega_{pm}^{+} - \omega_{pm}^{-} = 2\sqrt{2}\frac{\xi}{d_r}\frac{m}{p}[1+(-1)^{p-m+1}\cos\frac{2\pi}{a}\Delta x]^{1/2}\omega_{0p}, \tag{3.19}$$

where the angle measure of the phase shift, $\theta$, is $\theta = (2\pi/a)\Delta x$. If the corresponding integers are appointed to $p$ and $m$, Eq. (3.18) and (3.19) become

$$\omega_{31}^{\pm} = \left[1 \pm \frac{\sqrt{2}}{3}\frac{\xi}{d_r}[1-\cos\frac{2\pi}{a}\Delta x]^{1/2}\right]\omega_{03}, \tag{3.20}$$

$$\delta\omega_{31} = \omega_{31}^{+} - \omega_{31}^{-} = \frac{2\sqrt{2}}{3}\frac{\xi}{d_r}[1-\cos\frac{2\pi}{a}\Delta x]^{1/2}\omega_{03}, \tag{3.21}$$

or

$$f_{31}^{\pm} = \left[1 \pm \frac{\sqrt{2}}{3}\frac{\xi}{d_r}(1-\cos\frac{2\pi}{a}\Delta x)^{1/2}\right]f_{03}, \tag{3.22}$$

$$\delta f_{31}^{\pm} = f_{31}^{+} - f_{31}^{-} = \frac{2\sqrt{2}}{3}\frac{\xi}{d_r}\left[1-\cos\frac{2\pi}{a}\Delta x\right]^{1/2} f_{03}. \tag{3.23}$$

where $f_{03}$ is the cutoff frequency of the third mode for smooth waveguide. Eqs. (3.22) and (3.23) are another possible forms of Eqs. (3.20) and (3.21), respectively.

### 3.1.4. The Mechanism to Tune the Transmission Spectrum of a Periodically Corrugated Waveguide

The view of Eqs. (3.18) and (3.19) show that the parameter $\Delta x$ allows to introduce the mechanism to tune and control the transmision spectrum of a periodically corrugated waveguide.

A detailed analysis of Eqs. (3.18) and (3.19) is given here for two cases of the phase shift $\Delta x$: (1) $\Delta x = 0$, which may be called the case of asymmetric boundaries, and (2) $\Delta x = a/2$ that corresponds to a case of symmetrical boundaries (symmetry with respect to the centerline of the waveguide the $x$- axis). From Eqs. (3.18) and (3.19), it is seen that a value of the gap also depends on evenness of the mode indices $p$ and $m$.

#### 3.1.4.1. Asymmetric Waveguide ($\Delta x = 0$)

In this case, a seperation between the congruent boundaries is constant and equal to $d_r$ at any value of the $x$ coordinate. If both $p$ and $m$ are even or both are odd numbers, the expressions for the resonant cutoff frequencies and the gap

$$\omega_{pm}^{\pm} = \omega_{0p}, \tag{3.24}$$

$$\delta\omega_{pm} = \omega_{0p}^{+} - \omega_{0p}^{-} = 0, \tag{3.25}$$

If $p$ is even but $m$ is odd or vice versa

$$\omega_{pm}^{\pm} = \left[1 \pm 2\frac{\xi}{d_r}\frac{m}{p}\right]\omega_{0p}, \tag{3.26}$$

$$\delta\omega_{pm}^{\pm} = \omega_{0p}^{+} - \omega_{0p}^{-} = 4\frac{\xi}{d_r}\frac{m}{p}, \tag{3.27}$$

**3.1.4.2. Symmetric Waveguide (** $\Delta x = a/2$ **)**

In this case, a seperation between plates would vary with the $x$ coordinate between values $d+2\xi$ and $d-2\xi$. If both $p$ and $m$ are even or both are odd numbers, the expressions for the split cutoff frequency and $\delta\omega_{pm}$ are given by Eqs. (3.26) and (3.27). If $p$ is even and $m$ is an odd number or vice versa, the result is the same as for Eqs. (3.24), and (3.25).

From Eqs. (3.26) and (3.27), it is first seen that the forbidden gap $\delta\omega_{pm}$ is proportional, as expected, to the perturbation, ${}^{4\xi}\!/_{d_r}$, caused by the periodic corrugations. But Eq. (3.24) and (3.25) show that this common rule is not always valid. In the case of asymmetric waveguide, described by Eqs. (3.24) and (3.25), all Bragg gaps (*m*=*p*), for every mode, vanishes. Only the non-Bragg gaps, which have the order number *m* of different evenness than the mode index *p*, remain in the spectrum of every mode and they result in the reflections.

In the symmetric waveguide, the Bragg gaps as well as the subminizone gaps have the maximum value given by Eq. (3.27). The non-Bragg gaps do not open.

On increasing the thickness, each subsequent higher cutoff frequency would experience the analogous splitting. The value of the gap depends on the field configuration corresponding to the given cutoff frequency, and on the relative position of the boundaries (a position $\Delta x$). The gap has the maximum value, for example, in a case of asymmetric boundaries ($\Delta x = 0$) and asymmetric configuration of the field, i.e., when the mode indices $p$ and $m$ of the fundamental and $n = \pm 1$ space harmonics have a different evenness. In the opposite case, Eqs. (3.24) and (3.25), the electromagnetic field and the shape of the boundaries have such the symmetry that does not cause any shift of the cutoff frequency at all.

## 3.2. SHEMATIC OF EXPERIMENTAL SETUP AND EXPERIMENTAL STUDY

### 3.2.1. Assembling and Calibration of the Setup

The transmission properties of the planar periodically corrugated waveguide which we discussed theoritically in the preceding sections were investigated in this section experimentally. Both upper and lower plate of the waveguide have identical sinusoidal profile $y(x) = \xi \cos(qx)$, where $\xi$ and $a$ equal correspondingly to 0.415 and 3.15 cm in experimentation respectively. The length of the structure was 82 cm which corresponded to 26 periods of the corrugarion. The preliminary calibration measurement showed that a number of periods for optimal observation of the Bragg reflection ranges between 24 and 30. The width of the structure was chosen 70 cm, which was sufficient to model it as the planar waveguide and decrease significantly the influence of the z-component of the wave vector into the field distribution. The upper plate could slide with respect to the lower forming the phase shift $\Delta x$ between them. The relative position of the upper plate can be described, in this case, by the function $y_{up}(x) = d/2 + \xi \cos(qx + \frac{2\pi}{a}\Delta x)$.

### 3.2.2. Experimental Setup

The experimental setup is shown in Fig. 3.4. The standart microwave setup, consisting of oscillator, two couplers, Agilent E44196 power meter and two X-band pyramidal horn antennas was used for the measurements. The edges of the waveguide facing the receiving and transmitting antennas were flared in order to minimize reflections of the guided electromagnetic wave from edges. The schematic of the setup and the waveguide geometry are shown in Fig. 3.5. In the cartesian coordinate system the plates are paralel to the $zx-$plane.


Fig. 3.4. Experimental setup. It consists of oscillator, two couplers, Agilent E44196 power meter and two X-band pyramidal horn antennas. Flares were placed at the edges of the waveguide facing the receiving and transmitting antennas in order to minimize reflections of the guided electromagnetic wave from edges.

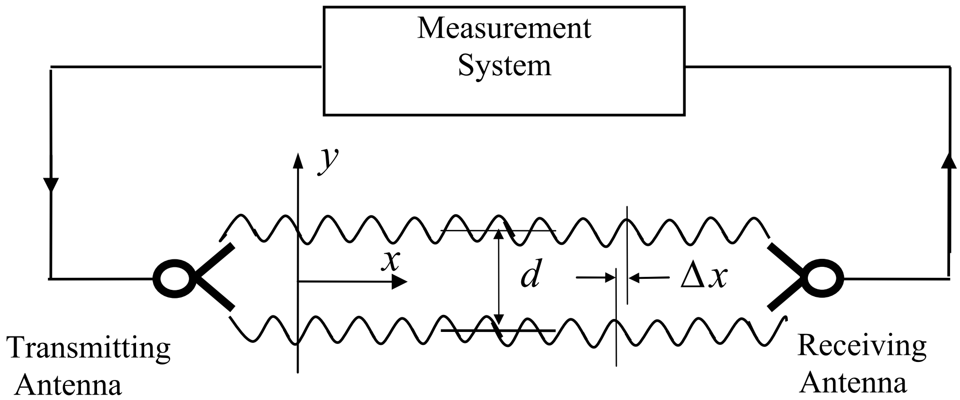


Fig. 3.5. Schematic of the experiment and geometry of the periodically corrugated waveguide. The *z*-axis is perpendicular to the plane of the picture.

### 3.2.3. Experimental Results

The propagation of the TE wave, having the polarization vector ***E*** paralel to the grooves of the corrugation (the $z$ axis), was investigated at the microwave range of frequency 8-12.5 GHz. At a certain waveguide thickness, $f_g$ can coincide with one of the cutoff frequencies $f_{0p}$; where $f_{0p} = \omega_{0p}/2\pi = (c/2d)p$. Here, the wave propagation at frequencies near the cutoff frequency of the third mode was examined.

$f_{03}$ is calculated for thickness $d_r = 4.5$ as 10.02 GHz. As it is seen from Eq. (3.23), a value of the gap, $\delta f_g = f_{31}^{+} - f_{31}^{-}$, depends on the phase shift $\Delta x$ between the plates. In a case of symmetrical waveguide (symmetry with respect to the $x$ axis), $\Delta x = a/2$, Eq. (3.23) gives $f_{31}^{+}$=10.63 GHz and $f_{31}^{-}$=9.40 GHz, with a gap $\delta f_{31}$=1.23 GHz. If $\Delta x = 0$ (asymmetric waveguide), the gap vanishes. Figure 3.6. shows the measured transmission properties for the case of the symmetric waveguide, $\Delta x = a/2$, yielded the 1.24 GHz Bragg gap. This gap vanished upon a shift of the upper plate by $\Delta x = a/2$ as shown in Fig. 3.7.

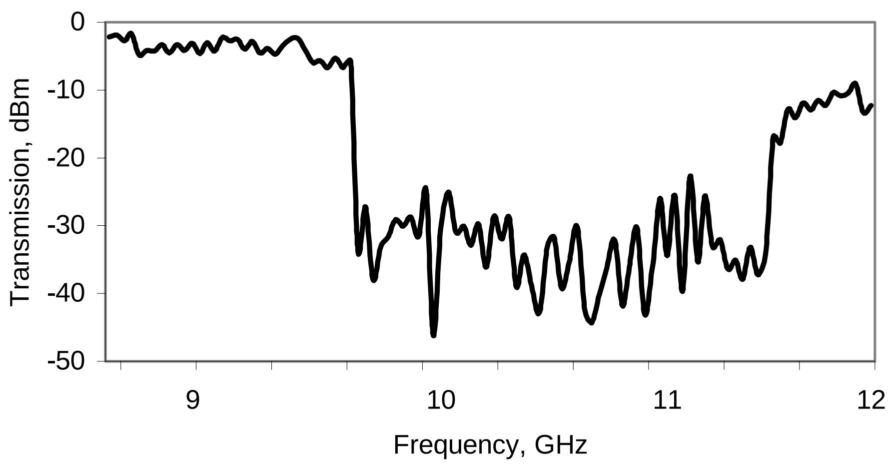


Fig. 3.6. Measured transmission characteristics for the periodically corrugated waveguide whose corrugations are symmetric, $\Delta x = a/2$.

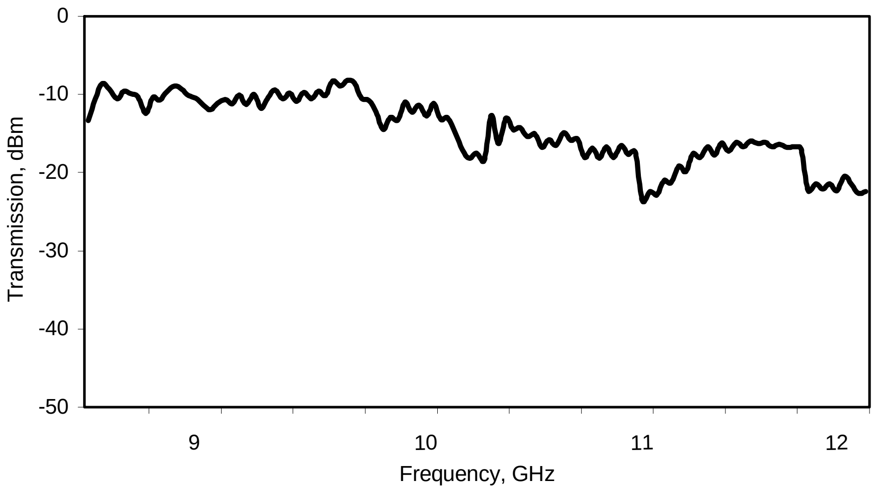


Fig. 3.7. Measured transmission characteristics for the planar periodically corrugated waveguide whose corrugations are assymmetric, $\Delta x = 0$. As shown from the figure, Bragg gap became vanished.

The numerically calculated dispersion for the waveguide with given dimensions are shown in Fig. 3.8. The Bragg gap, observed in the experiment, is shown by the shaded area. It is interesting to note that the gap is not real complete gap in the spectrum. As seen from Fig. 3.8., the $p = 2$ mode folded dispersion curve passes through the shaded frequency band. The intersection is shown by the dotted line. Therefore, the density of states is not equal to zero at these ranges of frequency. However, it had become possible to observe the gap because only the $TE_{10}$ mode was excited in the waveguide. The folded dispersion for this mode is shown in Fig. 3.8. by the thick solid line. From the graph, it is not hard to establish the validity of the geometric resonance condition, $\varpi_{03}^2 = \varpi_{01}^2 + q^2$ [see Eq. (3.11)], that appears numerically as $3^2 = 1^2 + \left(2\sqrt{2}\right)^2$.

It is appropriate to mention at this point that in both Fig. 3.6. and 3.7., one may realize that the baseline of the transmitted power falls down gradually. It occurs because the signal generator used in the experiments operates based on AM modulation. Many experiments were done in order to reveal its behaviour from different point of views in detail, and results can be found in Appendix V.

The dependence of the transmission on the phase shift is plotted in Fig. 3.9. for the selected band-gap frequency of 10.42 GHz. For this measurement, the initial position of the plates was chosen at $\Delta x = a/2$ and then one plate was gradually moved back and forth on one period of corrugation. The graph shows that the transmission varies from the minimum to the maximum value upon a shift of one periodic plate with respect to another on the half period of the corrugation, $a/2$.

Additionally, the scattered power experiments at stop and pass band frequency for $d_r = 4.5$ can be found in Appendix III

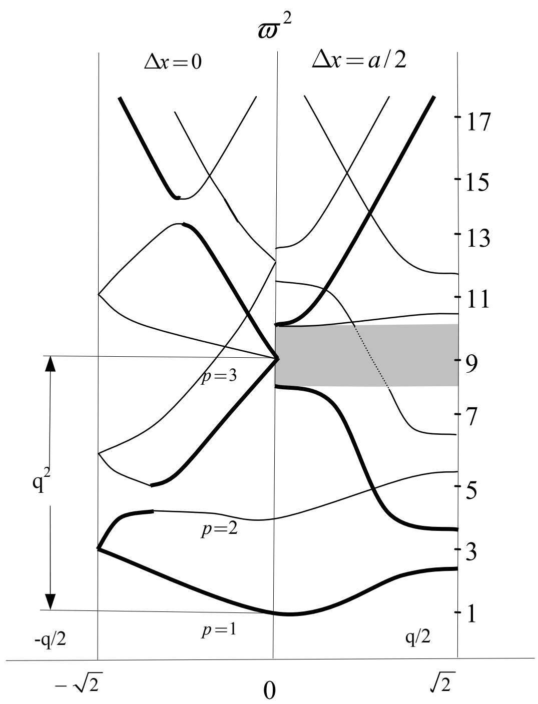


Fig. 3.8. Dispersion $\varpi^2(\kappa)$ for the periodic waveguide with the chosen dimensions. Here $\varpi = \omega/(ck_{01})$, $\kappa = k_x / k_{01}$, $q = q / k_{01}$ and $k_{01} = \pi / d$. The right side of the graph represents dispersions for the symmetric waveguide ($\Delta x = a/2$), the left for the asymmetric waveguide ($\Delta x = 0$). The dispersion for the $TE_{01}$ mode, investigated in the experiment, is shown by the thick line.

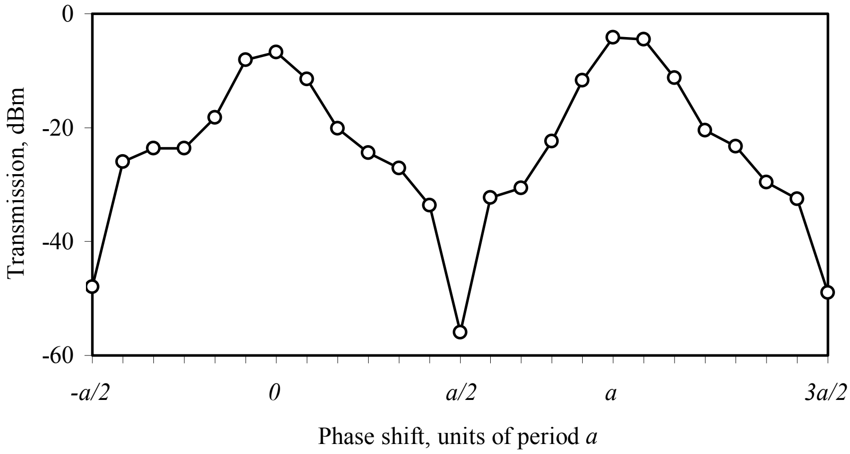


Fig. 3.9. The measured transmission through the corrugated waveguide at a fixed frequency of 10.42 GHz is plotted as a function of the phase shift $\Delta x$ between the plates.

### 3.3. Results and Discusion

The transmission properties of a planar periodically corrugated waveguide have been investigated theoritically and experimentally. The theoritical investigation shows that in a planar periodically corrugated waveguide, the geometric resonance arises under certain conditions. The phenomenon consist of resonant splitting of the cutoff frequency and the creation of the additional mode at a certain relation between the thickness and period of the waveguide.

Moreover, in the waveguide geometry, dispersions become more complex due to crossing of the folded dispersions. As a result, besides Bragg reflections, there arise non-Bragg reflections in the periodic waveguide.

The width of the gap depends on the phase shift, $\Delta x$, between two periodic plates and mode's evenness. It varies from zero to a maximum value upon shifting one plate with respect to another on the half period of the corrugation.

All the conclusion to which we came theoritically were also investigated experimentally. The Bragg gap of 1.24 GHz in the vicinity of the cutoff frequency of the third mode was observed experimentally. In a case of symmetrical waveguide (symmetry with respect to the $x$ axis), $\Delta x = a/2$, theoritical gives $f_{31}^{+}$=10.63 GHz and $f_{31}^{-}$=9.40 GHz, with a gap $\delta f_{31}$=1.23 GHz. If $\Delta x = 0$ (asymmetric waveguide), the gap vanishes. The measured transmission properties for the case of the symmetric waveguide, $\Delta x = a/2$, yielded the 1.24 GHz Bragg gap, close to the theoretical value of 1.23 GHz. This gap vanished upon a shift of the upper plate by $\Delta x = a/2$. In view of the results of both the theory and experiments, we can say that the experimental results found are in a good agreement with formula (3.23), to which we come, and which describes the controllable band gap in the spectrum for the periodically corrugated waveguide.

The wave properties of a periodic structure depend on a ratio between the wavelength and characteristic dimensions of the structure. Hence the observed microwave properties are useful for modeling of electron phenomena in periodic quantum structures. The principal condition of observation of the properties, caused by the periodicity in solids, is $l \gg a$, where $l$ is the electron mean free path, and $a$ is the period of the lateral modulation. It is a rigid enough condition that can be met usually at the helium temperature. The advantage of microwaves in such modeling is the very large "mean free path" of the electromagnetic wave, almost matching the electron mean free path in superconductors because losses in the hollow metallic waveguide are very small 0.1 $\mathrm{dBm}^{-1}$ at 10 GHz. Therefore, the mentioned condition is always met. Another advantage is that the microwave method enables an investigation of the dispersion of a seperate mode. From this point of view, the laterally modulated quantum well can be modeled by the planar periodically corrugated waveguide. Consequently, the microwave experiments assists the modeling the quantum phenomena in micro- and nanostructures and the observation of the effect of periodicity in the structures at the most favorable conditions.

In conclusion, this simple way of controlling bandwidth of the gap by the shifting of one periodic boundary with respect to another allows one to hope for the practical use of such a device.

# 4. THEORY AND EXPERIMENTAL RESULTS ON WAVE PROPAGATION IN A RANDOM WAVEGUIDE

Aside from considerable interest to the propagation of waves in periodic structures, one of the newest applications of which has been carried out in previous part, great interest to the propagation of waves in disordered structures by scientists has never been remained behind that of periodic structures.

A small impurity inside such a photonic band gap material will give rise to a naturally localized mode around this impurity. Moreover, since unintentional positional disorders are always present in the PBG (Photonic Band Gap) structures, it is important to address the influence of disorders on the photonic band gaps, cavity modes, and especially waveguides.

Moreover, huge number of studies in the field of photonic structures have shown that the existence of photonic gaps does not require long range periodic order. Therefore, investigation of disorder effects in photonic structures has a fundamental importance in pure and applied electromagnetics.

Not only does the interest come from light propagation in disordered metallic and dielectric systems but also the propagation of electrons in amorphous (semi)conductors. Besides, these fields mutually interact with each other in a manner such that existence of photonic band gaps, localization of classical waves in disordered photonic systems, defect modes are reminiscent of what is observed in electronic case. In other words, complete analogy to electronic Bloch bands in crystalline solids can be settled. For instance, it is well known that the amorphous semiconductors have similar band gaps compared to their crystalline counterparts.

Along with lots of work done in the fields of (semi)conductors and photonic structures regarding investigation of the effect of disorder in literature (and also in microwave frequency range), majority of studies, since field scattering by rough surface has been of interest due to its applications in radar and communication, concerning the effect of disorder in the microwave frequency range, to our knowledge, remain in the limit of scattering from rough surfaces which are modelled by Gaussian height distribution and Monte Carlo simulation. Only small part of studies have seemed different and still need additional contributions.

In this part of the thesis, the geometry of the random waveguide we designed is explained. Then, we try to find a proper geometrical and mathematical model from the various kinds of fields concerning disorder in a waveguide. Finally, the experimental results obtained from our waveguide are presented and discussed in "Results and Discussion" section.

It is worth repeating here that, since satisfactory studies have been done in the field of photonic crystals showing the effect of disorder we use the field of photonic crystals in the same way for our purpose by doing analogy as the scientists working on the photonic crystals take advantage of the similarities between photonic crystals and (semi)conductors.

## 4.1. Geometry and Manufacture of the Random Waveguide

### 4.1.1. Geometry of the Random Waveguide

Consider a periodically corrugated metal plate having the length of 120 cm and width of 6 cm, the corrugations of which vary sinusoidally. Let the period *a* and height of the corrugation $\xi$ be 3,2 cm and 0,8 cm, respectively. Instead of unique period of the corrugations, i.e. *a*=3,2 cm, we arranged the period of each of the corrugations by using Gaussian distribution. Gaussian distribution, or Normal distribution, is formulated as

$$f(x) = \frac{1}{\sqrt{2\pi}\sigma} e^{-\frac{(x-\mu)^2}{2\sigma^2}} \ , \ -\infty < x < +\infty \tag{4.1}$$

where $\sigma^2$ is the variance, $\mu$ is the mean value, and $\sigma$ is the standard deviation. We used the Microsoft Excel to generate consecutive random numbers between 0 and 1. The average of all the numbers generated, i.e. $\mu$, is ~0,5. Since the average of the random numbers is 0.5, and the average period we want to constitute is 3.2 cm, we used the number 6.4 as a coefficient. In what follows, we multiplied the coefficient by the random numbers generated from the computer in accordance with Gaussian distribution. Table 1. shows the generated numbers, the corresponding periods the random numbers constitute, and their position in the axis.

Table1. Random numbers generated by Excel and their corresponding position in the axis.

| No | Coefficient | Random numbers generated | Periods, cm | Position in the axis, cm |
|---|---|---|---|---|
| 1 | 6,4 | 0,18 | 1,152 | 1,152 |
| 2 | 6,4 | 0,87 | 5,568 | 6,72 |
| 3 | 6,4 | 0,47 | 3,008 | 9,728 |
| 4 | 6,4 | 0,25 | 1,6 | 11,328 |
| 5 | 6,4 | 0,84 | 5,376 | 16,704 |
| 6 | 6,4 | 0,78 | 4,992 | 21,696 |
| 7 | 6,4 | 0,25 | 1,6 | 23,296 |
| 8 | 6,4 | 0,60 | 3,84 | 27,136 |
| 9 | 6,4 | 0,50 | 3,2 | 30,336 |
| 10 | 6,4 | 0,25 | 1,6 | 31,936 |
| 11 | 6,4 | 0,34 | 2,176 | 34,112 |
| 12 | 6,4 | 0,15 | 0,96 | 35,072 |
| 13 | 6,4 | 0,92 | 5,888 | 40,96 |
| 14 | 6,4 | 0,18 | 1,152 | 42,112 |
| 15 | 6,4 | 0,85 | 5,44 | 47,552 |
| 16 | 6,4 | 0,25 | 1,6 | 49,152 |
| 17 | 6,4 | 0,79 | 5,056 | 54,208 |
| 18 | 6,4 | 0,22 | 1,408 | 55,616 |
| 19 | 6,4 | 0,48 | 3,072 | 58,688 |
| 20 | 6,4 | 0,67 | 4,288 | 62,976 |
| 21 | 6,4 | 0,77 | 4,928 | 67,904 |
| 22 | 6,4 | 0,93 | 5,952 | 73,856 |
| 23 | 6,4 | 0,35 | 2,24 | 76,096 |
| 24 | 6,4 | 0,57 | 3,648 | 79,744 |
| 25 | 6,4 | 0,20 | 1,28 | 81,024 |
| 26 | 6,4 | 0,45 | 2,88 | 83,904 |
| 27 | 6,4 | 0,85 | 5,44 | 89,344 |
| 28 | 6,4 | 0,30 | 1,92 | 91,264 |
| 29 | 6,4 | 0,77 | 4,928 | 96,192 |
| 30 | 6,4 | 0,62 | 3,968 | 100,16 |
| 31 | 6,4 | 0,74 | 4,736 | 104,896 |
| 32 | 6,4 | 0,15 | 0,96 | 105,856 |
| 33 | 6,4 | 0,07 | 0,448 | 106,304 |
| 34 | 6,4 | 0,05 | 0,32 | 106,624 |
| 35 | 6,4 | 0,81 | 5,184 | 111,808 |
| 36 | 6,4 | 0,68 | 4,352 | 116,16 |
| 37 | 6,4 | 0,39 | 2,496 | 118,656 |
| 38 | 6,4 | 0,55 | 3,52 | 122,18 |
| Average | | 0,502368 | | |

Fig. 4.1. demonstrates such a random arrangement. It is worth noting that corrugations are parallel to each other.

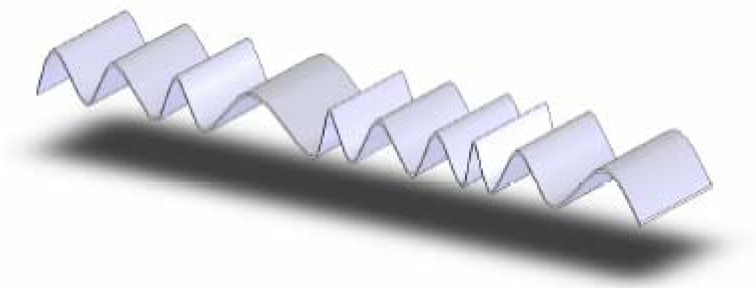

Fig. 4.1. The random corrugated plate part of the random waveguide. The heights of the corrugations are the same.

The structure demonstrated above can be considered as inhomogeneous. Fig. 4.2. shows such a structure. Variable creating inhomogeneity in the structure is the impedance change with respect to the direction of propagation of wave. The darkest and brightest areas may show the places where the impedance is the most and least concentrated.

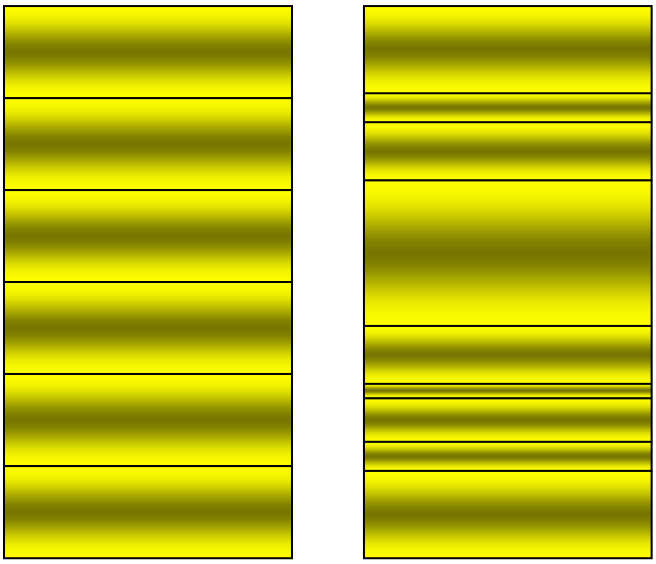

Fig. 4.2. One-dimensional complex structures. Homogeneity varies sinusoidally in both cases. The difference is that homogeneity distribution is made the same in all stacks in the left side wheras in the right the distributions are made individually.

### 4.1.2. Manufacture of the Random Waveguide

The length values of individual periods of the corrugations generated in accordance with the Gaussian distribution were lined up side by side so that we could find the positions of the starts and the ends of each corrugations in the *x*-axis. These positions are marked by a pen on the sheet of wooden having dimensions of 6x120 cm. By arranging the heights of the corrugations to 0,8 cm, and and also by avoiding making any sharp bends on the corrugations foil were stuck on the sheet of the wooden by glue. A 1 mm thick plane metal sheet having the same dimensions as the sheet of the wooden was stuck on the corresponding wooden sheet. The edges of the waveguide facing the receiving and transmitting antennas were flared in order to minimize reflections of the guided electromagnetic wave from edges. The side walls of the waveguides were also flared. Side walls were screwed to the wooden part of the bottom plate. the heights of the side walls were made long enough (30 cm) in order that we could make measurements in a wide range of average thickness. Fig. 4.3. shows the manufactured random waveguide. Note that in order to be able to demonstrate the inside of the waveguide, one side wall are removed.

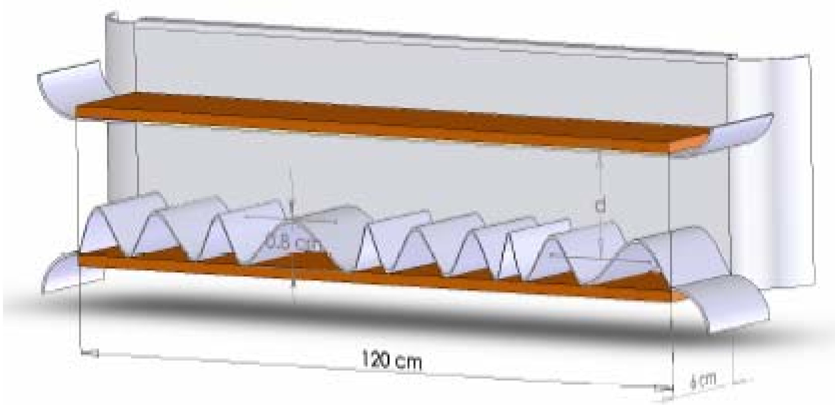


Fig. 4.3. Rectangular waveguide having random corrugations. The height of the corrugations are the same. One side wall are removed in order to demonstrate the inside the random waveguide.

## 4.2. Geometrical Modelling of the Random Waveguide

Complex structures can be constructed as one, two, or three-dimensional systems. In one dimension a complex material can be realized in the form of a multilayer structure, for instance by controlled etching of a semiconductor material (Cullis et al, 1997). One-dimensional structures have the advantage that they can be realized with almost arbitrary degree of disorder, which allows one to construct even complex deterministic non-periodic sequences like quasi-crystals.

The behaviour of waves in three-dimensional systems is often difficult to describe theoretically. The advantage of lower-dimensional structures is that an analytical theoretical description is often available, facilitating the interpretation of experimental results. Results on lower-dimensional structures can then be used to learn more about the complex behaviour of three-dimensional systems. In the case of one-dimensional (1D) structures one uses multilayers of different refractive index and thickness that are stacked either periodically or randomly, or via any other desired packing rule. An example for multilayer structure is shown in Fig. 4.4. Here, the layer are considered as homogeneous.

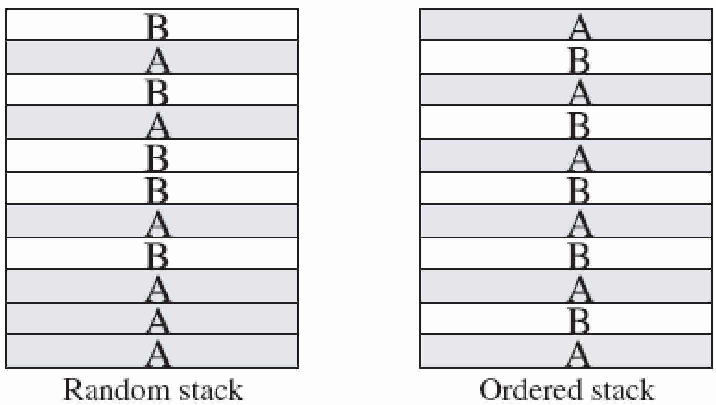


Fig. 4.4.One-dimensional complex photonic systems. By stacking two types of layers (A and B), one can obtain random or ordered one-dimensional structures. In principle any desired stacking rule can be used which allows one to explore the regime in between complete order and disorder. (Wiersma, 2005)

If the layers are etched orderly like a periodically corrugated waveguide, the interference will be constructive only in certain well-defined directions giving rise to

Bragg refraction and reflection. In the disordered case, the waves will perform a random walk. The occurrence of interference effects is now less obvious to understand; however, in random systems interference effects also turn out to be very important.

Quasi-crystals form one class of fascinating systems in between fully ordered and completely disordered. Quasicrystals are non-periodic structures that are constructed following a deterministic generation rule (Fujiwara and Ogawa, 1990). The transmission spectrum of a Fibonacci system also contains forbidden frequency regions called 'pseudo band gaps' similar to the band gaps of a photonic crystal (Nori and Rodriguez, 1986: Capaz et al, 1990).

A Fibonacci quasi-crystal is a deterministic aperiodic structure that is formed by stacking two different compounds A and B according to the Fibonacci generation scheme: $S_{j+1} = \{S_{j-1}S_j\}$ for $j \geq 1$; with $S_0 = \{B\}$ and $S_1 = \{A\}$. The lower order Fibonacci sequences are therefore $S_2 = \{BA\}$, $S_3 = \{ABA\}$, $S_4 = \{BAABA\}$, etc. For a 1D dielectric Fibonacci sample, the elements A and B are dielectric layers with different refractive index and thickness. In the present case layer A has a lower refractive index than layer B. The physical thickness of the layers can be chosen such that the optical thickness of both layers is equal to $\lambda_0 / 4$, where $\lambda_0$ is the central wavelength of the spectrum. This choice satisfies the maximum effective quasi-periodicity condition (Gellerman et al, 1994).

Wiersma et al (2005) report on 9th and 12th order Fibonacci samples as realized in porous silicon. The transmission spectra of these samples are reported in Fig. 4.5. In the transmission spectra in Fig. 4.5., pseudo band gaps are clearly visible both for the 9th and 12th order Fibonacci samples. In order to interpret the transmission spectra and to check the parameters of the multilayers, their transmission spectra within a transfer-matrix approach have numerically been calculated (Pendry, 1994: Kavokin et al, 2000).

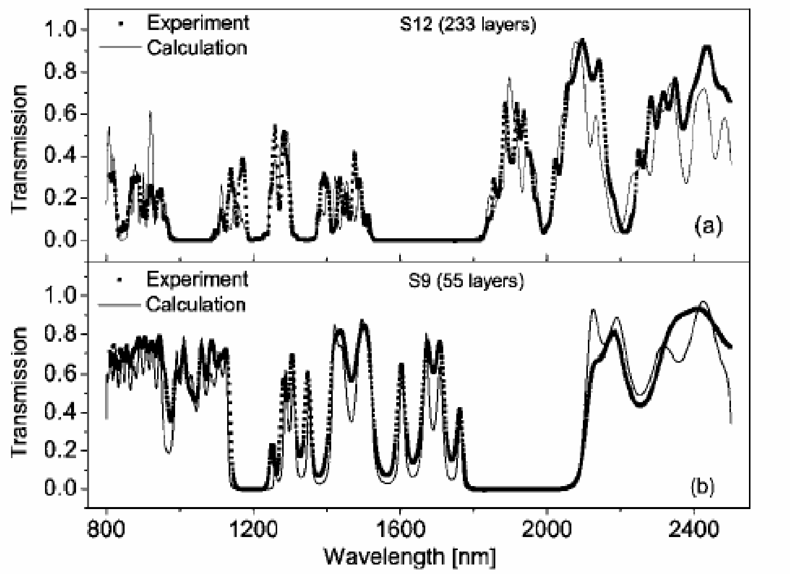


Fig. 4.5. Transmission spectra of Fibonacci samples $S_9$ (a) and $S_{12}$ (b). The solid lines are the results of a transfer-matrix calculation assuming optical path drifts of 1% (for $S_9$) and 4% (for $S_{12}$) and optical losses (absorption and scattering) of $\alpha \sim 120\,\mathrm{cm}^{-1}$. The dots denote the measured spectra. (Wiersma et al, 2005)

Since the systems stacked from different layers have band gap, can be arranged not only as Fibonacci sequence but as any distribution array, and is deterministic such systems can be a model for our structure.

One effective approach in finding a proper geometrical model to our structure is to use 2D photonic crystals having defects. The introduction of defects into the photonic crystal leads to the localization of light. A vacancy in the photonic crystals induces discrete localized photonic states in the previously complete bandgap with corresponding sharp spikes in the transmission spectra as shown in Fig. 4.6.

Photonic states localized on two separated defects can interact with each other, leading to a splitting of the original degenerate eigenmodes. The value of the splitting is proportional to the overlap of the localized photon eigenmodes of the two defects, which in the one-dimensional case of two coupled microcavities is proportional to the amplitude transmission coefficient of the Bragg mirror separating the two planar cavities (Kaliteevski, 1998). In a chain of microcavities, the split states transform into a miniband, which can be considered as the photonic analogue of the electronic minibands of a semiconductor superlattice. The width of the minibands is proportional to the value of the splitting of two nearest-neighbour localized states.

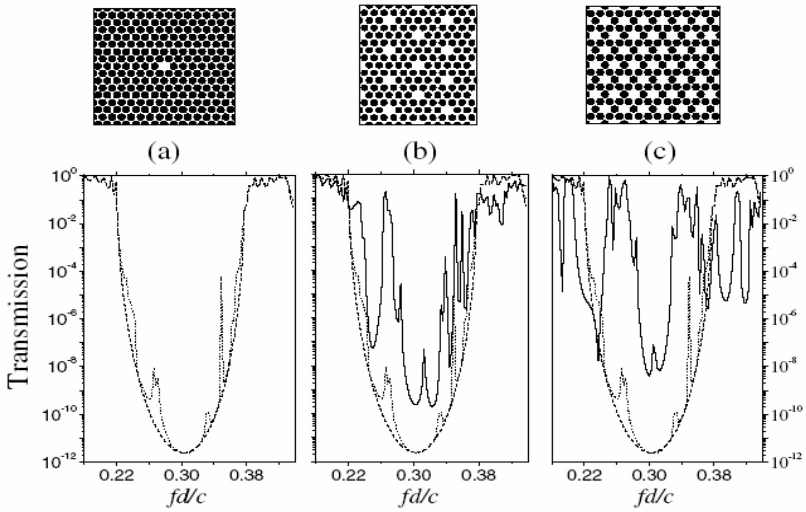


Fig. 4.6. (a) Transmission spectra for the supercell with a single vacancy (dotted curve). (b) Transmission spectra for photonic supercrystal PSC1 (solid curve). (c) Transmission spectra for photonic supercrystal PSC2 (solid curve). The transmission spectra of the ideal structure (dashed curve) and supercell with the single vacancy (dotted curve) are shown on all figures for comparison. (Kaliteevski et al, 2003)

Kaliteevsli et al (2003) interpret the findings in Fig. 4.6. that a periodic arrangement of vacancies leads to the formation of minibands in the photonic bandgap, and the position of the minibands is defined by the frequencies of the photonic states localized on a single vacancy. The width of the photonic minibands increases with increasing vacancy concentration. It should also be noted that the transmission spectrum of PSC1 has several additional smaller spikes which do not correspond to minibands. These could be explained as being due to the surface modes (Meade et al, 1991: Ramos-Mendieta and Halevi, 1999) of the PSC or to the interference of the Bloch modes of the PSC that are reflected from the front and back sides of the sample.

If the distribution of vacancies is arranged randomly rather than periodically light transmission in such structures can be considered as a hopping of photons from one defect to another, and such hopping becomes more efficient with increasing vacancy concentration. Fig. 4.7. shows the spectra of light transmission through the photonic crystal with randomly distributed vacancies with concentrations of (a) 2.9%, (b) 6.7% and (c) 8.3%.

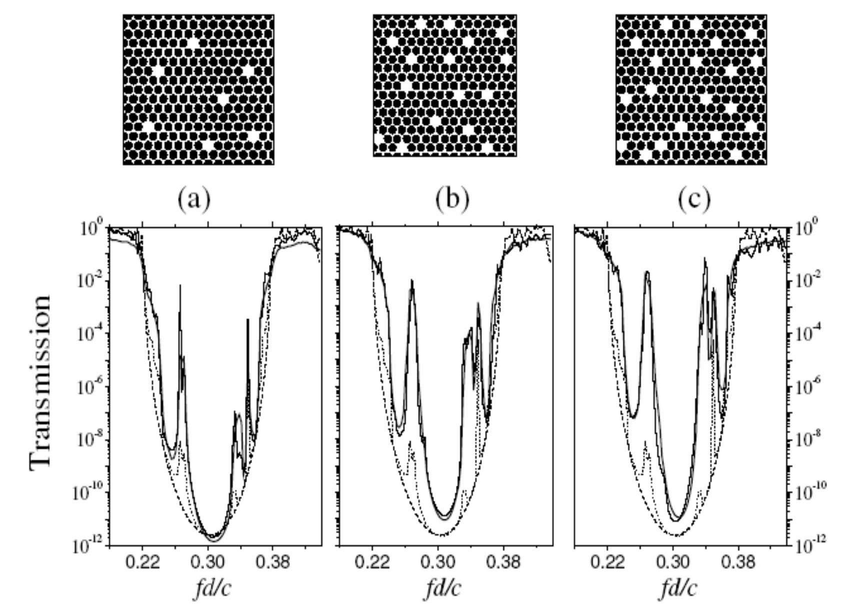


Fig. 4.7. Structures and transmission spectra of the disordered photonic crystals with different concentration of vacancies: (a) 2.9%; (b) 6.7%; (c) 8.3%. (Kaliteevski et al, 2003)

Comparing the enhancement of the light transmission for the structures shown in Figures 4.6.(b) and 4.7.(c) (which have the same 8.3% vacancy concentrations) one can conclude that transmission of light by means of the Bloch states of PSC is more efficient than by hopping from one vacancy to another in the case of a random distribution of vacancies. By varying the concentration of defects, the width of the minibands can be changed.

Kaliteevski et al (2003) have shown that in both cases photonic minibands appear in the former photonic bandgaps. The position of the minibands is defined by the energies of the photonic states localized on the individual vacancy, while the width of the minibands depends on the concentration of the vacancies.

It can be concluded that the minibands we are likely to encounter in our experiments can be evaluated in view of this study, and the experiments having different density of disorder can be compared with each other.

Özbay et al (2001) investigated the influence of disorder on photonic band gap characteristics of 2D dielectric and metallic photonic crystals. The positional disorder was introduced as follows. Each lattice point, $z_i$, was displaced according to $z_i \rightarrow z_i + re^{i\varphi}$, where $r$ is the randomness parameter, and $\varphi$ is a random variable between $\left[0-2\pi\right]$. Therefore, in this way, the degree of the disorder can be changed by varying the parameter $r$ between 0 and $a/4$.

For the periodic case, there appears a stop band extending from 8.67 to 13.25 GHz in Fig. 4.8.(a). When disorder is introduced, it is observed that (1) the width of the stop band becomes narrower, and (2) the upper band edge decreases nearly 15 dB. It is also observed that the photonic band gap persists even if large amount of disorder is introduced in Figs. 4.8.(b) and 4.8.(c). This observation is consistent with the argument that the long-range order is not necessary to achieve stop bands in dielectric photonic crystals. (Özbay et al, 2001)

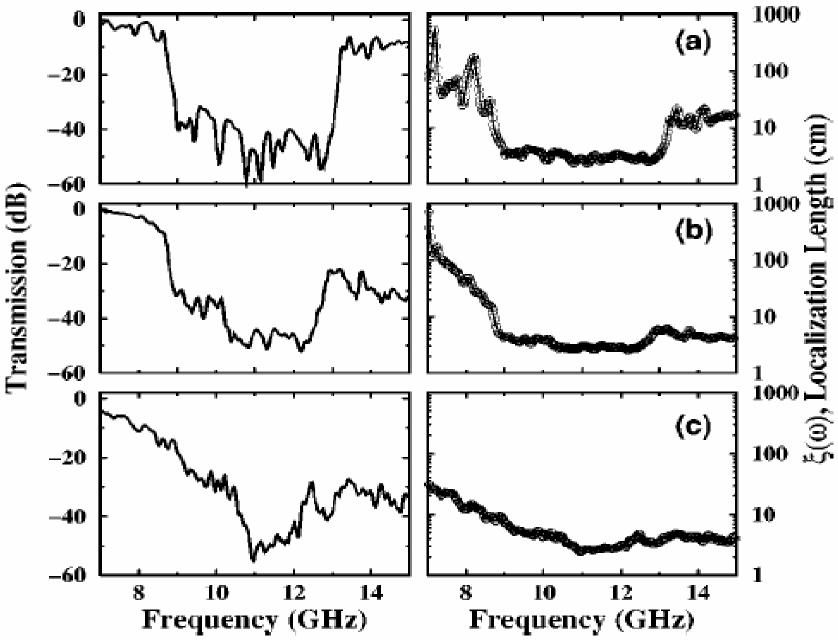


Fig. 4.8. The measured transmission spectra for (a) periodic ($r = 0$), and for disordered dielectric photonic crystals with (b) $r = a/9$ and (c) $r = a/4$. The photonic stop band shrank as the amount of disorder was increased. [Right panel] The localization length $\xi(\omega)$, as a function of frequency for the corresponding photonic crystals. The localization length became smaller than the length of the crystal in the presence of disorder. (Özbay et al, 2001)

Consequently, this results confirm our experimental results since we have found a band gap.

Since the following two important experiment couple are very important for our aim, before proceeding further, it is necessary to explain the discrepancy between the behavior of the photonic band gap for the disordered dielectric and metallic crystals. It can be explained by the underlying mechanism responsible for the formation of the photonic band gap. As described in the paper of Lidorikis et al (2000), the effect of disorder results in different changes to the system's properties. If the Bragg-like multiple scattering is the dominant one, the photonic band gaps should close quickly with increasing disorder. On the other hand, if the dominant mechanism is the Mie resonances, the photonic band gaps should survive even for large amounts of disorder, in a similar way that the electronic band gap survives in amorphous semiconductors. Under this explanation, the dominant mechanism for the formation of the photonic band gap is expected to be the Bragg scattering in metallic crystals, and the Mie resonances for the dielectric crystals.

The coupled-cavity waveguide (CCW) structures can be used in such photonic applications as lossless and reflectionless waveguides, waveguide bends (Bayındır et al, 2000), and dispersion compensators. Özbay et al (2001) investigated guiding of EM waves through CCW's in 2D dielectric and metallic photonic crystals. The influence of the weak disorder ($r = a/9$) on the guiding in the CCW's was also addressed.

In order to compare the effect of the disorder exactly it is desirable to start the measurement from the periodic case. A waveguiding band, or a defect band was observed (gray region in Fig. 4.9.) extending from 10.50 to 12.51 GHz. The bandwidth of the CCW's can be adjusted by changing the coupling strength between the localized cavity modes, i.e., decreasing the intercavity distance leads to a wider bandwidth. Then authors performed measurements on weakly disordered crystals with $r = a/9$. In this case, the guiding of EM waves along the coupled cavities was also achieved (dotted line in Fig. 4.9.) even if the waveguiding band significantly deformed for higher frequencies. Moreover, the resulting waveguiding band was narrower compared to the periodic CCW's.

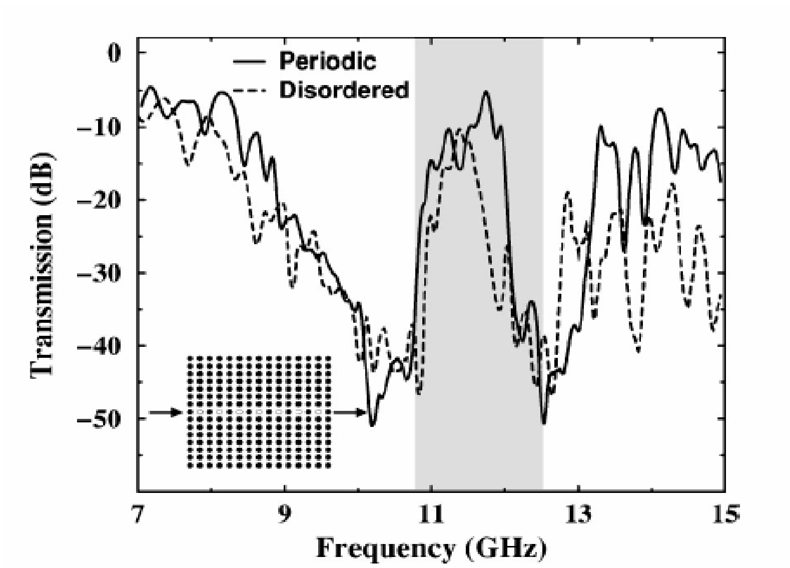


Fig. 4.9. Measured transmission through coupled cavities in two dimensional periodic (solid line) and weakly disordered (dotted line) dielectric photonic crystals. A waveguiding band (gray region) was formed due to coupling between localized defect modes. Inset: Schematic drawing of the coupled-cavity structure which was constructed by removing rods (O symbols) with a periodicity of 2*a*. (Özbay et al, 2001)

Özbay et al (2001) also investigated the waveguiding phenomena in 2D periodic and disordered metallic photonic crystals. Figure 4.10. displays the measured transmission spectra corresponding to periodic (solid line) and disordered (dotted line) straight CCW's. Two distinct guiding bands in metallic case were observed. While the lower band appeared within the metallicity gap, the higher band appeared inside the photonic band gap. This result is expected since introduction of a defect into the metallic crystal leads to two distinct defect modes in the metallicity and photonic band gaps. As shown in Fig. 4.10., it was observed that bandwidth of the defect band in the metallicity gap is narrower than bandwidth of the defect band in the photonic band gap. The introduction of disorder significantly affected the waveguiding properties of the metallic CCW's. As shown in Fig. 4.10., the disordered CCW structures had waveguiding bands with much lower transmission and bandwidths than the periodic metallic CCW structures. The defect band in the photonic band gap was significantly affected by the disorder.

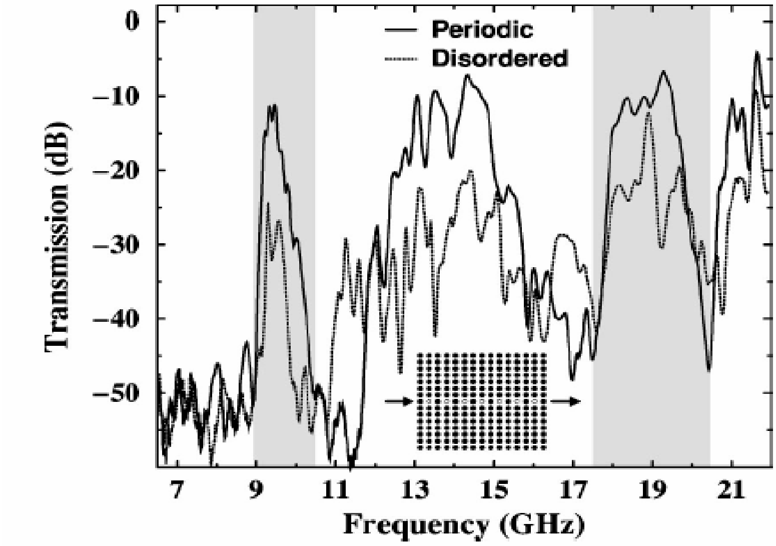


Fig. 4.10. Measured transmission through coupled cavities in two-dimensional periodic (solid line) and weakly disordered (dotted line) metallic photonic crystals. Two waveguiding bands (gray regions) were formed within the metallicity gap and the photonic band gap due to coupling between localized defect modes. Inset: Schematics of the coupled-cavity structure which was constructed by removing rods (O symbols) with a periodicity of 2*a*. (Özbay et al, 2001)

In view of the their geometry and behaviour when disorder is introduced, we can conclude that CCW's with disorder are very similar structure to our random waveguide. Therefore we can take advantage of their mathematical approximations in order to solve our problem.

Kuhl and Stöckmann (2001) show that by varying the lengths of the scatterers arbitrary sequences of site potentials can be realized.

According to Anderson's work the existence of transmission bands should be impossible in one-dimensional disordered systems, but recently it was shown by Izrailev and Krokhin (1999) that for a peculiar type of correlated disorder even here allowed bands and mobility-edges can be observed. Kuhl and Stöckmann (2001) give a review of microwave analogue experiments on the one-dimensional tight-binding model.

Fig. 4.11. shows the experimental set-up that Kuhl and Söckmann (2001) used. One hundred cylindrical scatterers can be introduced into a waveguide with dimensions a=20 mm, b=10 mm and a total length of 2.1 m. The lengths of all scatterers can be varied individually. The waveguide is so flexible that it can allow

not only to measure the total transmission but do measurements of the field intensities within the waveguide as well.

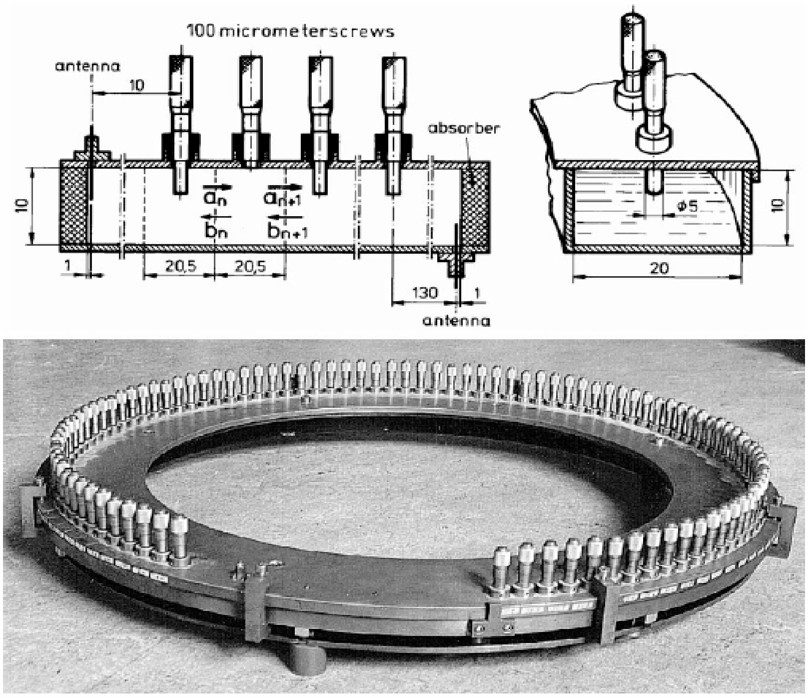


Fig. 4.11. (Top) Schematic view of the waveguide. The microwaves are coupled in through antenna 1 on the left and coupled out through antenna 2 on the right. (Bottom) Photograph of the apparatus. (Kuhl and Stöckmann, 2001)

The experiments were performed in the frequency range where only the first mode can propagate, ranging from the cutoff frequency of $\nu_{\min} = c/2a = 7.5$ up to $\nu_{\max} = c/2b = 15$, where the propagation of the second mode becomes possible.

The total transmission data presented in Fig. 4.12. are plotted as a function of the wave number $k$ in units of $\pi / d$, where $d$=20.5 mm is the distance between the scatterers. Here the scatterers were aranged periodically.

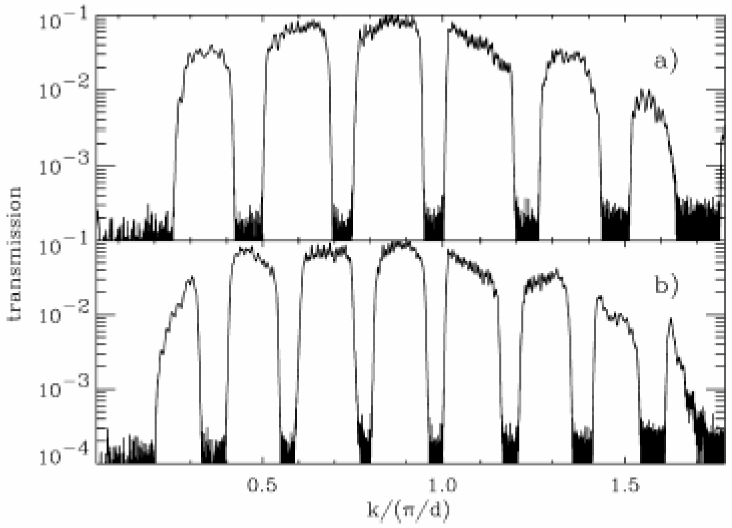


Fig. 4.12. Transmission through an array with every third (a) and every fourth (b) scatterer introduced. The plotted wave number range corresponds to a frequency range from 7.5 to 15 GHz. (Kuhl and Stöckmann, 2001)

After showing that such a structure has forbidded and transmission band spectrum, Kuhl and Stöckmann (2001) changed the $V_n$ from constant value to correlated disorder as Izrailev and Krokhin (1999) developed in their recent work a technique to calculate from an arbitrary prescribed transmission structure a sequence of site potentials reproducing this transmission structure. Fig. 4.13. shows a preliminary experimental example. It looks completely random, but actually there is an intricate hidden correlation between the sites. In the lower part the observed transmission spectrum is plotted, showing transmission for $k/(\pi/d)$ below 0.3, and in the range 0.5-0.8, with a gap in between.

In view of the experimental results Kuhl and Stöckmann (2001) performed, we can say that their experimental setup can constitute a good model for our structure, and we can make an analogy from its mathematical solution.

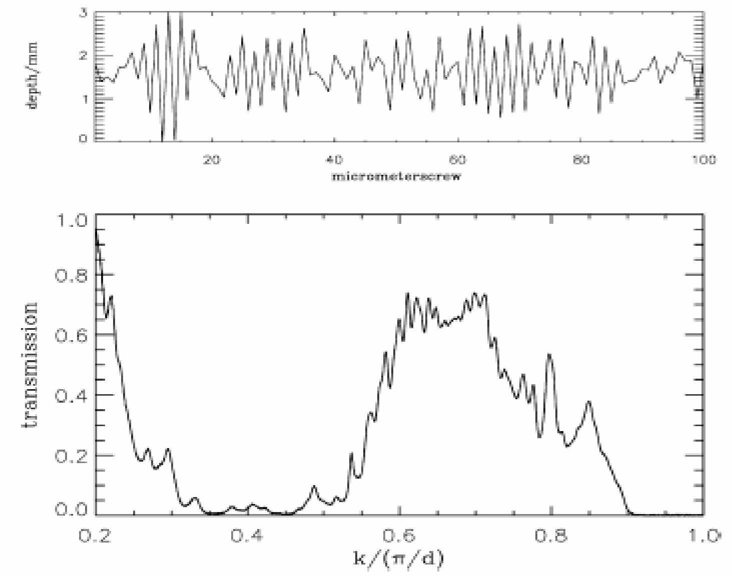


Fig. 4.13.(Top) Sequence of screw lengths with hidden correlated disorder. (Bottom) Transmission spectrum obtained with this sequence. (Kuhl and Stöckmann, 2001)

Song et al (2005) present a numerical study of the transmission properties in the corrugated waveguide. The real sample studied is a two-dimensional waveguide with corrugated surface, but it can be simplified to a waveguide consisting of randomly refractive index modulated thin layers in Fig. 4.14. by using the effective refractive index as the simulation of a normal DFB waveguide laser. This is reminiscent of two types of layers stacked, and arranged in accordance with a Fibonacci sequence shown in Fig. 4.4. a multilayer structure treatment can be adopted, electric field distribution and its spectrum can be numerically studied with the transfer matrix method. (Yeh et al, 1977: Cao et al, 1991: Song et al, 2003: Bliokh et al, 2004) Here, Song et al modified the simulation process further for simplification by keeping the refractive indices of the alternating layers as constants ($n_H$=1.545, $n_L$=1.515; here $n_H$ and $n_L$ are the effective refractive indices of $TE_0$ mode of the waveguide without and with silica sphere), but let the thickness of each layer be random between 75 nm to 120 nm (note that 75 nm is the diameter of the silica sphere). The modification should give the same simulation result as optical path $n \times L$ is the effective physical element ($n$ is the refractive index; $L$ is the thickness of each layer). The transmission through the multilayer-structure waveguide was simulated.

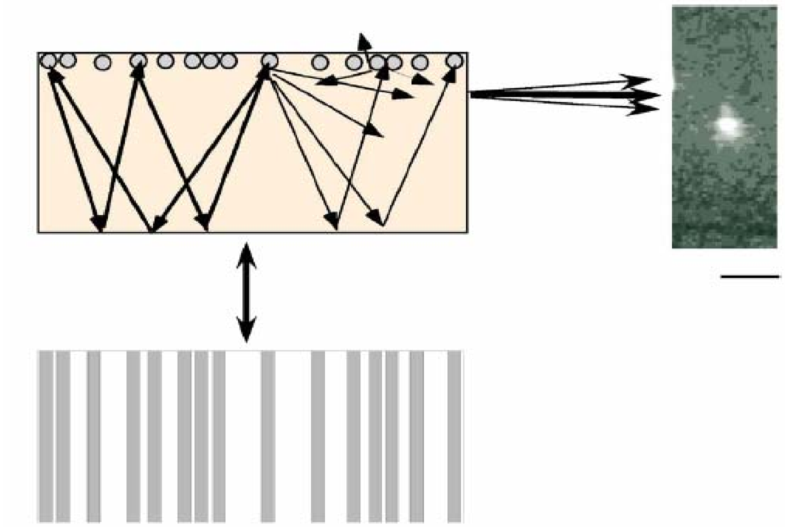

Fig. 4.14. (Color online) The schematic picture and far field picture of the emitter laser. (Song et al, 2005)

The dashed lines in Figs. 4.15(a) and 4.15(c) are the reflection spectra of 1000-layer, 1200-layer, and 2500- layer structures, respectively.

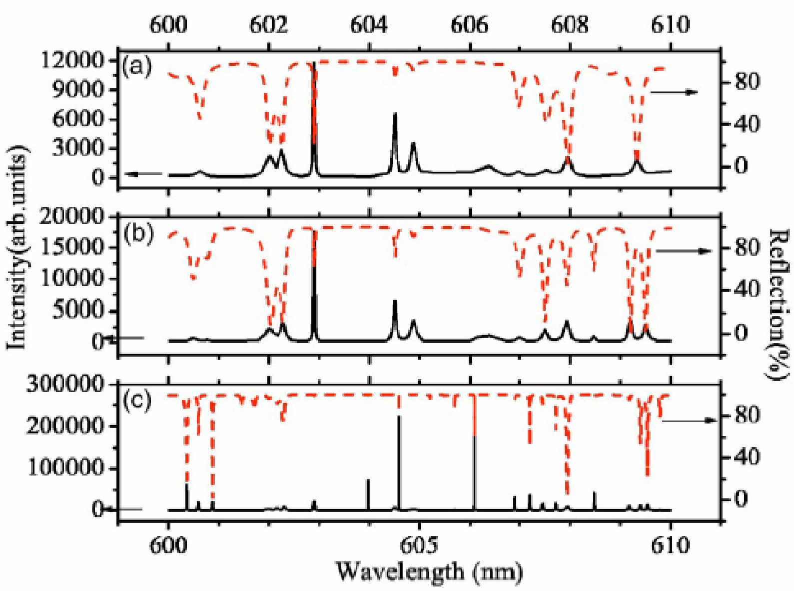


Fig. 4.15. (Color online) The spectra of reflection and the field distribution in (a) 1000-layer, (b) 1200-layer, and (c) 2500-layer structure. (Song et al, 2005)

In view of Fig. 4.14 showing a schematic picture of the waveguide we can deduce that geometry of the waveguide Song et al designed is almost the same as the geometry of the random waveguide we designed, except for that ours is inhomogeneous in the direction of propagation whereas the waveguide that Song et al proposed is of homogeneous nature.

### 4.3. Theoretical Approximations to Solve the Wave Propagation in the Random Waveguide

Anderson' paper (1958) lays the foundation for a quantum-mechanical theory for such processes as spin diffusion or conduction in the "impurity band." He studied the problem of localization of the eigensolutions of a tight-binding Hamiltonian in a 3D disordered systems. The theorem is that at sufficiently low densities, transport does not take place; the exact wave functions are localized in a small region of space.

Although Anderson's pioneering work is devoted to the observation of electronic localization in disordered solids, along with the studies concerning the localization in classical waves, such as electromagnetic waves in a disordered dielectric, or elastic waves in solids with a random ionic potential by scientists for the last two decades, it has been shown that the physical basis of the localization (Anderson localization) in both cases is essentially the same, i.e., the diffusion coefficient vanishes because of the coherent interference between waves scattered from random scatterers. This resulted in developing new mathematical models and techniques such as tight-binding model, transfer-matrix technique etc.

For example, using the transfer-matrix technique for the propagation of electromagnetic waves in dielectric structures, Sigalas et al (1993) calculate the transmission coefficient versus the frequency of the incident wave for different polarizations in two-dimensional periodic and/or random arrangements of dielectric cylinders. This technique has been applied to the case when the defects are present in an otherwise periodic system.

The study of Sigalas et al (1993) is interested in the propagation of EM waves in a system that consists of a periodic and/or a random array of infinitely long parallel, identical dielectric rods, characterized by a dielectric constant, $\varepsilon_a$, embedded in a background dielectric material characterized by a dielectric constant, $\varepsilon_b$. The rods are assumed to be parallel to the $x_3$ axis. The intersections of the rods with the $x_1x_2$ plane form a periodic 2D structure. The authors are mostly interested in studying the case where the EM waves propagate in a plane perpendicular to the axes of the dielectric rods, i.e., in the $x_1x_2$ plane. The *E* polarization, in which the electric field vector is parallel to the $x_3$ axis, is considered. The starting point is Maxwell's equations

$$\Delta \times E = i(\omega / c)E \tag{4.2}$$

where the dielectric constant $\varepsilon(r)$ is position dependent, and the authors seek solutions of Maxwell's equations which have the form $E(r)\exp(-i\omega t)$. The equation for the electric field *E* is

$$\left(\frac{\partial^2}{\partial x_1{}^2} + \frac{\partial^2}{\partial x_2{}^2}\right)E + \varepsilon\frac{\omega^2}{c^2}E = 0 \tag{4.3}$$

after the necessary mathematical operation, the authors come to

$$\left(4 - \frac{\omega^2 b^2}{c^2}\varepsilon_{i,j}\right)E_{i,j} - E_{i,j-1} - E_{i-1,j} - E_{i,j+1} - E_{i+1,j} = 0 \tag{4.4}$$

where the indices $i$ and $j$ denote the $x_1$ and $x_2$ axes, respectively, and $b$ is the distance between neighboring nodes in a uniform discrete 2D mesh. Eq. (4.3) can be solved by the plane-wave expansion method when the dielectric function $\varepsilon$ is a periodic function. It is proper to note here that comparison of the calculated transmission coefficient with experimental studies is excellent. However, Eq. (4.4) is exactly equivalent to the well-studied problem of the tight-binding model of electronic localization (MacKinnon and Kramer, 1981: Soukoulis et al, 1982: Pendry et al, 1992). In particular, the most successful method in obtaining the localized or extended nature of the wave functions in disordered and/or periodic electronic systems in the transfer-matrix technique. Eq. (4.4) can be solved by the transfer-matrix technique, where the electric fields $E$ on one side of a structure are related to those on the other. From this point, the transmission coefficient through a particular dielectric arrangement can be calculated. Eq. (4.4) can be used to calculate the transmission coefficients for disordered dielectric structures, as well as for a periodic dielectric structures with one or more imperfections.

Moreover, with the help of transfer matrix method, field distributions and the transmission spectra of Fibonacci samples can easily be calculated. (Pendry, 1994: Kavokin et al, 2000)

Kuhl and Stöckmann (2001) showed that there is a close correspondence between one-dimensional tight-binding systems, and the propagation of microwaves through a single-mode waveguide with inserted scatterers. Since the pioneering paper of Anderson (1958) a lot of work has been done in the theoritical studies of the one-dimensional tight-binding Scrödinger equation;

$$\psi_{n+1} + V_n\psi_n + \psi_{n-1} = E\psi_n \tag{4.5}$$

where $V_n$ are the potentials at site $n$, and $\psi_n$ is the amplitude of the wave function. Depending on the site potentials a number of different situations can be found. For constant $V_n$ regular allowed and forbidden transmission bands are observed, in complete analogy to electronic Bloch bands in crystalline solids.

Kuhl and Stöckmann also showed that a very similar transfer matrix equation governs the propagation of electromagnetic waves through a one-dimensional array of scatterers. This is the starting point of the experimental approach to the study of tight-binding Schrödinger equations.

Aside from Anderson localization, a more subtle kind of localization, "dynamical localization", may occur in classically chaotic systems. Here the disorder is not imposed on the system, but generated dynamically due to the chaotic features of the system (Casati et al, 1979: Fishman et al, 1982: Shepelyansky, 1986: Casati et al, 1987) . 2D chaotic billiards proposed recently as fruitful systems for the study of dynamical localization (Borgonovi et al, 1986) . At the interface between disorder and chaos are rough billiards, e.g. weakly deformed circular billiards introduced by Frahm and Shepelyansky (1997a: 1997b). It is this circular billiard perturbed by a rough boundary that the paper of Sirko et al (2000) addresses. They report the first experimental observation of dynamical localization in a rough billiard.

If we would like to approach the solution in finding the transmisson coefficient plane-wave method may be helpful; A different theory is developed to cope with the difficulty of the multiple-scattering problem in a random medium (RM) by Ogura (1975). The form of the solution has some analogy with Floquet's solution for a periodic medium. It is shown that there are two kinds of solutions in the one-dimensional RM: a travelling-wave mode and a cutoff mode. The former exists only when the power spectrum of the medium becomes zero at nearly double the wave number. Otherwise the wave is in the cutoff mode which is almost a standing wave whose envelope increases or decreases exponentially with distance. The average value of the wave and the transmission coefficient of a medium with finite thickness are also studied using the stochastic solution.

Although the theory is intended to be applicable to the three-dimensional (3D) case, Ogura (1975) starts his investigation with 1D case here. The refractive index of the medium is assumed to be a strictly stationary random process on the 1D coordinate.

To obtain a concrete solution, Ogura assumes that the random medium is a Gaussian stationary process generated by the Brownian-motion process, and accordingly the solution given in a possible form is expressed in terms of multiple Wiener integrals(Wiener, 1958: Ogura, 1972)

The method introduced here is also applicable to a lossy random medium immediately and to the other non-Gaussian random media, such as medium with random point scatterers: in this case the multiple Wiener integral with respect to the Poisson process can be useful. (Ogura, 1972)

Let the 1D wave equation be

$$\Delta^2\psi(x,\omega)+k^2n^2(x,\omega)\psi(x,\omega)=0, \quad \Delta\equiv\frac{d}{dx}, \tag{4.6}$$

where $\omega$ is the probability parameter denoting a sample point in the sample space $\Omega$, and the square of the random refractive index $n^2(x,\omega)=1+\varepsilon(x,\omega)$ where $\varepsilon(x,\omega)$ is the small fluctuating part with zero mean.

Ogura then comes to the solution;

$$\psi(x,\omega)=\exp\left(\int_0^x \lambda(T^a\omega)da\right)u(T^x\omega), \tag{4.7}$$

where $u(T^x\omega)$ is a stationary process derived from the random initial value $u(\omega)\equiv\psi(0,\omega)$. Eq. (4.7) gives a possible form of the solution, which is analogous to the well-known Floquet solution (Whittaker and Watson, 1927)

The cutoff mode never transports the energy through the infinite medium. If the medium is of finite thickness, however, the energy is transferred by the leakage like the tunnel effect though a cutoff microwave wave guide. Then, for a medium thick enough, the energy transfer decreases exponentially with increasing thickness. We treat this problem as a boundary-value problem using the two independent solutions of the cutoff modes. Let the increasing and decreasing modes be $\psi_1(x)$ and $\psi_2(x)$, respectively. Then the wave in the medium can be expressed as $\psi(x)=a\psi_1(x)+b\psi_2(x)$. Matching the boundary conditions at $x$=0, and $x$=$L$, where $L$ denotes the thickness, we obtain the complex transmission coefficient,

$$T = \frac{2ik \begin{pmatrix} \psi_1(0) & \psi_2(0) \\ \psi_1'(0) & \psi_2'(0) \end{pmatrix}}{\begin{pmatrix} \psi_1'(L) - ik\psi_1(L) & \psi_2'(L) - ik\psi_2(L) \\ \psi_1'(0) + ik\psi_1(0) & \psi_2'(0) + ik\psi_2(0) \end{pmatrix}} \tag{4.8}$$

The numerator is the Wronskian which is a constant independent of *L.* For large *L,* $\psi_2(L)$ and $\psi_2'(L)$ are negligible, so that asymptotic expression of $1/T$ becomes

$$\frac{1}{T} \sim \text{const x} \exp\left( -ikL + \int_0^L \lambda_A^*(T^x\omega)dx \right) \tag{4.8}$$

Eqs. (4.7) and (4.8) are the formulas calculating the transmission coefficient in a homogeneous random medium.

Klyatskin and Gurarie (1999) review a simple boundary value problem, namely the 1D stationary wave problem. They consider an inhomogeneous layered medium occupying strip $L_0 < x < L$. A plane wave of unit amplitude $u_0(x) = e^{-ik(x-L)}$ is incident upon it from the right half-space $x > L$. The wave field in the strip obeys the Helmholtz equation

$$\frac{d^2}{dx^2}u(x) + k^2\left[1 + \varepsilon(x)\right]u(x) = 0 \tag{4.9}$$

with function $\varepsilon(x)$ representing inhomogeneities of the media. They assume $\varepsilon = 0$ outside the strip, and $\varepsilon(x) = \varepsilon_1(x) + i\gamma$ within, the real part $\varepsilon_1(x)$ responsible for the wave scattering, while imaginary one $\gamma$ describing wave attenuation by the media. In the right half space $x > L$ the wave field is made of the incident and reflected components $u(x) = e^{-ik(x-L)} + R_L e^{ik(x-L)}$ where $R_L$ is the (complex) reflection coefficient. In the left half $x < L_0$ we have $u(x) = T_L e^{ik(L_0 - x)}$ with the (complex) transmission coefficient $T_L$. The boundary conditions for (4.9) are continuity relations for $u$ and its derivative $\frac{d}{dx}$ at $x = L$; $L_0$

$$\left.\frac{i}{k}\frac{du}{dx} + u\right|_{x=L} = 2$$
$$\left.\frac{i}{k}\frac{du}{dx} - u\right|_{x=L_0} = 0 \tag{4.10}$$

So the wave field in the inhomogeneous medium is determined by the boundary value problem of Eqs. (4.9) and (4.10)

If parameter $\varepsilon_1$ is random, one is interested in the statistics of the reflection and transmission coefficients: $R_L = u(L) - 1$, and $T_L = u(L_0)$, that depend on the boundary values of the wave-field Eqs. (4.9) and (4.10), as well as the field intensity $I(x) = |u(x)|^2$ within the layer (statistical radiative transport). Equation (4.9) implies the energy conservation (dissipation) law at $x < L$

$$kI(x) = \frac{d}{dx}S(x) \tag{4.11}$$

where $S(x)$ denotes the energy-density flux

$$S(x) = \frac{1}{2ik}\left[u(x)\frac{d}{dx}u^*(x) - u^*(x)\frac{d}{dx}u(x)\right] \tag{4.12}$$

Furthermore, one has

$$S(L) = 1 - |R_L|^2 ; S(L_0) = |T_L|^2 \tag{4.13}$$

If the medium does not dissipate waves $(\gamma = 0)$, then the energy-conservation yields

$$|R_L|^2 + |T_L|^2 = 1 \tag{4.14}$$

If it is turned to some special features of the stochastic boundary value of Eqs. (4.9) and (4.10), in the absence of medium fluctuations, $\varepsilon_1(x) = 0$, and sufficiently small attenuation, the field intensity decays exponentially inside the layer as

$$I(x) = |u(x)|^2 = e^{-k\gamma(L-x)} \tag{4.15}$$

It is proper to note that a clearly perceived exponential fall-off trend are observed accompanied by large intensity fluctuations, directed both ways (to zero and to infinity). They result from the multiple scattering processes in randomly inhomogeneous media, and demonstrate the so called dynamic localization.

Boundary value problems of Eqs. (4.9) and (4.10) could be solved by the imbedding method of the works (Casti and Calaba, 1973: Bellman and Wing, 1992: Kagiwada and Kalaba, 1974) that reformulates them as initial value problems in parameter *L*- the right boundary end of the strip [11]. Thus the reflection coefficient $R_L$ of Eqs. (4.9) and (4.10) obeys the Riccati equation in *L*,

$$\frac{d}{dL} R_L = 2ikR_L + \frac{ik}{2}\varepsilon(L)(1+R_L)^2; R_{L_0} = 0, \tag{4.16}$$

whereas field $u(x) = u(x;L)$ inside the layer obeys the linear equation

$$\begin{gathered} \frac{d}{dL} u(x;L) = iku(x;L) + \frac{ik}{2}\varepsilon(L)(1+R_L)u(x;L) \\ u(x;x) = 1 + R_x. \end{gathered} \tag{4.17}$$

Indeed, writing *R* in the phase-amplitude form $R = Ae^{i\phi}$, we can recast Riccati Eq. (4.16) as a coupled system

$$\begin{cases} \dfrac{d}{dL}\phi = k\left[(2+\varepsilon)A + \dfrac{\varepsilon}{2}\left(1+A^2\right)\cos\phi\right] \\ \dfrac{d}{dL}A = k\dfrac{\varepsilon}{2}\left(1-A^2\right)\sin\phi \end{cases} \tag{4.18}$$

Hence follows the equation for the squared modulus of the reflection coefficient $W_L = |R_L|^2$

$$\frac{d}{dL}W_L = -2k\gamma W_L - \frac{ik}{2}\varepsilon_1(L)(R_L - R_L^{\ *})(1-W_L), \qquad W_{L_0} = 0. \tag{4.19}$$

If boundary $L_0$ is completely reflective, the initial condition becomes $W_{L_0} = 1$. So in the absence of damping $(\gamma = 0)$ the incident wave is fully reflected, $W_L = 1$. Hence the reflection coefficient $R_L = \exp\{i\phi_L\}$, and Eq. (4.16) would imply the following evolution of the “reflection phase”

$$\frac{d}{dL}\phi_L = 2k + k\varepsilon_1(L)(1+\cos\phi_L) \tag{4.20}$$

valid through the entire range $(-\infty, \infty)$ of variable $\phi_L$.

Pogrebnyak (1980) investigated the reflection of plane monochromatic waves when the source is located inside a layer with a specularly reflecting wall. Although the one-dimensional problem has been investigated well enough in a theoretical respect, the choice of the particular model allows to obtain more detailed information about the process of multiple scattering. Problems of wave propagation in long lines and waveguides and of sound propagation in a plane-layer medium are reduced to the one-dimensional case.

A point source emitting plane monochromatic waves whose scalar field u(x) satisfies the stochastic differential equation is considered as

$$\frac{d^2u}{dx^2} + k^2\varepsilon'(x)u = -4x\delta(x)\,,\; k = \frac{\omega}{c} \tag{4.21}$$

It will be assumed that the randomly inhomogeneous medium occupies a layer of $0 \le x \le L$ , $-\infty \le y$ and $z \le \infty$ , and $\varepsilon'(x)$ describes the properties of the medium and is assigned within the layer in the form

$$\varepsilon'(x) = \varepsilon_1 + \varepsilon(x) \tag{4.22}$$

where $\varepsilon_1$ is the constant component and $\varepsilon(x)$ is a random function with an average of zero: $\langle \varepsilon(x) \rangle = 0$ . The rest of space is occupied by a medium with a constant value of $\varepsilon'(x) = \varepsilon_0$ . The interface x=0 represents a specularly reflecting wall for the waves, while the source is located at a point x=0 to the right of the mirror. Upon propagation from the source to the opposite boundary of the plate, the wave undergoes reflection from random inhomogeneities, which leads to a decrease in the wave amplitude at x=L and its increase near the source. The quantity

$$\langle D \rangle = \left\langle \frac{|u(0)|^2}{|u(L)|^2} \right\rangle \tag{4.23}$$

which is called the coefficient of internal reflection, can serve as a quantitative measure of such a redistribution of field intensity.

Pogrebnyak (1980) seeks the solution for $\langle D \rangle$ by taking the process $\varepsilon(x)$ as $\delta$ -correlated with a correlation function of the form

$$\langle \varepsilon(x)\varepsilon(x+\tau) \rangle = B\delta(\tau) \qquad B = \int_{-\infty}^{\infty} d\tau \langle \varepsilon(x)\varepsilon(x+\tau) \rangle \tag{4.24}$$

i.e., it is assumed that $\varepsilon(x)$ is a uniform steady process.

The statement of the problem in the form presented above is equivalent to another statement in which the source lies in the middle of a plate occupying the space of $-L \le x \le L$, with $\varepsilon(x)$ being an even function of x: $\varepsilon(x) = \varepsilon(-x)$. In this case, however, the $\delta$-correlation of the process $\varepsilon(x)$ in the interval of $-L \le x \le L$ is not satisfied owing to the parity of the function $\varepsilon(x)$, so that the initial equation must be reduced to the interval $0 \le x \le L$. It must also be noted that a problem with a source inside a layer is connected by the reciprocity principle with the problem of the field produced in the layer by an external source. Applying the standard technique for finding mean values for Markov processes, Pogrebnyak (1980) obtain the following result:

$$\langle D \rangle = \frac{\varepsilon_1 + \varepsilon_0}{2\varepsilon_1} \exp\left( \frac{k^2 BL}{2\varepsilon_1} \right) - \exp\left( \frac{k^2 BL}{4\varepsilon_1} \right) \left\{ \frac{\varepsilon_0 - \varepsilon_1}{2\varepsilon_1} \cos(2k\sqrt{\varepsilon_1} L) + \frac{kB(\varepsilon_1 + 3\varepsilon_0)}{16\varepsilon_1^{\delta/2}} \sin(2k\sqrt{\varepsilon_1} L) \right\} \quad (4.25)$$

Equation (4.25) is an expansion of the exact solution for $\langle D \rangle$ with respect to the small parameter $kB/\varepsilon_1 \ll 1$. As one would expect, the reflectivity of a randomly inhomogeneous plate increases exponentially with an increase in the thickness of the plate. It is important to note that the quantity $\varepsilon_0$ appears in the preexponential factor in Eq. (4.25). This means that for a plate of any thickness the interface of the media will make a contribution proportional to $\varepsilon_0$. It would seem that an increase in the thickness L of the layer must reduce the influence of the interface owing to the attenuation of the field in such a way that $\varepsilon_0$ should not appear in the answer as $L \to \infty$. This is not so, however; the dependence of Eq. (4.25) obtained indicates the coherent nature of the contribution from scatterers located on any sections of the wave propagation path.

### 4.4. Experimental Results and Discussion

#### 4.4.1. Experiment Mechanism

The transmission properties of the rectangular random waveguide which we modelled geometrically and theoretically in the preceding sections were investigated in this section experimentally. The lower plate of the waveguide has the profile the corrugations of whose heights $\xi$ are of the same, whereas the upper plate has plane plate. $d$ is the average thickness between the random and smooth plates, the bottom and the top surface of the waveguide respectively. The length of the structure is 120 cm which corresponded to 37 individual corrugations. The width of the structure is 6 cm, which is suitable for working with $TE_{10}$ only. The experiment setup is shown in Fig. 4.16.

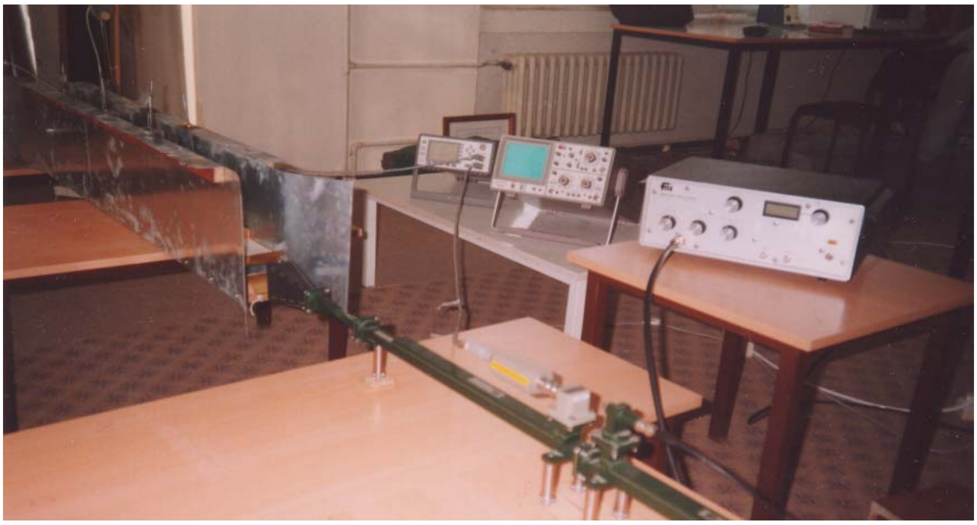

Fig. 4.16 Setup of the experiment. It consists of a digital power meter, an oscilloscope, a signal generator, and two X-band pyramidal horn antennas. Flares in both transmitting and receiving sides are added to the waveguide in order that they prevent undesirable reflections.

The standart microwave setup, consisting of oscillator, two couplers, Agilent E44196 power meter and two X-band pyramidal horn antennas were used for the measurements. The edges of the waveguide facing the receiving and transmitting antennas were flared in order to minimize reflections of the guided electromagnetic wave from edges. The schematic of the setup and the waveguide geometry are shown in Fig. 4.17. In the cartesian coordinate system the plates are paralel to the $zx-$plane.

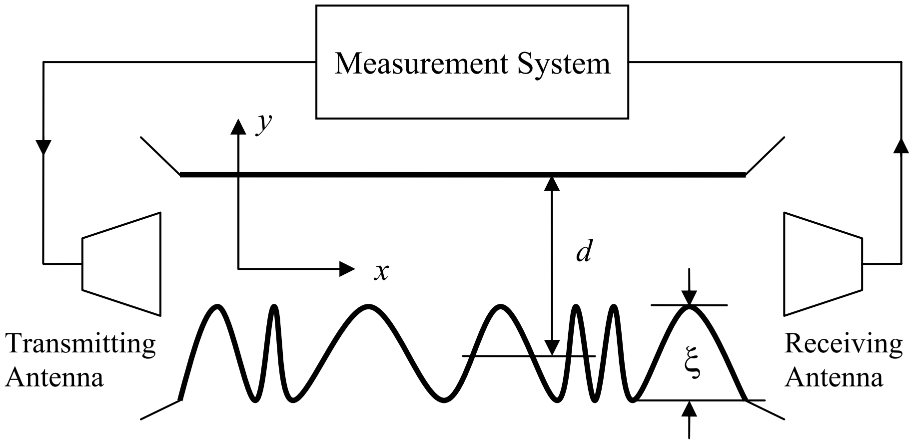


Fig. 4.17. Schematic of the experiment and geometry of the periodically corrugated waveguide. The *z*-axis is perpendicular to the plane of the picture.

**4.4.2. Experimental Results and Discussion**

The propagation of the TE wave, having the polarization vector ***E*** paralel to the grooves of the corrugation (the *z* axis), was investigated at the microwave range of frequency 8-12.5 GHz.

Fig. 4.18. shows the experimental data acquired with the thickness 31 mm. It is easily seen that the waveguide with random corrugations can create stop band like in a periodically corrugated waveguide. The gap starts from 9,643 GHz and ends 11,941 GHz, corresponding to 2,268 GHz band width.

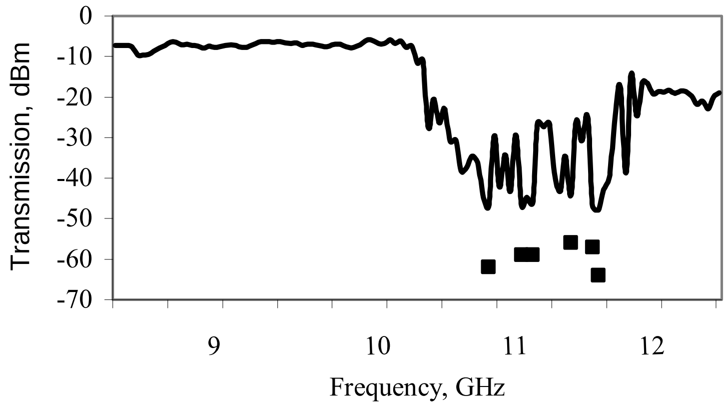


Fig. 4.18. Measured transmission characteristics for the rectangular waveguide having random corrugation with the average thickness $d$=31 mm. The width of the stop band is 2,268 GHz.

We measured the transmission characteristics of the random waveguide with different average thickness $d$ to investigate the effect on the transmission spectrum. Experiments showed that the more thickness of the waveguide we arrange, the narrower gap we obtain. Figs. 4.19. and 4.20. demonstrate the transmission characteristics obtained experimentally with the thicknesses 30 and 32 mm, respectively. If we take the data obtained from the experiment with $d$=31 mm into account for comparison as well we can conclude that the width of the stop band varies with the average thickness of the waveguide. The higher thickness we arrange the wider band we obtain. Experimental data are summarized in Table 4.1.

Table 2. Data obtained from the three consecutive experiments are summarized.

| Thickness, mm | Gap starts at, GHz | Gap ends at, GHz | Gap width, GHz |
|---|---|---|---|
| 30 | 9,659 | 12,169 | 2,51 |
| 31 | 9,643 | 11,911 | 2,268 |
| 32 | 9,333 | 11,349 | 2,016 |

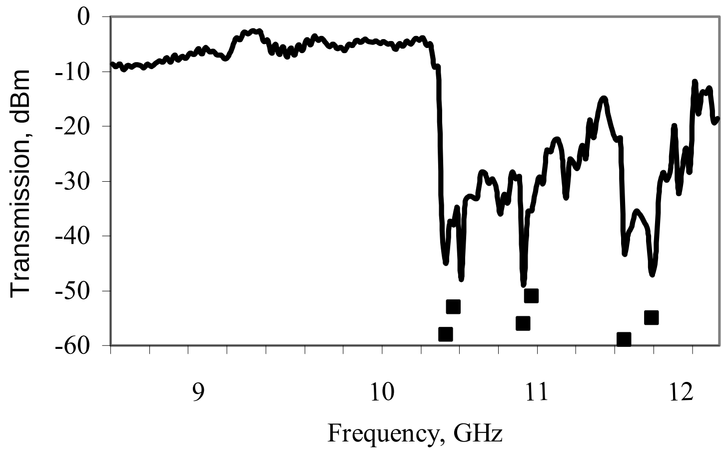


Fig. 4.19. Measured transmission characteristics for the rectangular waveguide having random corrugation with the average thickness $d$=30 mm. The width of the stop band is 2,51 GHz.

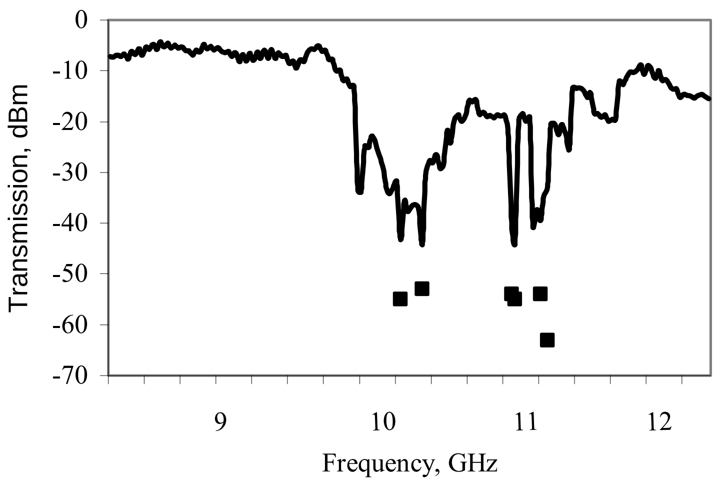


Fig. 4.20. Measured transmission characteristics for the rectangular waveguide having random corrugation with the average thickness $d$=32 mm. The width of the stop band is 2,016 GHz.

We also studied the effect of the dielectric material placed in the random waveguide. We have found that like in a periodically corrugated waveguide, a dielectric material such as foam rubber causes a shift in the spectrum in random waveguide. The comparison of the two experiments done with the same average thickness $d$=31 mm revealed this truth. A dielectric material such as foam rubber shifts the stop band to the lower frequency from 9,643 GHz to 9,341 GHz, corresponding to the shift of 0,302 GHz.

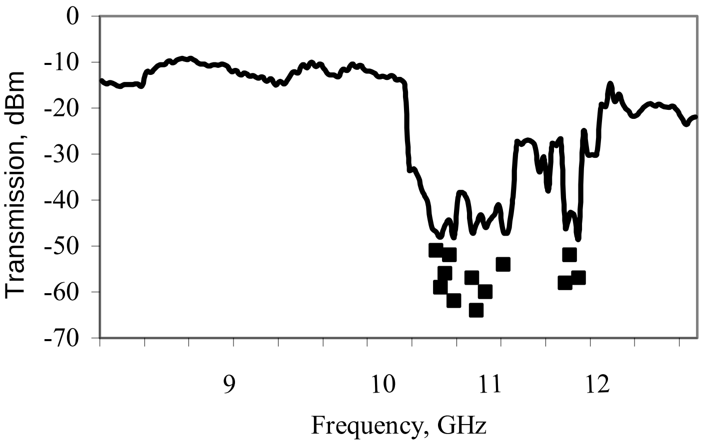


Fig. 4.21. Measured transmission characteristics for the rectangular waveguide having random corrugation with the average thickness $d$=31 mm. Foam plastic material is placed inside the waveguide to investigate the shift. The width of the stop band is 2,268 GHz which is the same value as in the experiment done with the averagege thickness $d$=31 mm, but without foam plastic material.

In view of the above experimental results we performed we see that in the transmission spectrum of the random waveguide, stop and pass bands appeared. This can be explained by localization phenomena. The wave is localized in the random waveguide, i.e. we proved the localization of waves in random medium as in the experiments done with photonic crystals, quasicrystals and laser.

Upon trying to find and constitute a geometrical and mathematical model for our random waveguide we took notice of the mechanism of the disorder and its effects to transmission spectrum of interest as from periodic to disordered case. The similar thing can be applied to our random waveguide. The random waveguide we designed is a new arrangement, yet we can compare the results obtained with the transmission spectrum of the periodically corrugated waveguide which we also designed and investigated theoritically and experimentally in this thesis. The period of the corrugation in the periodically corrugated waveguide we designed was 3.2 cm which was also the average of the random periods in the random waveguide of ours. In fact, the average period 3.2 cm was chosen intentionally in order that we can have an opportunity to compare both. The periods of the random waveguide vary between 0 and 6.4 cm, to which Gaussian probability distribution was applied in order to obtained average period 3.2 cm.

If compared, as expected, the stop band in the transmission spectrum of the random waveguide contains defect modes whereas the stop band resulting from Bragg reflection has no defect modes in the periodically corrugated waveguide.

In conventional lasers, emission is stimulated into well-defined cavity modes and emerges as a coherent beam. Care is taken to suppress scattering within the cavity since this would shorten the photon residence time in the lasing mode and thereby raise the excitation power required to initiate lasing. In the opposite limit of a random amplifying medium, however, multiple scattering impedes the flow of light out of the gain region (Letokhov, 1968: Ambartrsumyan et al, 1970). This has led to a search for lasing action in random amplifying media. However, multiple scattering also impedes the flow of the incident pump light into the sample (Genack and Drake, 1994: Wiersma et al, 1995). This creates a shallow gain region and allows subsequently emitted photons to escape promptly as diffuse luminescence. As a result, the lasing threshold in these diffusive systems is not appreciably lower than the power level at which stimulated emission surpasses spontaneous emission in a neat dye solution.

It is shown that (Milner and Genack, 2005) a collimated laser beam is produced at greatly reduced lasing threshold in a stack of microscope cover slides with interspersed dye films. The photon localization laser described is of simple design, which can be literally slapped together. Lasing is facilitated by resonant excitation of localized modes at the pump laser wavelength, which are peaked deep within the sample with greatly enhanced intensity. Emission occurs into long-lived localized modes overlapping the localized gain region. This mechanism overcomes a fundamental barrier to reducing lasing thresholds in diffusive random lasers, in which multiple scattering restricts the excitation region to the proximity of the sample surface.

From this point of view, a random amplifying medium can be modeled by the random waveguide we designed. Consequently, the microwave experiments assists the modeling the quantum phenomena in micro- and nanostructures and the observation of the effect of disorder in the structures at the most favorable conditions.

# 5. CONCLUSION

In conclusion, the tunability of the transmission spectrum of a planar periodically corrugated waveguide have been investigated theoretically and experimentally.

The 1.24 GHz band gap in the vicinity of the cutoff frequency of the third mode has been observed. Upon a shift of one of the plates with respect to another on a half period of corrugation, the gap vanished. In the latter case, that of the congruent boundaries, an electromagnetic wave was propagated in the periodic waveguide without Bragg reflection indicating on gapless folding of dispersions in the spectrum for a periodic waveguide.

In solid state terminology, the spectrum transformation corresponds to the metal-insulator transition, when the Fermi energy matches the gap. It is of interest to note that manifestations of periodicity in physics of the 0.5 nm diameter and 1 $\mu$m length carbon nanotube and of the above described corrugated waveguide have much in common. The conductive properties of carbon nanotubes depend strongly on the helicity of the lateral hexagonal periodicity along the tube and on the tube diameter. An atomic size change in the pitch of helicity, altering the symmetry of the periodicity from “armchair” to ”zigzag,” causes the metal insulator transition in the nanotube.

The wave properties of a periodic structure depend on a ratio between the wavelength and characteristic dimensions of the structure. Hence the observed microwave properties are useful for modeling of electron phenomena in periodic quantum structures. The principal condition of observation of the properties, caused by the periodicity in solids, is $l \gg a$, where $l$ is the electron mean free path, and $a$ is the period of the lateral modulation. It is a rigid enough condition that can be met usually at the helium temperature. The advantage of microwaves in such modeling is the very large “mean free path” of the electromagnetic wave, almost matching the electron mean free path in superconductors because losses in the hollow metallic waveguide are very small 0.1 $\mathrm{dBm}^{-1}$ at 10 GHz. Therefore, the mentioned condition is always met. Another advantage is that the microwave method enables an investigation of the dispersion of a seperate mode. Whereas in the physics of solids, it is a serious experimental problem. From this point of view, the laterally modulated quantum well can be modeled by the planar periodically corrugated waveguide. Consequently, the microwave experiments assists the modeling the quantum phenomena in micro- and nanostructures and the observation of the effect of periodicity in the structures at the most favorable conditions.

Aside from the investigation of the planar periodically corrugated waveguide the transmission spectrum of a random waveguide which we designed, manufactured, and tried to find geometrical and mathematical model was investigated experimentally. experimental results showed that stop and pass bands appeared in the transmission spectrum of the random waveguide. This can be explained by localization phenomena. The wave is localized in the random waveguide, i.e. we proved the localization of waves in random medium as in the experiments done with photonic crystals, quasicrystals and laser.

Upon trying to find and constitute a geometrical and mathematical model for our random waveguide we took notice of the mechanism of the disorder and its effects to the transmission spectrum of interest as from periodic to disordered case. The similar thing can be applied to our random waveguide. The random waveguide we designed is a new arrangement, yet we can compare the results obtained with the transmission spectrum of the periodically corrugated waveguide which we also designed and investigated theoritecally and experimentally in this thesis. The period of the corrugation in the planar periodically corrugated waveguide we designed was 3.2 cm which was also the average of the random periods in the random waveguide of ours. In fact, the average period 3.2 cm was chosen intentionally in order that we can have an opportunity to compare both. The periods of the random waveguide vary between 0 and 6.4 cm, to which Gaussian probability distribution was applied in order to obtained average period 3.2 cm.

When compared, as expected, the stop band in the transmission spectrum of the random waveguide contains defect modes whereas the stop band resulting from Bragg reflection has no defect modes in the periodically corrugated waveguide.

In conventional lasers, emission is stimulated into well-defined cavity modes and emerges as a coherent beam. Care is taken to suppress scattering within the cavity since this would shorten the photon residence time in the lasing mode and thereby raise the excitation power required to initiate lasing. In the opposite limit of a random amplifying medium, however, multiple scattering impedes the flow of light out of the gain region (Letokhov, 1968: Ambartrsumyan et al, 1970). This has led to a search for lasing action in random amplifying media. However, multiple scattering also impedes the flow of the incident pump light into the sample (Genack and Drake, 1994: Wiersma et al, 1995). This creates a shallow gain region and allows subsequently emitted photons to escape promptly as diffuse luminescence. As a result, the lasing threshold in these diffusive systems is not appreciably lower than the power level at which stimulated emission surpasses spontaneous emission in a neat dye solution.

It is shown that (Milner and Genack, 2005) a collimated laser beam is produced at greatly reduced lasing threshold in a stack of microscope cover slides with interspersed dye films. The photon localization laser described is of simple design, which can be literally slapped together. Lasing is facilitated by resonant excitation of localized modes at the pump laser wavelength, which are peaked deep within the sample with greatly enhanced intensity. Emission occurs into long-lived localized modes overlapping the localized gain region. This mechanism overcomes a fundamental barrier to reducing lasing thresholds in diffusive random lasers, in which multiple scattering restricts the excitation region to the proximity of the sample surface.

From this point of view, a random amplifying medium can be modeled by the random waveguide we designed. Consequently, the microwave experiments assists the modeling the quantum phenomena in micro- and nanostructures and the observation of the effect of disorder in the structures at the most favorable conditions.

## REFERENCES


ABEELUCK A. K., LITCHINITSER N. M., HEADLEY C., EGGLETON B. J., 2002. Analysis of Spectral Characteristics of Photonic Bandgap Waveguides. Optical Society of America, 1320-1333.

AGIO M., SOUKOULIS C. M., 2001. Ministop Bands in Single-defect Photonic Crystal Waveguides. Physical Review E, Volume 64, 055603.

AMBARTRSUMYAN R. V., BASOV N. G., KRYUKOV P. G., LETOKHOV V. S., 1970. progress in Quantum Electronics. Pergamon, Oxford, pp. 107.

ANDERSON P. W., 1958. Absence of Diffusion in Certain Random Lattices. Physical Review, Vol. 109, No. 5, pp. 1492-1505.

ARYA K., SU Z. B., BIRMAN J. L., 1986. Anderson Localization of Electromagnetic Waves in a Dielectric Medium of Randomly Distributed Metal Particles. Physical Review Letters, Vol. 57, No. 21, Pp. 2725-2728.

ASFAR O. R., 1997. A Novel Narrowband Waveguide Filter. IEEE, 2526-2529.

AXLINE R. M., FUNG A. K., 1978. Numerical Computation of Scattering from a Perfectly Conducting Random Surface. IEEE Transactıons on Antennas and Propagation, Vol. Ap-26, No. 3, pp. 482-488.

BAHAR E., RAJAN G. G., 1979. Depolarization And Scattering of Electromagnetic Waves by Irregular Boundaries for Arbitrary Incident and Scatter Angles Full-Wave Solutions. IEEE Transactıons on Antennas and Propagation, Vol. Ap-21, No. 2, pp. 214-225.

BAHAR E., 1980. Full-Wave Solutions for the Scattered Radiation Fields From Rough Surfaces with Arbitrary Slope and Frequency. IEEE Transactions on Antennas and Propagation, Vol. Ap-28, No. 1, pp. 11-21.

BAHAR E., FITZWATER M. A., 1984. Scattering Cross Sections For Composite Models Of Non-Gaussian Rough Surfaces For Which Decorrelation Implies Statistical Independence. IEEE, APS-2-2, pp. 41-44.

BAHAR E., 1991. Full Wave Analysis For Rough Surface Diffuse, Incoherent Radar Cross Sections With Height-Slope Correlations Included. IEEE Transactions On Antennas And Propagation, Vol. 39, No. 9, pp. 1293-1304.

BAHAR E., El-SHENAWEE M., 1991. Use Of Supercomputers To Evaluate Singly And Multiply Scattered Electromagnetıc Fields From Rough Surfaces. IEEE Transactions On Magnetics, Vol. 27, No. 5, pp. 4287-4290.

BAHAR E., EL-SHENAWEE M., 1993. Full Wave Multiple Scattering from one Dimensional Random Rouge Surfaces and High Frequency Stationary Phase Approximations. IEEE, pp. 1316-1319.

BAHAR E., EL-SHCNAWCE M., 1993. High Frequency Approximations to Multiple Scatter by Rough Surfaces That Exhibit Enhanced Backscatter. IEEE, pp. 234-236.

BAHAR E., LEE B. S., 1995. Full Wave Vertically Polarized Bistatic Radar Cross Sections for Random Rough Surfaces-Comparison with Experimental and Numerical Results. IEEE, pp. 205-213

BAHAR E., ZHANG Y., 1995. Scatter Cross Sectıons For Sea Surfaces Characterized A New Unified Full Wave Approach By Pearson-Moskowltz Spectral Density Function. IEEE, pp. 1728-1731.

BAHAR E., LEE B. S., 1996. Scatter Cross Sections For Two-Dimensional Random Rough Surfaces-Full Wave Analysis. IEEE, pp. 2180-2182.

BAL G., FREILIKHER V., PAPANICOLAOU G., RYZHIK L., 2000. Wave Transport along Surfaces with Random Impedance. Physical Review B, Vol. 62, No. 10, pp. 6228-6240.

BASS F. G., FREULICHER V. D., FUKS I. M., 1974. Propagation in Statistically Irregular Waveguides-Part I: Average Field. IEEE Transactions on Antennas and Propagation, Ap. 22, No. 22, pp. 278-288.

BAYINDIR M., TEMELKURAN B., OZBAY E., 2000. Tight-Binding Description of the Coupled Defect Modes in Three-Dimensional Photonic Crystals. Phys. Rev. Lett. Vol. 84, pp. 2140.

BAYINDIR M., TEMELKURAN B., OZBAY E., 2000. Propagation of photons by hopping: A waveguiding mechanism through localized coupled cavities in three-dimensional photonic crystals. Physical Review B, VOLUME 61, No. 18.

BAYINDIR M., CUBUKCU E., BULU I., TUT T., OZBAY E., SOUKOULIS C. M., 2001. Photonic Band Gaps, Defect Characteristics, and Waveguiding in Two-Dimensional Disordered Dielectric and Metallic Photonic Crystals. Physical Review B, Vol. 64, 195115-1 195115-7.

BAYINDIR M., CUBUKCU E., BULU I., OZBAY E., 2001. Photonic Band-Gap Effect, Localization, and Waveguiding in the Two-Dimensional Penrose Lattice. Physical Review B, Vol. 63, 161104(R).

BAYINDIR M., AYDIN K., OZBAY E., MARKOS P., SOUKOULIS C. M., 2002. Transmission Properties of Composite Metamaterials in Free Space. Applied Physics Letters Vol. 81, Number 1, 120-122.

BECKER K. M., 2004. Effect of Various Surface-Height-Distribution Properties on Acoustic Backscattering Statistics. IEEE Journal of Oceanic Engineering, Vol. 29, No. 2, pp. 246-259.

BORGONOVI F., CASATI G., LI B., 1996. Diffusion and Localization in Chaotic Billiards. Phys. Rev. Lett., Vol.77, pp. 4744.

BOURLIER C., BERGINC G., SAILLARD J., 2001. Theoretical Study On Two-Dimensional Gaussian Rough Sea Surface Emission And Reflection In The Infrared Frequencies With Shadowing Effect. IEEE Transactions On Geoscience And Remote Sensing, Vol. 39, No. 2, pp. 379-392.

BROSCHAT S. L., THORSOS E. I., ISHIMARU A., 1990. A Heuristic Algorithm For The Bistatic Radar Cross Section For Random Rough Surface Scattering IEEE Transactions On Geoscience And Remote Sensing. Vol. 28, No. 2, pp. 202-206.

BROSCHAT S. L., 1993. The Phase Perturbation Approximation For Rough Surface Scattering From A Pierson-Moskowitz Sea Surface. IEEE Transactions On Geoscience And Remote Sensing, Vol 31, No. 1, pp. 278-283.

BROCKELMAN R. A., HAGFOORS T., 1966. Note on the Effect of Shadowing on the Backscattering of Waves from a Random Rough Surface. IEEE Transactions on Antennas and Propagation,Vol. Ap-14, No. 5, pp. 621-62

BROWN G. S., 1978. Backscattering From A Gaussian-Distributed Perfectly Conducting Rough Surface. IEEE Transactions On Antennas And Propagation, Vol. Ap-26, No. 3, pp. 472-482.

BULATOV A., LIVDAN D., BIRMAN J. L., 1998. Statistical Properties of the Cumulative Phase of Electromagnetic Radiation Transmitted through a Waveguide with Random Scatterers. Physical Review E Vol. 57, No. 3, Pp. 3574-3578.

BURIN A. L., RATNER M. A., CAO H., CHANG S. H., 2002. Random Laser in One Dimension. Physical Review Letters, Vol. 88, No. 9, 093904.

BUSCH K., SOUKOULIS C. M., 1995. Transport Properties of Random Media: A New Effective Medium. Physical Review Letters, Vol. 75, No. 19, pp. 3442-3445.

CAO Z. Q., HU C., JIN G. L., 1991. Method of Equivalent Refractive indices in Multi-Quantum-Well Waveguides with Arbitrarily Shaped Base Periods**.** J. Opt. Soc. Am. B 8, 2519.

CAPAZ R. B., KOILLER B., DE QUEIROZ S. L. A., 1990. Gap States and Localization Properties of One-Dimensional Fibonacci Quasicrystals. Phys. Rev. B, Vol. 42, pp. 6402.

CASATI G., CHIRIKOV B. V., FORD J., IZRAILEV F. M., 1979. Stochastic Behaviour in Classical and Quantum Hamiltonian Systems. Lecture Notes in Physics, Vol. 93, Springer, Berlin, pp. 334.

CASATI G., CHIRIKOV B.V., GUARNERI I., SHEPELYANSKY D.L., 1987. Relevance of classical chaos in quantum mechanics: The hydrogen atom in a monochromatic field Phys. Rep., 154, 77.

CHABANOV A. A., GENACK A. Z., 2001. Photon Localization in resonant Media. Physical Review Letters, Vol. 87, No. 15, 153901.

CHAN C. T., DATTA S., HO K. M., SOUKOULIS. C. M., 1994. A7 Structure: A Family of Photonic Crystals. Physical Review B, Vol. 50, No. 3, 1988-1991.

CHAN T. K., KUGA Y., ISHIMARU A., CHARLIE T. C. 1996. Experimental Studies Of Bistatic Scattering From Two-Dimensional Conducting Random

Rough Surfaces. IEEE Transactions On Geoscience And Remote Sensing, Vol 34, No 3, pp. 674-680.

COLLARO A., FRANCESCHETTI G., MIGLIACCIO M., RICCIO D., 1999. Gaussian Rough Surfaces And Kirchhoff Approximation. IEEE Transactions on Antennas and Propagation, Vol. 47, No. 2, pp. 392-398.

COLLIN R. E., 1992. Electromagnetic Scattering From Perfectly Conducting Rough Surfaces (A New Full Wave Method). IEEE Transactions on Antennas and Propagation, Vol. 40, No.12, pp. 1466-1477.

COLLIN R. E., 1994. Scattering Of An Incident Gaussian Beam By A Perfectly Conducting Rough Surface. IEEE Transactions On Antennas And Propagation, Vol. 42, No. 1, pp. 70-74.

CULLIS A. G., CANHAM L. T., CALCOTT P. D., 1997. The Structural and Luminescence Properties of Porous Silicon. J. Appl. Phys. Vol. 82, pp. 909.

DATTA S., CHAN C. T., HO K. M., SOUKOULIS C. M., 1992. Photonic Band Gaps in Periodic Dielectric Structures: The Scalar Wave Approximation. Physical Review B, Vol. 46, No. 17, 10650-10656.

DE BOER J. F., VAN ROSSUM M. C. W., VAN ALBADA M. P., NIEUWENHUIZEN T. M., LAGENDIJK A., 1994. Probabilty Distribution of Multiple Scattered Light Measured in Total Transmission. Physical Review Letters, Vol. 73, No. 19, pp. 2567-2570.

DEMIR M. A., JOHNSON J. T., 2003. Fourth and Higher Order Small Perturbation Solution for Scattering From Dielectric Rough Surfaces. IEEE, pp. 412-415

DESIDERI J. P., MACON L., SORNETTE D., 1989. Observation of Critical Modes in Quasiperiodic Systems. Physical Review Letters, Volume 63, No. 4, 390-393.

DEYCH L. I., ZASLAVSKY D., LISYANSKY A. A., 1998. Statistics of the Lyapunov Exponent in 1D Random Periodic-on Average Systems. Physical Review Letters, Vol. 81, No. 24, pp. 5390-5393.

DEYCH L. I., YAMILOV A., LISYANSKY A. A., 2001. Local Polariton Modes and Resonant Tunneling of Electromagnetic Waves Through Periodic Bragg Multiple Quantum Well Structures. Physıcal Review B, Volume 64, 075321.

DEYCH L. I., EREMENTCHOUK M. V., LISYANSKY A. A., 2003. Scaling Properties of the One-Dimensional Anderson Model with Correlated Diagonal Disorder. Physical Review B, Vol. 67, 024205.

DEYCH L. I., EREMENTCHOUK M. V., LISYANSKY A. A., 2003. Statistics of Transmission in One-Dimensional Disordered Systems: Universal Characteristics of States in the Fluctuation Tails. Physical Review B, Vol. 68, 174203.

DOMINGUEZ-ADAME F., MALYSHEV V. A., 2004. A Simple Approach to Anderson Localization in One-Dimensional Disordered Lattices. American Association of Physics Teachers pp. 226-230.

ECONOMOU E. N., ZDETSIS A., 1989. Classical Wave Propagation in Periodic Structures. Physical Review B, Vol. 40, No. 2, 1334-1337.

EDREI I., KAVEH M., SHAPIRO B., 1989. Probability Distribution Functions for Transmission of Waves Through Random Media: A New Numerical Method. Physical Review Letters, Vol. 62, No. 18, pp. 2120-2123.

ELACHI C., 1976. Waves in Active and Passive Periodic Structures. Proceedings of IEEE, 1666-1698.

EL-KADY I., SIGALAS M. M., BISWAS R., HO K. M., SOUKOULIS C. M., 2000. Metallic Photonic Crystals at Optical Wavelengths. Physical Review B, Vol. 62, No. 23, 15299-15302.

EOM H. J., FUNG A. K., 1983. A Comparison Between Backscattering Coefficients Using Gaussian And Non-Gaussian Surface Statistics. IEEE Transactions On Antennas And Propagation, Vol. Ap-31, No. 4, July 1983, Pp. 635-638.

ESPINOSA F. R. M. D., JIMÉNEZ E., TORRES M., 1998. Ultrasonic Band Gap in a Periodic Two-Dimensional Composite. Volume 80, Number 6 Physical Review Letters, 1208-1211.

ESTEBAN J., REBOLLAR J. M., 1991. Characterization of Corrugated Waveguides by Modal Analysis. IEEE Transactıons On Microwave Theory And Techniqes, Vol. 39, No. 6, 937-943.

FISHMAN S., GREMPEL D. R., PRANGE R.E., 1982. Quantum, Recurrence, and Anderson Localization.

FUJIWARA T., OGAWA T., 1990. Quasicrystals (Berlin:Springer).

FOTEINOPOULOU S., 2001. In- and out-of-Plane Propagation of Electromagnetic Waves in Low Index Contrast Two Dimensional Photonic Crystals. Journal of Applied Physics Volume 89, Number 2, 824-830.

FRAHM K. M., SHEPELYANSKY D. L., 1997a. Quantum Localization in Rough Billiards. Phys. Rev. Lett., Vol. 78, pp. 1440.

FRAHM K. M., SHEPELYANSKY D. L., 1997b. Emergence of Quantum Ergodicity in Rough Billiards. Phys. Rev. Lett. Vol. 79, pp. 1833.

FREI W. R., JOHNSON H. T., 2004. Finite-Element Analysis of Disorder Effects in Photonic Crystals. Physical Review B, Vol. 70, 165116.

FREILIKHER V. D., TARASOV Y. V., 1991. Localization of the Field of a Point Source in a Randomly Layered Medium. IEEE Transactions on Antennas and Propagation, Vol. 39, No. 2, pp. 197-203.

FREILIKHER V. D., LIANSKY B. A., YURKEVICH I. V., MARADUDIN A. A., MCGURN A. R., 1995. Enhanced Transmission due to Disorder. Physical Review E, Vol. 51, No. 6, pp. 6301-6304.

FREILIKHER V., PUSTILNIK M., YURKEVICH I., 1997. Statistical Properties of the Reflectance and Transmittance of an Amplifying Random Medium. Physical Review B, Vol. 56, No. 10, pp. 5974-5977.

FUNG A. K., TJUATJA S., 2003. Advanced Models For Backscattering From Rough Surfaces. IEEE, KIMAS, pp. 659-663.

GALDI V., FELSEN L. B., CASTAÑON D. A., 2001. Quasi-Ray Gaussian Beam Algorithm For Time-Harmonic Two-Dimensional Scattering By Moderately Rough Interfaces. IEEE Transactions On Antennas And Propagation, Vol. 49, No. 9, pp. 1305-1314.

GARCIA-MARTIN A., LÓPEZ-CIUDAD T., SÁENZ J. J., NIETO-VESPERINAS M., 1998. Statistical Distribution of Intensities Reflected from Disordered Media. Physical Review Letters Vol. 81, No. 2. pp. 329-332.

GARCIA-MARTIN A., TORRES J.A., SÁENZ J. J., 1998. Intensity Distribution of Modes in Surface Corrugated Waveguides. Physical Review Letters, Vol. 80, No. 19, Pp. 4165-4168.

GARCIA-MOLINA R., RUIZ J., CHICAN R., ORTUNO M., GUNN J. M F., 1990. Reflection of electromagnetic Waves from rough Waveguides. IEEE Transactions on Microwave Theory and Techniques, Vol. 38, No. 4, pp. 445-448.

GARCIA-PABLOS D., SIGALAS M., ESPINOSA F. R. D. M., TORRES M., KAFESAKI M., GARCIA M., 2000. Theory and Experiments on Elastic Band Gaps. Physical Review Letters, Vol. 84, No. 19, 4349-4352.

GELLERMAN W., KOHMOTO M., SUTHERLAND B., TAYLOR P. C., 1994. Socalization of Light Waves in Fibonacci Dielectric Multilayers. Physical Review Letters, Vol. 72, No. 5, pp. 633-636.

GENACK A. Z., DRAKE J. M., 1994. Nature (London), Vol. 368, pp. 400.

GILBERT' M. S., JOHNSON J. T., 2003. A Study Of Rough Surface Scattering Effects Using The Higher-Order Small Slope Approximation. IEEE, pp. 557-560.

GIORGIO A., PASQUA D., PERRI A. G., 2003. Multiple Defect Characterization in Finite-Size Waveguiding Photonic Bandgap Structures. IEEE Journal of Quantum Electronics, Vol. 39, No. 12, pp. 1537-1547.

GU B., HUO C., GAN Z., YANGG., WANG J., 1992. Effects of Various Obstacles and Tunneling Disorder on the Quantized Conductance of an Electron Waveguide: Model of Two Coupled Chains. Physical Review B, Vol. 46, No. 20, pp. 13274-13288.

HARTMANN C. S., PLESSKY V. P., JEN S., 1995. 112O-LITA03 Periodic Waveguides. 1995 IEEE ULTRASONICS SYMPOSIUM, 63-66.

HASTINGS F. D., SCHNEIDER J. B., BROSCHAT S. L., THORSOS E. I., 2001. an FDTD Method for Analysis of Scattering From Rough Fluid–Fluid Interfaces. IEEE Journal of Oceanic Engineering, Vol. 26, No. 1, pp. 94-101.

HASTINGS F. D., SCHNEIDER J. B., BROSCHAT S. L., 1995. A Monte-Carlo FDTD Technique For Rough Surface Scattering. IEEE Transactions On Antennas And Propagation, Vol. 43, No. 2 , pp. 1183-119.

HATTORI T., TSURUMACHI N., KAWATO S., NAKATSUHA H., 1994. Photonic Dispersion Relation in a One-Dimensional Quasicrystal. Physical Review B, Vol. 50, No. 6, pp. 4220-4223.

HAWWA M. A., Asfar O. R., 1994. Coupled-Mode Analysis of Love Waves in a Filter Film with Periodically Corrugated Surfaces. IEEE Transactions on Ultrasonics, Ferroelectronics, and Frequency Control, Vol. 41, No. 1, 13-18.

HAWWA M. A., 1997. Acoustic/Elastic Stop-Band Interaction in Waveguides Involving Two Periodicities. Acoustical Society of America Vol. 102, 137-142.

HILL D. A. , 1989. Reflection Coefficient of a Waveguide With Slightly Uneven Walls. IEEE Transaction on Microwave Theory and Techniques, Vol. 37, No.1, pp. 244-252.

HO K. M., CHAN C. T., SOUKOULIS C. M., 1990. Exsistence of a Photonic Gap in Periodic Dielectric Structures. Physical Review Letters, Vol. 65, No. 25, 3152-3155.

HUANG X., GONG C., 1998. Property of Fibonacci Numbers and the Periodiclike Perfectly Transparent Electronic States in Fibonacci Chains. Physical Review B, Vol. 58, No. 2, pp. 739-744.

HUANG W., GUO Q., WU C., 1996. A Polarization-Independent Distributed Bragg Reflector Based on Phase-Shifted Grating Structures. IEEE Journal of Lightwave Technology, Vol. 14, No. 3, 469-473.

ISHIMARU A, PHU P., KUGA Y., 1987. Pulse Beam Wave Scattering from one-Dimensıonal Very Rough Surfaces: Experimental and Numerıcal Studies. IEEE, pp. 237-239.

ISHIMARU A., 1991. Electromagnetic wave Propagation, Radiation And Scattering. Prentice Hall, New Jersey.

ISHIMARU A., PHU P., KUGA Y., 1993. Pulse Beam Wave Scattering from One-Dimensional Very Rough Surfaces: Experimental and Numerical Studies.Geoscience and Remote Sensing Symposium. IGARSS'03. 'Better Understanding of Earth Environment.', International, Vol. 1, pp. 237-239.

ITO S., ADACHI S., 1997. Multiple Scattering Effect on Backscattering from a Random Medium. IEEE Transactions on Antennas And Propagation, pp. 205-208.

IZRAILEV F. M., MENDEZ-BERMUDEZ J. A., LUNA-ACOSTA G. A., 2003. Ballistic Localization in Quasi-One-Dimensional Waveguides with Rough Surfaces. Physical Review E 68, 066201.

IZRAILEV F. M., MAKAROV N. M., 2003. Onset of Delocalization in Quasi-One-Dimensional Waveguides with Correlated Surface Disorder. Physical Review B 67, 113402.

IZRAILEV F. M., MAKAROV N. M., 2005. Anomalous Transport in Low-Dimensional Systems with Correlated Disorder. J. Phys. A: Math. Gen., 0507629 V1.Pp. 1-26.

JOANNOPOULOS J. D., COHEN M. L., 1974. Effect of Disorder on the Electronic Density of States of III-V Compounds. Physical Review B, Vol. 10, No. 4, pp. 1545-1559.

JOHN S., 1984. Electromagnetic Absorption in a Disordered Medium near a Photon Mobility Edge. Physical Review Letters, Vol. 53, No. 22, pp. 2169-2172.

JOHN S., 1987. Strong Localization of Photons in Certain Disordered Dielectric Superlattices. Physical Review Letters, Vol. 58, No. 23, pp. 2486-2489.

KACZKOWSKI P. J., THORSOS E. I., 1994. Accuracy of Several Alternative Forms of The Operator Expansion Solution For Scattering From 1-D Randomly Rough Dirichlet Surfaces. IEEE, pp. 1096-1099.

KAFESAKI M., SOUKOULIS C. M., AGIO M., 2004. Losses and Transmission in Two-Dimensional Slab Photonic Crystals, Journal of Applied Physics, Vol. 96, No. 8, 4033-4038.

KAFESAKI M., SIGALAS M. M., GARCIA N., 2000. Frequency Modulation in the Transmittivity of Wave Guides in Elastic-Wave Band-Gap Materials. Physical Review Letters, Vol. 85, No. 19, 4044-4047.

KALITEEVSKI M. A., MARTINEZ J. M., CASSAGNE D., ALBERT J. P., BRAND S., ABRAM R. A., 2003. Appearance of Photonic Minibands in

Disordered Photonic Crystals. Journal of Physics: Condensed Matter 15, 785-790.

KALITEEVSKII M. A., 1998. Tech. Phys., Vol. 43, pp. 565.

KARL F. WARNICK, DAVID V. A., 1998. Finite Frequency Generalization of the Geometrical Optics Rough Surface Scattering Coefficient, IEEE, 1078-1081

KAVOKIN A., MALPUECH G., DI CARLO A., LUGLI P., ROSSI F., 2000. Photonic Bloch Oscillations in Laterally Confined Bragg Mirrors. Phys. Rev. B, Vol. 61, pp. 4413.

KAWAKAMI S., 2002. Analytically Solvable Model of Photonic Crystal Structures and Novel Phenomena. Journal of Lightwave Technology, Vol. 20, No. 8, pp. 1644-1650.

KLYATSKIN V. I., GURARIE D., 1999. Coherent Phenomena in Stochastic Dynamical Systems. Uspekhi Fizicheskikh Nauk. pp. 1-72.

KOENDERINK A. F., VOS W. L., 2005. Optical Properties of Real Photonic Crystals: Anomalous Diffuse Transmission. J. Opt. Soc. Am. B Vol. 22, No. 5, pp. 1075-1084.

KOHMOTO M., SUTHERLAND B., IGUCHI K., 1987. Localization in Optics: Quasiperiodic Media. Physical Review Letters, Vol. 58, No. 23, pp. 2436-2438.

KOSCHNY T., MARKOS P., ECONOMOU E. N., SMITH D. R., VIER D. C., SOUKOULIS C. M., 2005. Impact of Inherent Periodic Structureon Effective Medium Description of Let-Handed and Related Metamaterials. Physical Review B, Vol. 71, No. 245105.

KRISHEN K., KOEPSEL W. W., DURRANI S. H., 1966. Cross-Polarization Measurements and Their Relation to Target Surface Properties. IEEE Transactions on Antennas and Propagation, Vol. Ap-14, No. 5, pp. 629-635

KROHA J., SOUKOULIS C. M., WÖLFLE P., 1993. Localization of Classical Waves in a Random Medium: A Self –Consistent Theory. Physical Review B, Vol. 47, No. 17, pp. 11093-1096.

KROKHIN A., IZRAILEV F., KUHL U., STÖCKMANN H.-J., ULLOA S.E., 2002. Random 1D Structures as Filters for Electrical and Optical Signals. Physica E 13, pp. 695 – 698.

KUHL U., IZRAILEV F. M., KROKHIN A. A., STÖCKMANN H. J., 2000. Experimental Observation of the Mobility Edge in a Waveguide with Correlated Disorder. Applied Physics Letters Vol. 77, No. 5, pp. 633-635.

KUHL U., STÖCKMANN H.-J., 2001. Microwave Transmission Spectra in Regular and Irregular One-Dimensional Scattering Arrangements. Physica E 9 pp. 384-388.

KWAK J. H., JUN K. H., LIM K. S., 2002. Light Scattering Effect by Rough Surface of the Solar Cell Material. IEEE, pp. 1134-1137.

LETOKHOV V. S., 1968. JETP, Vol. 26, pp. 835

LI B., CHEN R. T., 2001. Optical Waveguide Superprism in 2-D Low Index Contrast Photonic Crystal. IEEE Conference proceedings, 149-150.

LI Q., CHAN C. T., HO K. M., SOUKOULIS C. M., 1996. Wave Propagation in Nonlinear Photonic Band-Gap Materials. Physical Review B, Vol. 53, No. 23, 15577-15585.

LI Z., JIN Y., 2000. Bistatic Scattering From Fractal Rough Surface in Numerical Finite Element Method. IEEE, pp. 382-385

LICCIARDELLO D. C., ECONOMOU E. N., 1975. Study of Localization in Anderson's Model for Random Lattices. Physical Review B, Vol. 11, No. 10, pp. 3697-3717.

LIDORIKIS E., SIGALAS M. M., ECONOMOU E. N., SOUKOLIS C. M., 1998. Tight-Binding Parametrization for Photonic Band Gap Materials. 7 Physical Review Letters, Volume 81, Number 7, 1405-1408.

LIDORIKIS E., SIGALAS M. M., ECONOMOU E. N., SOUKOULIS C. M., 2000. Gap Deformation and Classical Wave Localization in Disordered Two-Dimensional Photonic-Band-Gap Materials. Phys. Rev. B, Vol. 61, pp. R 13 458.

LIN C. Y., WANG L.A., 2001. A Wavelength- and Loss-Tunable Band-Rejection Filter Based on Corrugated Long-Period Fiber Grating. IEEE PHOTONICS TECHNOLOGY LETTERS, VOL. 13, NO. 4, 332-334.

LIU D., SARMA S. D., 1994. Universal Scaling of Strong-Field Localization in an Integer Quantum Hall Liquid. Physical Review B, Vol. 49, No. 4, pp. 2677-2690.

LOUZA S., AUDEH N. F., SANDHU G., 1989. Scattered Fields By Rough Surfaces. IEEE Proceedings - Southeastcon Session 11B2, pp. 566-571.

LOUZA S., AUDEH N. F., 1990. Scattering Of Horizontally Polarized Electromagnetic Fields By Random Surfaces. IEEE, pp. 157-160.

LOURTIOZ J. M., LUSTRAC D. A., et. al., 1999. Toward Controllable Photonic Crystals for Centimeter- and Millimeter-Wave Devices. Journal of Lightwave Technology, Vol. 17, 2025-2031.

LU J. P., BIRMAN J. L., 1986. Mistakes in Quasilattices. Physical Review Letters, Vol. 57, No. 21, pp. 2706-270.

MACKINNON A., KRAMER B., 1981. One-Parameter Scaling of Localization Length and Conductance in Disordered Systems. Phys. Rev. Lett., Vol. 47, pp. 1546-1549.

MAKAROV N. M., TARASOV Y. V., 1998. The Resonance Expansıon Method in Surface Scattering Problems: Transmittance of Narrow Rough-Boundary 2D Strips, MMET'98 proceedings, VIIth International Conference on Mathematical Methods in Electromagnetic Theory, Kharkov, Ukraine, pp. 891-893.

MAKAROV N. M., TARASOV Y. V., 1998. Localization of Waves in a Single-Mode Waveguide with Statistically Identical Rough Boundaries. MSMW'98 Symposium Proceedings, Kharkov, Ukraine, pp. 466-468.

MAKAROV N. M., TARASOV Y. V., 2001. Electron Localization in Narrow Surface-Corrugated Conducting Channels: Manifestation of Competing Scattering Mechanisms. Physical Review B, Volume 64, 235306 1-14.

MALLICK A. K., SANYAL G. S., 1978. Electromagnetic Wave Propagation in a Rectangular Waveguide with Sinusoidally Varying Width. IEEE Transaction on Microwave Theory and Techniques, Vol. MTT-26, no. 4, 243-249.

MARKOS P., SOUKOULIS C. M., 2005. Intensity Distribution of Scalar Waves propagating in a Random Media. Physical Review B, Vol. 71, 054201.

MATSUMOTO M., TSUTSUMI M., KUMAGAI N., 1986. Bragg Reflection Characteristics of Millimeter Waves in a Periodically Plasma-Induced Semiconductor, IEEE Tansaction on Microwave Theory and Techniques, MTT-34, no:4, 406-411.

MAYSTRE D., 1983. Electromagnetic Scattering from Perfectly Conducting Rough Surfaces in Resonance Region. IEEE Transactıons on Antennas and Propagation, Vol. Ap-31, No. 6, pp. 885-895.

MEADE R. D., BROMMER K. D., RAPPE A. M., JOANNOPOULOS J. D., 1991. Electromagnetic Bloch Waves at the Surface of a Photonic Crystal. Phys. Rev. B, Vol. 44, pp. 10961.

MEADE R. D., BROMMER K. D., RAPPE A. M., JOANNOPOULOS J. D., 1991. Photonic Bound States in Periodic Dielectric Materials. Physical Review B, Vol. 44, No. 24, pp. 13772-13774.

MEECHAM W. C., LIN W., 1987. Radiation Reflected From Random Rough Surfaces IEEE Journal of Oceanic Engineering, Vol. 12, No. 2, pp. 357-361.

MERLIN R., BAJEMA K., CLARKE R., JUANG F. Y., BHATTACHARYA P. K., 1985. Quasiperiodic GaAs-AlAs Heterostructures. Physical Review Letters, Vol. 55, No. 17, pp. 1768-1770.

MILNER V., GENACK A. Z., 2005. Photon Localization Laser: Low-Threshold Lasing in a Random Amplifying Layered Medium via Wave Localization. Physical Review Letters, Vol. 94, pp. 073901.

MIYAZAKI H., HASE M., MIYAZAKI H. T., KUROKAWA Y., SHINYA N., 2003. Photonic Material for Designing Arbitrarily Shaped Waveguides in two Dimensions Physical Review B 67, 235109.

MIZRAHI A., SCHACHTER L., 2003. Dielectric Bragg Accelerator. IEEE Proceedings of the 2003 Particle Accelerator Conference, 728-730.

MOUSSA R., POTEINOPOULOU S., ZHANG L., TUTTLE G., GUVEN K., OZBAY E., SOUKOULIS C. M., 2005. Negative Refraction and Superlens Behaviour in a Two-Dimensional Photonic Crystal. Physical Review B, Vol. 71, No. 085106.

NAKAYAMA J., OGURA H., 1977. Wave Propagation in a Random Periodic Structure. IEEE, AP-S Session 17, 1350.

NIELSEN J. B., SØNDERGAARD T., BARKOU S. E., BJARKLEV A., BROENG J., 2000. Two-Dimensional Kagomé Photonic Bandgap Waveguide. IEEE Photonics Technology Letters, VOL. 12, NO. 6, 630-632.

NIEUWENHUIZEN T. M., ROSSUM M. C. W. V., 1995. Intensity Distributions of Waves Transmitted through a Multiple Scattering Medium. Physical Review Letters, Vol. 74, No. 14, pp. 2674-2677.

NORI F., RODRIGUEZ J. P., 1986. Acoustic and Electronic Properties of One-Dimensional Quasicrystals. Phys. Rev. B, Vol. 34, pp. 2207.

OGURA H., 1972. IEEE Trans. Inform. Theory IT-18, 473.Orthogonal Functionals of the Poisson Process. Information Theory, IEEE Transactions. Vol. 18, pp. 473-481.

OGURA H., 1975. Theory of Waves in a Homogeneous Random Medium. Physical Review A, Vol. 11, No. 3, pp. 942-956.

OGURA H., WANG Z. L., 1994. Scattering of Guided Waves in a Waveguide with a Slightly Rough Boundary: Stochastic Functional Approach. Physical Review E, Vol. 50, No. 6, pp. 5006-5016.

OHNUKI S., CHEW W. C., 2004. A High-Frequency Approximation For Random Rough Surface Problems. IEEE, pp. 619-622.

OZBAY E., TUTTLE G., SIGALAS M., SOUKOULIS C. M., HO K. M., 1995. Defect Structures in a Layer-by-Layer Photonic Band-Gap-Crystal. Physical Review B, Vol. 51, No. 20, pp. 13961-13966.

PAK K., TSANG L., CHAN C. H.,1994. Studies Of Large Scale Random Rough Surface Problems With The Sparse-Matrix Flat-Surface Iterative Approach. IEEE, pp. 267-269.

PENDRY J. B., MACKINNON A., 1992. Calculation of Photon Dispersion Relations. Physical Review Letters, Vol. 69, No. 19, pp. 2272-2275

PENDRY J. B., MACKINNON A., ROBERTS P. J., 1992. Proc. R. Soc. London Ser. A 437, 67.

PENDRY J. B., 1994. Adv. Phys. Vol. 43, pp. 461.

PERAL E. CAPMANY J., 1997. Generalized Bloch Wave Analysis for Fiber and Waveguide Gratings. Journal of Lightwave Technology, Vol. 15, No. 8, pp. 1295-1302.

PLIHAL M., MARADUDIN A. A., 1991. Photonic Band Structure of Two-Dimensional Systems: The Triangular Lattice. Physical Review B, Vol. 44, No. 16, 8565-8571.

POGREBNYAK V. A., 1980. Field of a Point Source in a One-Dimensional, Randomly Inhomogeneous Medium with a Specularly Reflecting Wall. Plenum Publishing Corporation, 0033-8443/79/2211-0983$07.50

POGREBNYAK V. A., 2003. Geometric Resonances in a Periodic Waveguide, Journal of Applied Physics, 776-778.

POGREBNYAK V. A., 2004. Non-Bragg Reflections in a Periodic Waveguide, Optics Communications 202, 201-207.

PURICA M., BUDIANU E., KUSKO M., et.al., 2003. Analysis and Optimization of the Bragg Reflector for Tunable Photodetector with Planar Mirror Optical Microcavity on Silicon Substrate. IEEE, 155-158.

RAHMAT-SAMII Y., MOSALLAEI H., 2001. Electromagnetic Band-gap Structures: Classification, Characterization, and Application. IEEE 11th International Conference on Antennas and Propagation, 480, pp. 560-564.

RAHMAT-SAMII Y., 2003. The Marvels of Electromagnetic Band Gap (EBG) Structures: Novel Microwave and Optical Applications. IEEE, pp. 265-275.

RAMOS-MENDIETA F., HALEVI P., 1999. Surface Electromagnetic Waves in Two-Dimensional Photonic Crystals: Effect of the Position of the Surface Plane. Phys. Rev. B, Vol. 59, pp. 15112.

RICHARDS J. A., 1983. Analysis of Periodically Time-Varying Systems. Springer-Verlag.

RO R., VARADAN V. V., MA Y., VARADAN V. K., 1988. Facet Ensemble Method for Wave Scattering From Rough Surface. IEEE Ultrasonic Symposium, pp. 1075-1078.

ROBERTSON W. M., ARJAVALINGAM G., MEADE R. D., BROMMER K. D., RAPPE A. M., JOANNOPOULOS J. D., 1992. Measurement of Photonic Band Structure in a Two- Dimensional Periodic Dielectric Array. Physical Review Letters, Vol. 68, No. 13, 2023-2027.

SANCHEZ-GIL J. A., MARADUDIN A. A., LU J. Q., FREILIKHER V. D., 1995. Transmission of Electromagnetic Waves through Thin Metal Films with Randomly Rough Surfaces. Physical Review B, Vol. 51, No. 23, pp. 17100-17116.

SANCHEZ-GIL J. A., FREILIKHER V., YURKEVICH I., MARADUDIN A. A., 1998. Coexsistence of Ballistic Transport, Diffusion, and Localization in Surface Disordered Waveguides. Phys. Rev. Lett., Vol. 80, No. 5, 948-951.

SANCHEZ-GIL J. A., FREILIKHER V., MARADUDIN A. A., YURKEVICH I. V., 1999. Reflection and Transmission of Waves in Surface-Disordered Waveguides. Physical Review B 15, Vol. 59, No. 8, pp. 5915-5925.

SCALORA M., FLYNN R. J., REINHARDT S. B., FORK R. L., TOCCI M. D., BOWDEN C. M., LEDBETTER H. S., BENDICKSON J. M., DOWLING J. P., LEAVITT R. P., 1996. Ultrashort Pulse Propagation at the Photonic Band Edge: Large Tunable Group Delay With Minimal Distortion and Loss. Physical Review E, Vol. 54, No. 2, R1078-R1081.

SCHOMERUS, 2001. Transmission Delay Times of Localized Waves. Physical Review B, Vol. 64, 026606.

SELTZER J. E., 1972. Spatial Densities for Specular Points on a Gaussian Surface. IEEE Transactions on Antennas and Propagation, Vol. Ap-20, No. 6, pp. 723-731.

SHEPELYANSKY D.L., 1986. Localization of Quasienergy Eigenfunctions in Action Space. Phys. Rev. Lett. Vol. 56, pp. 677.

SIGALAS M. M., SOUKOULIS C. M., ECONOMOU E. N., CHAN C. T., HO K. M., 1993. Photonic Band Gaps and Defects in Two Dimensions: Studies of the Transmission Coefficient. Physical Review B, Vol. 48, No. 19, pp. 14121-14126.

SIGALAS M., SOUKOULIS C. M., ECONOMOU E. N., CHAN C. T., HO K. M., 1993. Photonic Band Gaps and Defects in Two Dimensions: Studies of the Transmission Coefficient. Physical Review B, Vol. 48, No. 19, pp. 14121-14126.

SIGALAS M. M., SOUKOULIS C. M., CHAN C. T., HO K. M., 1994. Electromagnetic-wave Propagation Through Dispersive and Absorptive Photonic-Band-Gap Materials. Physical Review B, Vol. 49, No. 16, 11080-11087.

SIGALAS M. M., CHAN C. T., HO K. M. SOUKOULIS C. M., 1995. Metallic Photonic Band-Gap Materials. Physical Review B, Vol. 52, No. 16, pp. 11744- 11751.

SIGALAS M. M., SOUKOULIS C. M., 1995. Elastic-Wave Propagation Through Disordered and/or Absorbtive Layered Systems. Physical Review B, Vol. 51, No. 5, pp. 2780-2789.

SIGALAS M. M., SOUKOULIS C. M., CHAN C.-T., TURNER D., 1996. Localization of Electromagnetic Waves in Two-Dimensional Disordered Systems. Physical Review B, Vol. 53, No. 13, pp. 8340-8348.

SIGALAS M. M., 1997. Elastic wave band gaps and defect states in two-dimensional composites. J. Acoust. Soc. Am. 101 (3), pp. 1256-1261.

SIGALAS M. M., HO K. M., BISWAS R., SOUKOULIS C. M., 1998. Theoretical Investigation of Defects in Photonic Crystals in the Presence of Dielectric Losses. Physical Review B Volume 57, Number 7, pp. 3815-3820.

SIGALAS M. M., BISWAS R., HO K. M., SOUKOULIS C. M., 1998. Theoretical Investigation of Off-Plane Propagation of Electromagnetic Waves in Two-Dimensional Photonic Crystals. Physical Review B, Vol. 58, No. 11, 6791-6794.

SIGALAS M. M., SOUKOULIS C. M., CHAN C. T., BISWAS R., HO K. M., 1999. Effect of Disorder on Photonic Band Gaps. Physical Review B, Vol. 59, No. 20, pp. 12767-12770.

SIRKO L., BAUCH S., HLUSHCHUK Y., KOCH P.M., BLUMEL R., BARTH M., KUHL U., STÖCKMANN H.-J, 2000. Observation of Dynamical Localization in a Rough Microwave Cavity. Physics Letters A 266, pp. 331–335

SØNDERGAARD T., ARENTOFT J., KRİSTENSEN M., 2002. Theoretical Analysis of Finite-Height Semiconductor-on-Insulator-Based Planar Photonic Crystal Waveguides. IEEE Journal of Lightwave Technology, Vol. 20, No. 8, 1619-1626.

SONG Q. H.,. LIU L. Y, LING T., XU L., WANG W. C., 2003. Narrow-Band Polarized Light Emission from Organic Microcavity Fabricated by Sol-Gel Technique. Appl. Phys. Lett., Vol. 82, pp. 2939.

SONG Q., WANG L., XIAO S., ZHOU X., LIU L., XU L., 2005. Random Laser Emission from a Surface-Corrugated Waveguide. Physical Review B 72, 035424.

SOUKOULIS C. M., ECONOMOU E. N., 1980. Localization in Disordered Two-Dimensional Systems. Physical Review Letters, Vol. 45, No. 19, pp. 1590-1593.

SOUKOULIS C. M., WEBMAN I., GREST G. S., ECONOMOU E. N., 1982. Study of Electronic States with Off-Diagonal Disorder in Two Dimensions. Phys. Rev. B, Vol. 26, pp. 1838-1841.

SOUKOULIS C. M., GREST G. S., 1991. Localization in Two-Dimensional Quantum Percolation. Physical Review B, Vol. 44, No. 9, pp. 4684-4688.

SOUKOULIS C. M., DATTA S., ECONOMOU E. N., 1994. Propagation of Classical Waves in Random Media. Physical Review B, Vol. 49, No. 6, pp. 3800-3811.

STADNIK Z. M., 1999. Physical Properties of Quasicyrstals, Springer-Verlag, Berlin-Heidelberg.

STERKE C. M. D., 1998. Superstructure Gratings in the Tight-Binding Approximation. Physical Review E, Vol. 57, No. 3, 3502-3509.

TAMIR T., WANG H. C., OLINER A. A., 1964. Wave Propagation in Sinusoidally Stratified Dielectric Media, IEEE Transactions on Microwave Theory And Techniques, 323-335.

TATARSKII V. I., TATARSKII V. V., 1998. Comparison of Scattering From Gaussian and Non-Gaussian Rough Surfaces Having The Same Spectrum. IEEE, pp. 1451-1454.

TATEIBA M., NANBU Y., 1994. Numerical Analysis of the Effective Propagation Constant of a Space Where Small Spheres With High Permittivity are Randomly Distributed. IEEE, pp. 554-556.

TEMELKURAN B., BAYINDIR M., OZBAY E., KAVANAUGH J. P., SIGALAS M. M., TUTTLE G., 2001. Quasimetallic Silicon Micromachined Photonic Crystals. Applied Physics Letters Volume 78, Number 3, 264-266.

TOPORKOV J. V., BROWN G. S., 2000. Numerical Simulations of Scattering from Time- Varying, Randomly Rough Surfaces. IEEE Transactions on Geoscience and Remote Sensing, Vol. 38, No. 4, pp. 1616-1625.

TSUJI M., MATSUMOTO S., SHIGESAVA H., TAKIYAMA K., 1983. Guided Wave Experiments with Dielectric Waveguides Having Finite Periodic Corrugation. IEEE Transaction on Microwave Theory and Techniques, MTT-31, no. 4, 337-344.

TSUJI M., SHIGESAVA H., TAKIYAMA K., 1983. Wave-Guiding Characteristics of Partially Corugated Dielectric Waveguides. IEEE MTT-S Digest, 296-298.

VAN LANGEN S. A., BROUWER P. W., BEENAKKER C. W. J., 1996. Nonperturbative Calculation Of The Probability Distribution Of Plane-Wave Transmission Through A Disordered Waveguide. Physical Review E, Vol. 53, No. 2, Pp. R1344-R1347.

VAN ALBADA M. P., DE BOER J. F., LAGENDIJK A., 1990. Observation of Long-Range Intensity Correlation in the Transport of Coherent Light through a Random Medium. Physical Review E, Vol. 64, No. 23, pp. 2787-2790.

VILLENEUVE P. R., PICHE M., 1992. Photonic Band Gaps in Two-Dimensional Square and Hexagonal Lattices. Physical Review B, Vol. 46, No. 8, 4969-4972.

VILLENEUVE P. R., PICHE M., 1992. Photonic Band Gaps in Two-Dimensional Square Lattices: Square and Circular Rods. Physical Review B, Vol. 46, No. 8, 4973-4975.

WANG C., BARRIO R. A., 1988. Theory of the Raman Response in Fibonacci Superlattices. Physical Review Letters, Vol. 61, No. 2, pp. 191-194.

WEBER J.-P., 1993. Spectral Characteristics of Coupled-Waveguide Bragg-Reflection Tunable Optical Filter. IEEE Proceedings, Vol. 140, No. 5, 275-284.

WEISS M., MÉNDEZ-BERMÚDEZ J. A., KOTTOS T., 2006. Resonance Width Distribution for High-Dimensional Random Media. Physical Review B, Vol. 73, No. 045103.

WHITTAKER E. T., WATSON G. N., 1927. Modern Analysis. Cambridge U. P., Cambridge, 4th ed.

WIENER N., 1958. Nonlinear Problems in Random Theory. M.I.T. Press, Cambridge, Mass. and Wiley, New York.

WIERSMA D., VAN ALBADA M. P., LAGENDJIK A., 1995. Nature (London), Vol. 373, pp.203.

WIERSMA D.S., SAPIENZA R., MUJUMDAR S., COLOCCI M., GHULINYAN M., PAVESI L., 2005. Optics of Nanostructured Dielectrics. Journal of Optics A: Pure and Applied Optics, S-190-S197.

WINGHAM D. J., DEVAYYA R. H., 1992. A Note On The Use Of The Neumann Expansion in Calculating The Scatter From Rough Surfaces. IEEE Transactions On Antennas And Propagation, Vol. 40, No. 5, pp. 560-563.

WU T. D., CHEN K. S., SHI J., FUNG A. K., 2001. A Transition Model For The Reflection Coefficient In Surface Scattering. IEEE Transactions On Geoscience And Remote Sensing, Vol. 39, No. 9, pp. 2040-2050.

WU S. C., CHEN M. F., FUNG A. K., 1988. Scattering From Non-Gaussian Randomly Rough Surfaces-Cylindrical Case. IEEE Transactions On Geoscience And Remote Sensing, Vol. 26, No. 6, pp. 790-798.

XIA M. Y., CHAN C. H., LI S. Q., HU J. L., TSANG L., 2001. Wavelet-Based Simulations Of Electromagnetic Scattering From Large-Scale Two-

Dimensional Perfectly Conducting Random Rough Surfaces. IEEE Transactions On Geoscience And Remote Sensing, Vol. 39, No. 4, pp. 718-725.

XIE X. C., WANG X. R., LIU D. Z., 1998. Kosterlitz-Thouless-Type Metal Insulator Transition of a 2D Electron Gas in a Random Magnetic Field. Physical Review Letters, Vol. 80, No. 16, pp. 3563-3666.

YABLANOVICH E., GMITTER T. J., MEADE R. D., RAPPE A. M., BROMMER K. D., JOANNOPOULOS J. D., 1991. Donor and Acceptor Modes in Photonic Band Structure. Physical Review Letters, Vol. 67, No. 24, pp. 3380-3383.

YANG T., BROSCHAT L., 1992. A Comparasion Of Scattering Model Results For Two-Dimensional Randomly Rougy Surfaces. IEEE Transactions On Antennas And Propagation, Vol. 40, No. 12, pp. 1505-1512.

YANG N., CHEN Z. N., 2005. Microstrip Line Periodic Structures with Capacitive and Resonant Element Loads. IEEE 391-394.

YARIV A., 1973. Coupled-Mode Theory for Guided-Wave Optics. IEEE Journal of Quantum Electronics, Vol. Qe-9, No. 9, 919-933.

YARIV A., NAKAMURA M., 1977. Periodic Structures for Integrated Optics. IEEE Journal of Quantum Electronics, 233-253.

YEH P., YARIV A., HONG C-S., 1977. Electromagnetic Propagation in Periodic Stratified Media. I. General Theory. J. Opt. Soc. Am. 67, 423.

YOON K., TAIEIBA M., UCHIDA K., 1999. Analysis of Electromagnetic Wave Scattering From Building Walls with Periodic and Random Surface. Electromagnetic Compatibility, IEEE, International Symposium, 19A305, pp. 284-287.

YU K., BLIOKH YU. P., FREILIKHER V. D., 2004. Resonances in One-Dimensional Disordered Systems: Localization of Energy and Resonant Transmission. J. Opt. Soc. Am. B, Vol. 21, pp. 11.

ZHANG B., KAHRIZI M., 2003. Wide Range Periodic Waveguide Temperature Sensor. IEEE 117-120.

ZHANG X., ZHANG Z., 2002. Non-Rayleigh Distribution of Reflected Speckle Intensities from Localized States Inside the Gap of Disordered Photonic Crystals. Physical Review B, Vol. 65, 245115.

ZHANG Z. Q., WONG C. C., FUNG K. K., HO Y. L., CHAN W. L., KAN S. C., CHAN T. L., CHEUNG N., 1998. Observation of Localized Electromagnetic Waves in Three-Dimensional Networks Of Waveguides. Physical Review Letters, Volume 81, Number 25, pp. 5540-5543.

ZHOU L., TSANG L., JANDHYALA V., CHEN C., 2001. Studies On Accuracy Of Numerical Simulations Of Emission From Rough Ocean-Like Surfaces. IEEE Transactions On Geoscience And Remote Sensing, Vol. 39, No. 8, pp. 1757-1763.

## AUTOBIOGRAPHY

I was born in Adana on 13th of June 1977. I had my high school education in Adana Engine Vocational School between years 1991-1994. I entered the Electrical&Electronics Engineering Department of Ege University from which I graduated in 2001.

As soon as I graduated I started to work at a company serving in the medical field as Field Clinical Engineer (FCE). For the first one and half year my duty was to implant pacemaker, Heart Failure Device, and Implantable Cardioverter Defibrillator into patients with doctors in operating room. Moreover, I had also been technical service responsible for the life saving devices called external defibrillators and AED's (Automated External Defibrillators)

In 2003, I started my Master programme (MSc) at Electrical&Electronics Engineering Department of Cukurova University. The field of the study in the Master program was on Tunable Tranmission Spectrum of a Periodically Corrugated Waveguide in microwave frequency range. Besides, I took two courses related to medical instruments in order to support my job scientifically.

As from the very beginning of 2003, I continued my work to serve as an FCE in electrophysiology field, by especially focusing on mapping of and navigation through heart as Turkey region responsible. I composed the 123 pages booklet explaining everything about Non-contact mapping, navigation systems named 'Ensite 3000+ advanced mapping and Navigation System' both in English and Turkish languages

I completed my MSc program in 2006. During my research work in the master programme, the scientific results I obtained were presented both in national and international conferences, and published in a journal. Details of the conferences participated in, and the journal are given in the introduction section of the present thesis.

On the other hand, I took many trainings and their certificates regarding the jobs I have done. Details are below;

1. Zoll Medical U.K., Manchester/UK. 1-4/March/2006 Technical Training on Zoll 1400/2000 Pacemaker/Defibrillator Full Service.

2. Zoll Medical U.K., Manchester/UK. 4-8/April/2005 Technical Training on Zoll Charger Products&Batteries Full Service.

3. Zoll Medical U.K., Manchester/UK. 4-8/April/2005 Technical Training on Zoll M-Series Pacemaker/Defibrillator Full Service.

4. Endocardial Solutions, Minneapolis/Minnesota/USA. 9-13/August/2004 Technical Training on the Basics of Ensite System and Simultaneous Mapping.

5. Endocardial Solutions, Brussel/Belgium. 12-14/August/2003 Technical Training on the Basics of Ensite System and Introduction to Mapping.

6. Cardiac Impulse, Florence/Italy. 12-14/May/2003 Technical Training on the Basics of Pacemaker.

7. Guidant, Brussels/Belgium. 4-8/February/2002 Technical Training on the Basics and Implantation Procedures of Pacemaker.

## APPENDICES

### Appendix I: Analog and Digital Powermeter Comparison Experiments

Comparative power meter sensitivity experiment in a smooth planar waveguide with two different kinds of powermeters. Thickness between parallel plates is 18 mm. Cutoff frequency is 10.824 GHz. If results obtained from analog powermeter in Fig. I.1. are compared with that of Fig. I.2., it is easily realized that digital power meter is more sensitive and precise than analog power meter.

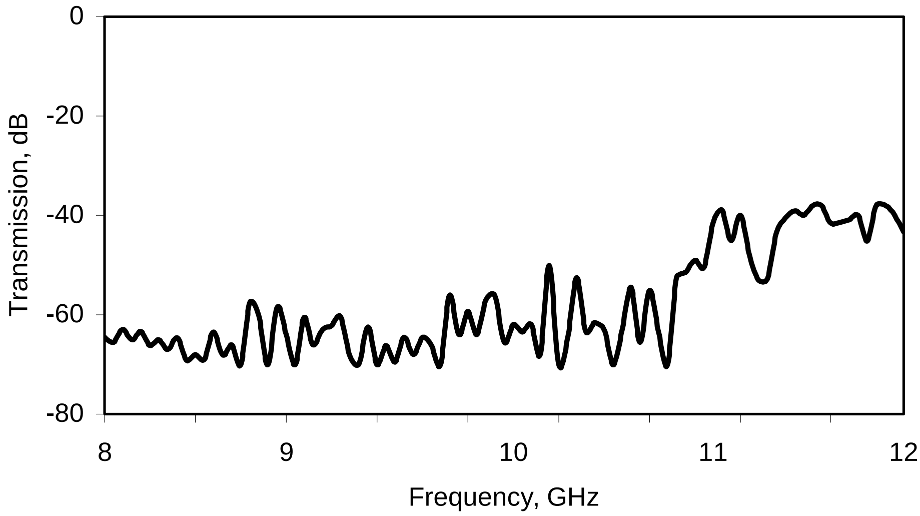


Fig I.1. Values acquired from analog powermeter in dB.

In view of this experimental result, we concluded that using digital power meter in our experiments will provide us more precise measurement than that of analog power meter, and therefore we used the digital power meter for all of the measurements of ours.


Fig. I.2. Values acquired from digital powermeter in dBm

**Appendix II:**

**Definition, and Investigation Experiments of Cutoff Frequency in Rectangular Smooth Waveguide**

How cutoff frequency arises in a rectangular waveguide is demonstrated here theoritically in a parallel plate waveguide for simplicity and is investigated experimentally in a rectangular smooth waveguide.

Consider a wave propagating along a parallel plate waveguide. The wave is also arranged as the wave which is the superposition of two plane waves bouncing back and forth obliquely between the two conducting plates ($TM_1$, for example) as shown in Fig. II.1.

Propagation takes place only when $\cos\theta = \dfrac{\pi}{\beta b} = \dfrac{\lambda}{2b}$. Here $\beta$, $\lambda$ and $b$ are propagation constant, wavelength and the distance between parallel plates respectively. As shown from the above equation solution exist only when $\dfrac{\lambda}{2b} \le 1$.

$\dfrac{\lambda}{2b} = 1$, or $f = \dfrac{1}{2b\sqrt{\mu\varepsilon}} = 1$, is the special case in which the waves bounce forth and back in the *y*-direction, normal to the parallel plates, and there is no propagation in the *z*-direction. It is called the Cutoff frequency.

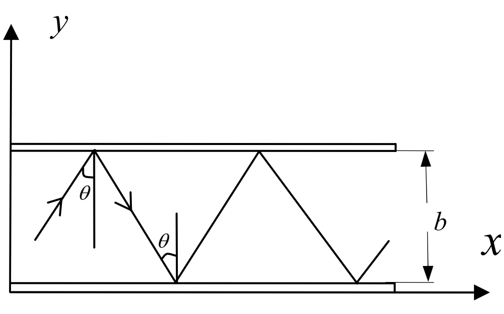


Fig. II.1. Propagation in parallel plate waveguide having metallic plates.

Cutoff frequency in a rectangular smooth waveguide having its rectangular cross section of sides *a* and *b* can be found by the following formula

$$\left(f_c\right)_{mn} = \frac{1}{2\sqrt{\varepsilon\mu}}\sqrt{\left(\frac{m}{a}\right)^2 + \left(\frac{n}{b}\right)^2} \quad \text{(Hz)} \qquad \text{(II.1)}$$

Here *m* and *n* denote mode numbers of wave propagating in the waveguide. On the other hand, because in our experiments $TE_{10}$ mode are investigated, the above formula takes such form

$$\left(f_c\right)_{10} = \frac{1}{2a\sqrt{\varepsilon\mu}} \quad \text{(Hz)} \qquad \text{(II.2)}$$

In Table I. cutoff frequencies for such a rectangular waveguide are calculated with the above formula.

Table I. Theoritical and experimental values corresponding to the concerning thickness are shown in Fig. II.1.

| Thickness (*a*), mm | Cutoff Frequency, GHz | | Frequency difference between theoritical and experimental, GHz |
|---|---|---|---|
| | Theoritical | Experimental | |
| 14 | 10,714 | 11,609 | 0,895 |
| 16 | 9,375 | 10,405 | 1,03 |
| 18 | 8,33 | 9,225 | 0,895 |

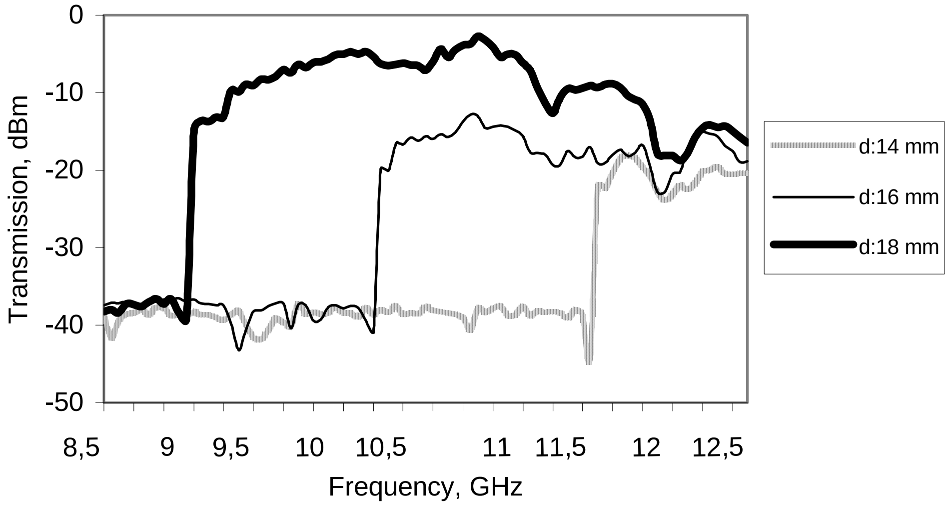


Fig. II.2. Cutoff frequencies in rectangular smooth waveguide with different thickness.

**Appendix III: Finding Permittivity of a Dielectric Material**

It is possible to find the permittivity of any dielectric material by a rectangular smooth waveguide, and it was also done in our experiments. The dimensions of the rectangular waveguide is as follows: length 1200 mm, thickness 16 mm, and width 60 mm. It is also suitable to say here that the thickness of the rectangular smooth waveguide can be varied between 0 and 200 mm so that it provides the user enough flexibility to cope. As discussed in Appendix II., cutoff frequency for $TE_{10}$ mode can be found with

$$(f_c)_{10} = \frac{1}{2d\sqrt{\varepsilon\mu}} \tag{III.1}$$

we expected to find the value for the case when the waveguide is hollow as 9,375 GHz theoritically, but we found 10, 206 GHz. Experimental results is shown in Fig. III.1 Since we did relative measurement the error contribution was not important because we have a chance to apply the same error upon calculating the cutoff frequency for the case when the waveguide is filled with the foam plastic material (dielectric material). We also found 9,829 GHz when the waveguide was filled with foam plastic material. The rate of cutoff frequencies of both cases gives the relative permittivity of the dielectric material of interest.

$$\frac{\left[(f_c)_{10}\right]_{free} = \dfrac{1}{2d\sqrt{\varepsilon_0\mu}}}{\left[(f_c)_{10}\right]_{dielectric} = \dfrac{1}{2d\sqrt{\varepsilon_r\varepsilon_0\mu}}} = \sqrt{\varepsilon_r} \tag{III.2}$$

With the help of above formula we found that the permittivity of the foam plastic material is $\varepsilon_r = 1{,}019$.

With this manner, the permittivity of any dielectric material can be calculated.

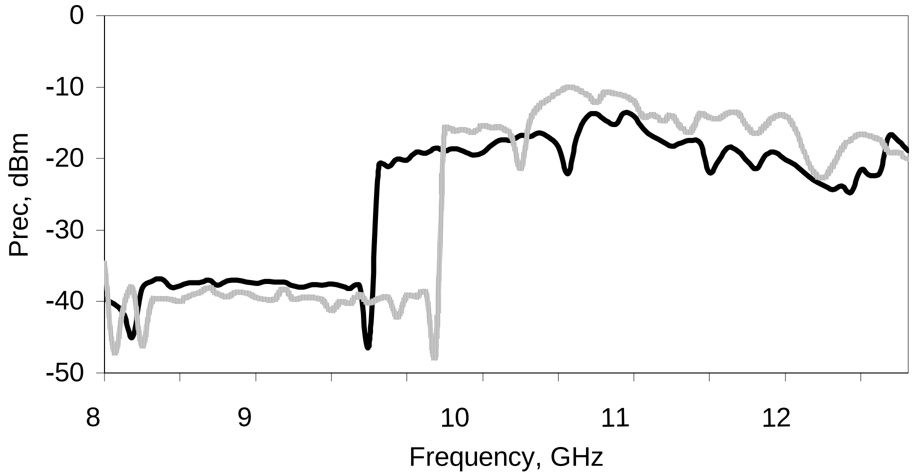


Fig. III. 1. The results of two experiments shown above provide us to compare the cut-off frequencies with the same thickness d:16 mm. Black line demonstrates the cutoff frequency when the waveguide is filled with foam plastic material whereas gray line denotes the cutoff frequency when the waveguide is hollow.

In conclusion, rectangular smooth waveguide can be used to calculate the permittivity of any dielectric material.

**Appendix IV: Additional Experiments**

Fig IV.1. shows the experimental result of Bragg band gap with the thickness $d$= 5,4 cm. The average depth and width of the gap are about 40 dB and 0.998 GHz, respectively.

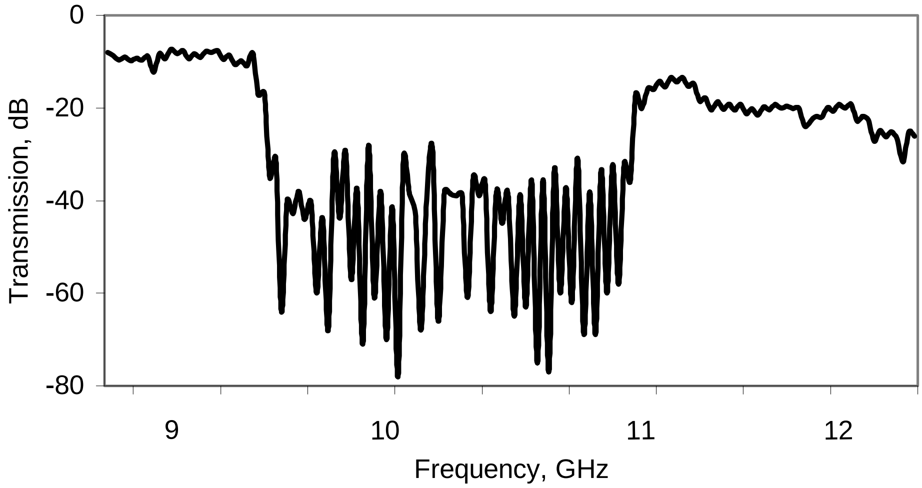


Fig IV.1. Experimental result of the Bragg band gap in periodically corrugated waveguide.

Fig. IV.2. shows the phase shift done in periodically corrugated waveguide. If compared with Fig. 3. 9., here oscillation arises in the vicinity of $\Delta x = a/2$ upon having been moved in the $x$-direction.

Additionally, two consecutive experiments were done to reveal the scattering behaviour of the planar periodically corrugated waveguide for two different, but fixed frequencies, one of which was in Bragg region while the other was chosen in non-Bragg side. Fig. IV.3. shows the scattered electromagnetic waves from periodically corrugated waveguide. The fixed frequency was chosen at Bragg gap region. (Gap starts from 9.40 GHz to 10.63 GHz, with a gap 1.23 GHz with the chosen thickness $d_r = 4.5$). Additional horn antenna was positioned in the place opposite the corrugations, and moved along the $x$-direction in order to measure the scattered power due to the corrugations. Measurement was started from the receiving side. Abbreviations are as follows: F: far, M: middle, C: close. (The points are named by taking the distance with respect to the *z*-axis into notice).

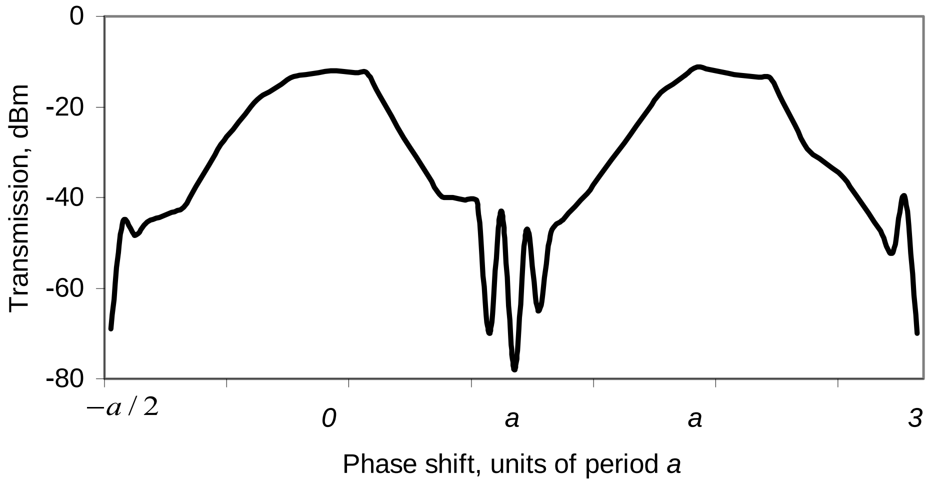


Fig. IV.2. Phase shift experiment.

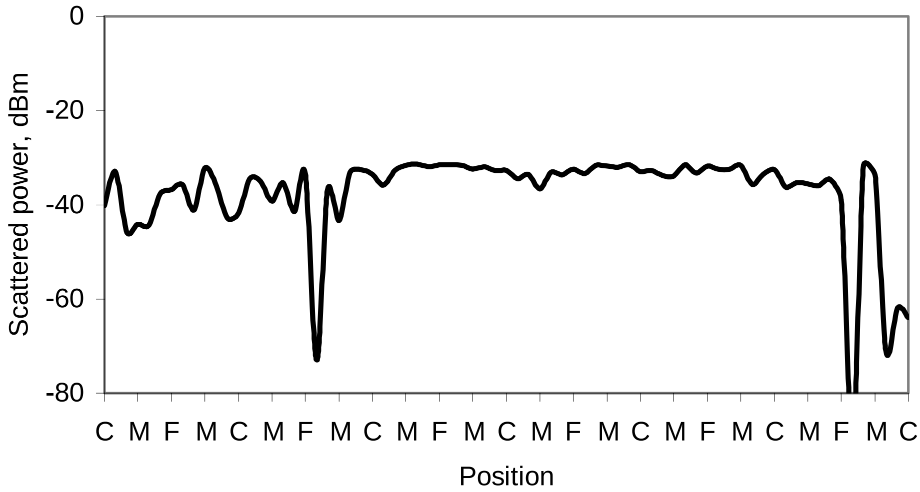


Fig. IV.3. Scattered power at Bragg frequency 10.164 GHz

Fig. IV.4. shows the scattered waves from the waveguide. The fixed frequency here was chosen outside of Bragg gap region. If both results are compared one realizes that in the experiment done with the fixed frequency chosen within the Bragg region there almost appears no electromagnetic wave along the waveguide, i.e., almost all of of the electromagnetic waves is reflected by the structure whereas in the experiment done with the fixed frequency chosen outside of the Bragg region sinusodal fluctuation is seen.

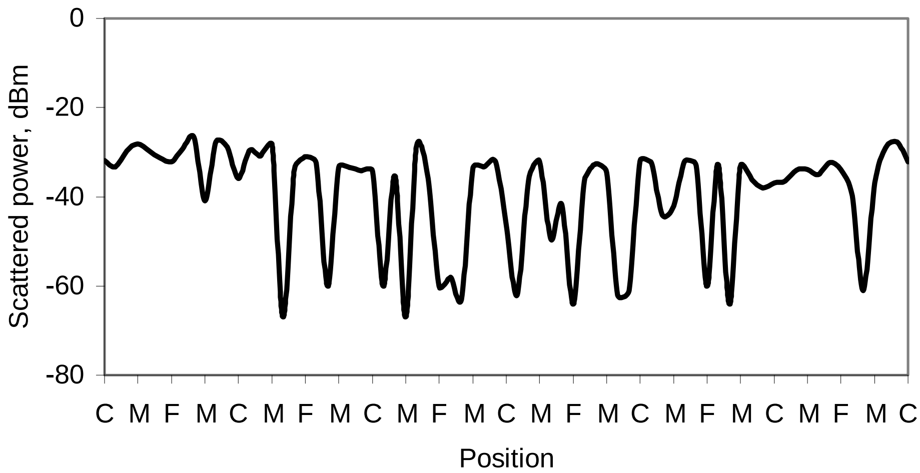


Fig. IV.5. Scattered power at frequency 8.9 GHz from pass band range

## Appendix V: Experiments for Finding the Transmitting Power of the Signal Generator on Frequency

In almost all of the experiments investigating the band structure of the waveguides (both smooth, rectangular, planar, and periodically corrugated) here, the frequency spectrum studied exhibited the power pattern declining upon frequency increased. The reason is that the signal generator makes AM modulation. Four experiments were done in order to reveal the behaviour of the signal generator. Two horn antennas were positioned face to face with three different distances (d) between them. Fig. V.1. shows the power pattern of the generator. In these experiments, between transmitting and horn antennas was nothing. Although all the three experiments exhibited the same pattern, one realizes that the experiment done with d:0 cm is different in terms of its several respective peaks. It resulted from the resonance of horn antennas. The antennas was almost in contact with each other but despite this, due to the shape of face of the horn antennas it was not possible to match them so that we faced such a resonace contribution.

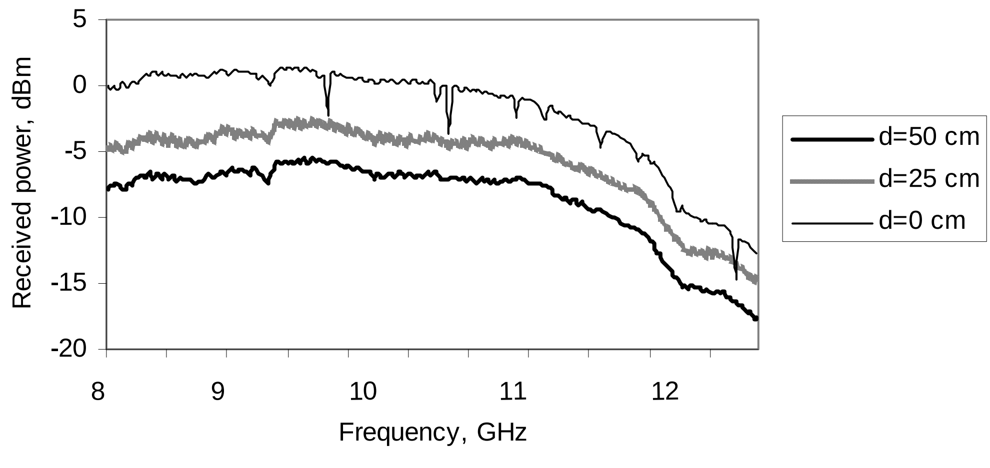


Fig. V.1. Power curves of signal generator FMI 449X. ‘d’ denotes the distance between transmitting and receiving antennas.

We also investigated the behaviour of the signal generator when between the transmitting and receiving antennas was a rectangular smooth waveguide. More truly, the effect of the rectangular smooth waveguide on the power pattern of the signal generator was investigated. The length, width, and thickness of the waveguide are 120 cm, 6 cm, 2,4 cm respectively. Both transmitting and receiving antennas are 5 cm away from the waveguide. Fig. V.2. shows the experimental data. As expected, because of the AM modulation the power pattern tend to decline upon increasing the frequency. Apart from this, from the start to the middle of the frequency spectrum there appeared an increase, or on the contrary, upon proceeding to the start of frequency spectrum from the middle point power pattern tend to decline. This resulted from the interference of the modes.

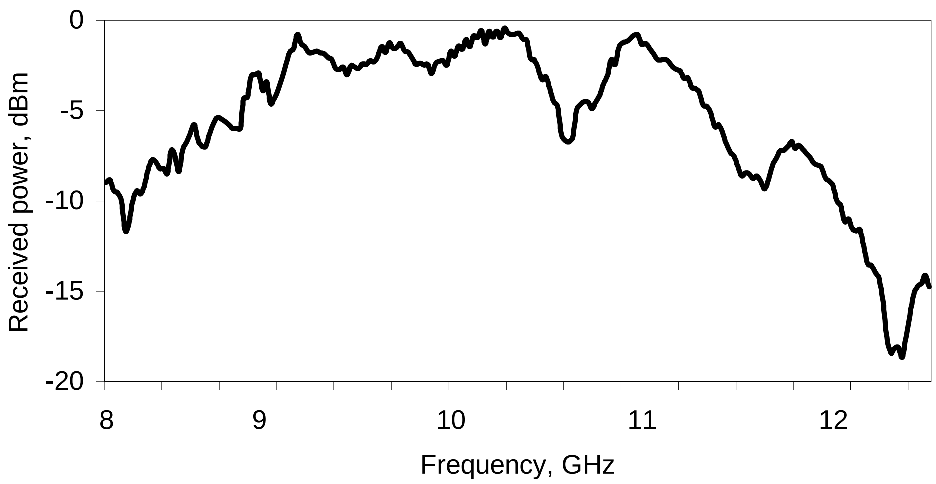


Fig. V. 2. Transmission Power through the rectangular smooth waveguide generated by the signal generator FMI 449X.